Structure and biological activities of hydrophobic short chain pyroglutamyl peptides in fermented foods and food protein hydrolysates

Saki Shirako

2020

The table on contents

General Introduction

Food peptides are usually produced by protease digestion of food proteins. Furthermore, peptides are generated by fermentation. Some peptides in foods have been demonstrated to exert beneficial activities beyond amino acid source.[1,2] It was, however, assumed that most of the peptides in food are degraded into amino acids during the digestion and absorption processes. Recently, it has been demonstrated that some peptides can resist protease digestion and can be absorbed into the blood circulation system.[3,4]

It has been shown that some peptides in foods are chemically modified during processing and storage. Pyroglutamyl (5-oxoprolyl) peptide is spontaneously generated from peptides with a glutaminyl residue at the amino terminal during processing and storage as shown in Figure below.[5,6] Short chain pyroglutamyl peptides resist to endoproteinases and exopeptidases digestions.[7] There are several reports demonstrating *in vivo*[8–11] and *in vitro*[12,13] biological activities of short chain pyroglutamyl peptides. Pyroglutamyl leucine (pyroGlu-Leu or pEL) was first identified in a wheat gluten hydrolysate and demonstrated to attenuate hepatitis in animal model.[8] The administration of pyroGlu-Leu and other pyroglutamyl peptides have been demonstrated to attenuate colitis and colitis-induced disturbance of microbiota[9,11] and anti-depressant like effect in animal models[10] at relatively low doses. *In vitro* studies have demonstrated that some hydrophobic pyroglutamyl peptides show anti-inflammatory activities.[12,13] Pyroglutamyl peptides are widely distributed in food protein hydrolysates[5,8,14] and some Japanese traditional fermented foods.[15,16]

Japanese diet (washoku) has been believed to contribute to longevity of Japanese. One of characteristics of washoku is using traditional fermented seasonings, such as salted soy paste (miso), soy sauce (shoyu), and Japanese rice wine (sake). A number of reports have demonstrated the health benefits of washoku. Tomata *et al.* have found that the Japanese dietary pattern (rice, miso soup, seaweeds, pickles, green and yellow vegetables, fish and green tea) is significantly associated with a lower risk of incidence of dementia in elderly people.[17] Zhang *et al.* also have shown that the Japanese dietary pattern is associated with

longer disability-free survival time in elderly people.[18] There are also a number of reports showing the effects of Japanese traditional fermented foods. A prospective study showed that higher intake of fermented soy products including miso is inversely associated with high blood pressure.[19] Yang *et al.* have demonstrated that Japanese men taking miso and say sauce frequently show lower concentration of inflammatory marker interleukin-6 (IL-6).[20] In addition, a cohort study demonstrated that women taking miso soup every day have lower HOMA-IR.[21] Although, there are a number of reports showing the effects of washoku and Japanese traditional fermented foods, the study on the active compounds in them is limited.

More than 19 pyroglutamyl peptides were identified in Japanese rice wine.[15] Some pyroglutamyl peptides, which can attenuate colitis in animal model, were identified in Japanese rice wine in addition to pyroGlu-Leu. Thus, there is a possibility that pyroglutamyl peptides in Japanese traditional fermented seasoning might exert beneficial activities as suggested by epidemiological studies. However, there is limited information on structure, content, and biological activities of pyroglutamyl peptides in other Japanese traditional fermented seasonings such as miso.

The present study shows the structure, content, and biological activity of pyroglutamyl peptides in miso in Chapter 1. Chapter 2 provides new mechanism for attenuation of high fat diet-induced dysbiosis by pyroGlu-Leu. In chapter 3, the tissue distribution of short chain hydrophobic pyroglutamyl peptides after oral administration is shown. In addition, generation of a novel peptide; propionyl-Leu by the administration of hydrophobic pyroglutamyl peptides is reported.

Figure

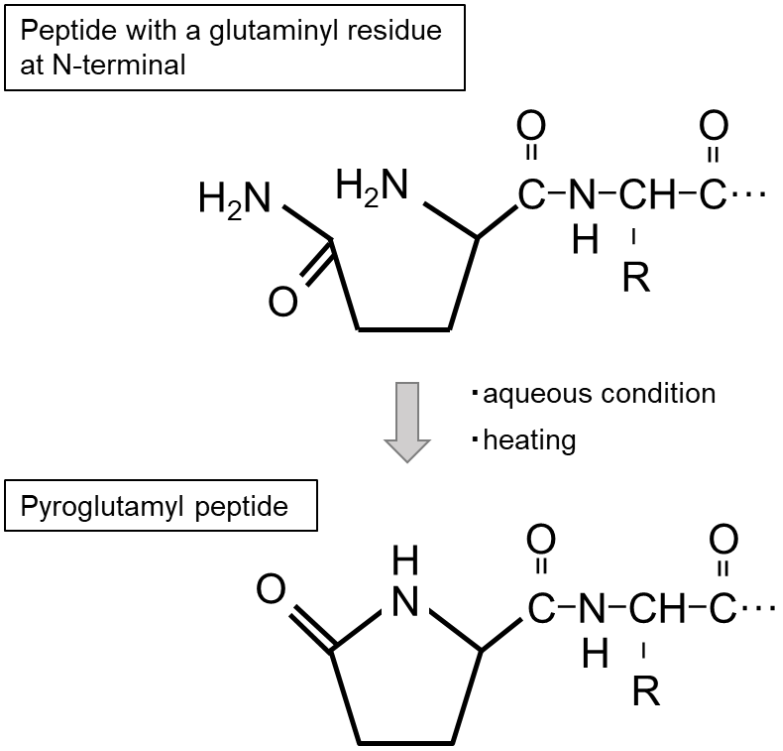

Figure. Structure of pyroglutamyl peptide

Peptide with a glutaminyl residue at the amino terminal is spontaneously converted to pyroglutamyl peptide by heating in aqueous condition.

References for General Introduction

1. Hartmann, R. & Meisel, H. Food-derived peptides with biological activity: from research to food applications. *Curr. Opin. Biotechnol.* **18**, 163–169 (2007).
2. Möller, N. P., Scholz-Ahrens, K. E., Roos, N. & Schrezenmeir, J. Bioactive peptides and proteins from foods: indication for health effects. *Eur. J. Nutr.* **47**, 171–182 (2008).
3. Sato, K. Structure, content, and bioactivity of food-derived peptides in the body. *J. Agric. Food Chem.* **66**, 3082–3085 (2018).
4. Nwachukwu, I. D. & Aluko, R. E. Structural and functional properties of food protein-derived antioxidant peptides. *J. Food Biochem.* **43**, e12761 (2019).
5. Sato, K. *et al.* Occurrence of indigestible pyroglutamyl peptides in an enzymatic hydrolysate of wheat gluten prepared on an industrial scale. *J. Agric. Food Chem.* **46**, 3403–3405 (1998).
6. Higaki-Sato, N. *et al.* Occurrence of the free and peptide forms of pyroglutamic acid in plasma from the portal blood of rats that had ingested a wheat gluten hydrolysate containing pyroglutamyl peptides. *J. Agric. Food Chem.* **54**, 6984–6988 (2006).
7. Chen, L. *et al.* Presence of exopeptidase-resistant and susceptible peptides in a bacterial protease digest of corn gluten. *J. Agric. Food Chem.* **67**, 11948–11954 (2019).
8. Sato, K. *et al.* Identification of a hepatoprotective peptide in wheat gluten hydrolysate against D-galactosamine-induced acute hepatitis in rats. *J. Agric. Food Chem.* **61**, 6304–6310 (2013).
9. Wada, S. *et al.* Ingestion of Low dose pyroglutamyl leucine improves dextran sulfate sodium-induced colitis and intestinal microbiota in mice. *J. Agric. Food Chem.* **61**, 8807–8813 (2013).
10. Yamamoto, Y. *et al.* Antidepressant-like effect of food-derived pyroglutamyl peptides in mice. *Neuropeptides* **51**, 25–29 (2015).
11. Kiyono, T. *et al.* Identification of pyroglutamyl peptides with anti-colitic activity

in Japanese rice wine, sake, by oral administration in a mouse model. *J. Funct. Foods* **27**, 612–621 (2016).

12. Hirai, S. *et al.* Anti-inflammatory effect of pyroglutamyl-leucine on lipopolysaccharide-stimulated RAW 264.7 macrophages. *Life Sci.* **117**, 1–6 (2014).
13. Oishi, M. *et al.* pyroGlu-Leu inhibits the induction of inducible nitric oxide synthase in interleukin-1β-stimulated primary cultured rat hepatocytes. *Nitric Oxide* **44**, 81–87 (2015).
14. Ejima, A., Nakamura, M., Suzuki, Y. A. & Sato, K. Identification of food-derived peptides in human blood after ingestion of corn and wheat gluten hydrolysates. *J. Food Bioact.* **2**, 104–111 (2018).
15. Kiyono, T. *et al.* Identification of pyroglutamyl peptides in Japanese rice wine (sake): Presence of hepatoprotective pyroGlu-Leu. *J. Agric. Food Chem.* **61**, 11660–11667 (2013).
16. Sato, K. & Kiyono, T. Modified peptides in foods; Structure and function of pyroglutamyl peptides. *FFI J.* **222**, 216–222 (2017).
17. Tomata, Y. *et al.* Dietary patterns and incident dementia in elderly Japanese: The Ohsaki cohort 2006 study. *Journals Gerontol. Ser. A Biol. Sci. Med. Sci.* **71**, 1322–1328 (2016).
18. Zhang, S., Tomata, Y., Sugawara, Y., Tsuduki, T. & Tsuji, I. The Japanese dietary pattern is associated with longer disability-free survival time in the general elderly population in the Ohsaki cohort 2006 study. *J. Nutr.* **149**, 1245–1251 (2019).
19. Nozue, M. *et al.* Fermented soy product intake is inversely associated with the development of high blood pressure: The Japan public health center–based prospective study. *J. Nutr.* **147**, 1749–1756 (2017).
20. Yang, X. *et al.* Associations between intake of dietary fermented soy food and concentrations of inflammatory markers: a cross-sectional study in Japanese workers. *J. Med. Investig.* **65**, 74–80 (2018).

21. Ikeda, K. *et al.* Dietary habits associated with reduced insulin resistance: The Nagahama study. *Diabetes Res. Clin. Pract.* **141**, 26–34 (2018).

Chapter 1

Identification of hydrophobic short chain pyroglutamyl peptides in Japanese traditional fermented food, miso, and their potential anti-obesity activity

Introduction

Japanese salted soy paste (miso) is one of Japanese traditional fermented foods.[1] Japanese diet, referred to washoku, is mainly composed of steamed rice, main and side dishes (fish, meat, or vegetables), and miso soup. Miso soup is prepared by putting one spoonful (approximately 12 g per one serve) of miso into soup stock made such as from dried bonito flake (katsuobushi), dried kelp (konbu), and so on. Miso also can be used as seasonings for cooked meats including fish. Miso is still important ingredient for Japanese diet, while the consumption of miso has continuously decreased from 1970's.

Miso is a fermented product made from steamed soybeans, fungus starter (koji), and salt. Koji is prepared by inoculating *Aspergillus oryzae* to steamed rice, barley, or soybean, and cultured at approximately 30°C for 40 hours, which are referred to rice koji, barely koji, or soybean koji, respectively. Soybean is steamed after washing and sinking in water. Steamed soybeans are mixed with the koji and salt and aged for several weeks (short aging type) or months (long aging type). In Japan, different types of miso are produced, depending on ingredients and fermentation period. On the basis of koji ingredients, final miso product is called as rice miso, barely miso, or soybean miso. In Japan, approximately 80% of miso is rice miso, 10% is barely miso and others. Protein in soybean and barley or rice is degraded into peptides and amino acids to show umami taste by proteases of it. In addition, characteristic flavor and aroma are generated by Maillard reaction and also fermentation by air-born lactic acid bacteria and yeasts.

There are several reports demonstrating health benefits by consumption of miso. A cross-sectional study has showed that people who take miso soup in high frequency tend to show lower heart rate.[2] Nagahama prospective cohort study found that women taking miso soup every day show lower HOMA-IR, which is a homeostasis model assessment

to estimate insulin resistance.[3] Kondo *et al* also have reported that intake of miso for 8 weeks reduces nighttime blood pressure in human subjects.[4] Okouchi *et al* have reported that the administration of daily dose of miso suppressed visceral fat accumulation in mice to tend to suppress high fat diet-induced body weight gain.[5] Some compounds in miso have been suggested to be responsible for the beneficial activity of miso. However, it has not been confirmed even by animal experiment.

As mentioned in General Introduction, the presences of pyroglutamyl peptides in food protein hydrolysates[6–8] and some Japanese traditional fermented foods[9,10] have been demonstrated. The administration of pyroGlu-Leu and other pyroglutamyl peptides have been shown to exert attenuation of colitis and colitis-induced disturbance of microbiota,[11,12] anti-inflammation,[13,14] and anti-depressant like effect.[15] These facts suggest that pyroglutamyl peptides in miso might be, at least partially, responsible for the beneficial activities of miso. However, there is little information on peptides in miso. The objective of Chapter 1 was to elucidate structure, content, and biological activity of pyroglutamyl peptides in miso. Consequently, hydrophobic short chain pyroglutamyl peptides suppressed high fat diet-induced body weight gain.

Methods

Material

Different types of Japanese soy paste, miso, were commercially obtained in local market. Rice miso (short aging type and long aging type: Marumi koji honten, Soja, Japan), barley miso (Marumi koji honten), and soybean miso (Kakukyu, Okazaki, Japan) were used.

Reagents

Acetonitrile (HPLC grade) was purchased from Nacalai Tesque (Kyoto, Japan). 1H-benzotruazol-1-yloxy-tri (pyrrolidino) phosphonium hexafluorophosphate (PyBOP), 1-hydroxybenzotriazole (HOBt), 9-fluorenylmethoxycarbonyl (Fmoc) amino acid

derivatives, *N*-(*tert*-Butoxycarbonyl)-L-pyroglutamic acid (Boc-Pyr-OH), L-proline *tert*-butyl ester hydrochloride (H-Pro-OtBu・HCl), L-valine *tert*-butyl ester hydrochloride (H-Val-OtBu・HCl), L-isoleucine *tert*-butyl ester hydrochloride (H-Ile-OtBu・HCl), and L-leucine *tert*-butyl ester hydrochloride (H-Leu-OtBu・HCl) were purchased from Watanabe Chemical Industries (Hiroshima, Japan).

Identification of pyroglutamyl peptides in miso

Pyroglutamyl peptides fraction was obtained by the method as described previously.[8] Briefly, a strong cation exchanger (AG50W-×8, hydrogen form, 100-200 mesh, Bio-Rad Laboratories, Hercules, CA, USA) was washed with 50% methanol and packed into a spin column (15 mm × 7 mm i.d., 5.0 μm pore size, Ultrafree-MC, Merck, Darmstadt, Germany). The resin was further washed with 200 μL of 50% methanol and eluted by spin down at 815 × g (three times). Furthermore, resin was equilibrated with 200 μL of 0.1% formic acid containing 10% of acetonitrile (twice). Soybean miso was added with 3-volume of ethanol and stirred vigorously for minutes. The suspension was centrifuged at 12,000 × g for 10 min at 4°C. The supernatant (200 μL) was loaded onto the spin column and eluted by centrifugation at 815 × g. The eluent was used as pyroglutamyl peptide fraction for following LC-MS/MS analyses.

Aliquots of the pyroglutamyl peptide fraction were subjected to a liquid chromatography electrospray ionization tandem mass spectrometer (LC-MS/MS, LCMS 8040, Shimadzu, Kyoto, Japan) connecting Inertsil ODS-3 column (5 μm, 2.1 mm i.d. × 250 mm, GL Science, Tokyo, Japan). A binary liner gradient was used with 0.1% formic acid (solvent A) and 0.1% formic acid containing 80% acetonitrile (solvent B) at a flow rate of 0.2 mL/min. The gradient program was as follows: 0–30 min, 0–30% B; 30–240 min, 30–100% B; 40–50 min, 100% B; 50–50.1 min, 100–0% B; 50.1–60 min, 0% B. The column was maintained at 40°C. Total ion intensity was monitored at a positive mode in the scan range of mass to charge ratio (*m/z*) =50-150, 150-200, 250-300, and 300-500 (total ion scan). Pyroglutamyl peptides were specifically detected by selecting precursor ions, which generated immonium ion of pyroglutamic acid residue (*m/z*=84.1) at collision

energy -35 V in a positive mode in the scan range of *m/z*=50-150, 150-200, 250-300, and 300-500 (precursor ion scan). The *m/z* of pyroglutamyl peptide peaks were recorded and used for product ion scanning to estimate the peptides structure at collision energies -15, -25, and -35V.

Peptides synthesis

Peptides were synthesized through Fmoc strategy using a PSSM-8 peptide synthesizer (Shimadzu). Synthetic peptides were purified via RP-HPLC using a Cosmosil 5C18-MS-II column (10 mm i.d. × 150 mm, Nacalai Tesque). A binary liner gradient was used with 0.1% formic acid (solvent A) and 0.1% formic acid containing 80% acetonitrile (solvent B) at a flow rate of 2 mL/min. The gradient program was as follows: 0–20 min, 0–50% B; 20–30 min, 50–100% B; 30–35 min, 100% B; 35–35.1 min, 100–0% B; 35.1–45 min, 0% B. The column was maintained at 40°C. Elution of peptides was monitored at 214 and 254 nm. Purity of the peptide was confirmed via LC-MS. Content of the peptide was evaluated via amino acid analysis of HCl hydrolysate.[17] Pyroglutamyl proline (pyroGlu-Pro or pEP), pyroglutamyl valine (pyroGlu-Val or pEV), pyroglutamyl isoleucine (pyroGlu-Ile or pEI), and pyroglutamyl leucine (pyroGlu-Leu or pEL) were also synthesized in liquid phase through Boc strategy as described previously[7] for animal experiments.

Peptides determination

Aliquots (10 μL) of pyroglutamyl peptide fraction of miso were subjected to LC-MS/MS in multiple reaction monitoring (MRM) mode using Inertsil ODS-3 column. The synthetic peptides were used as standard for optimization of MRM condition. A binary liner gradient was used with 0.1% formic acid (solvent A) and 0.1% formic acid containing 80% acetonitrile (solvent B) at a flow rate of 0.2 mL/min. The gradient program was as follows: 0–20 min, 0–30% B; 20–25 min, 30–100% B; 25–30 min, 100% B; 30–30.1 min, 100–0% B; 30.1–40 min, 0% B. The column was maintained at 40°C.

Preparation of samples for animal experiment

Soybean miso was suspended with 4 volumes of water and stirred vigorously. The suspension was centrifuged at 3,000 × g for 10 min. The supernatant was collected and used as crude water extract. Pyroglutamyl peptides in the crude water extract were fractionated by column chromatography in reversed phase and strong cation exchange modes. SepPak Vac 35cc (10 g) C18 Cartridges (Waters, Milford, MA, USA) was washed successively with acetonitrile (50 mL) and 0.1% acetic acid (50 mL). The crude water extract (100 mL) was applied onto the column by syringe (50 mL). Fifty milliliters of 0.1% acetic acid was loaded onto the column. The effluents were combined and used as non-absorbed (N-A) fraction. The compound absorbed to the column were successively eluted with 0.1% acetic acid containing 10% and 30% of acetonitrile (50 mL) and used as 10% ACN and 30% ACN fraction, respectively.

To obtain pyroglutamyl peptide fraction, the N-A, 10% ACN, and 30% ACN fractions were passed through strong cation exchange column (AG50W-×8). AG50W-×8 was washed with 60% acetonitrile and packed into a column (16 mm i.d. ×200 mm, K column, GE Healthcare Chicago, IL, USA). The column was equilibrated with water. Each fraction was loaded to the column by Perista Pump (ATTO, Tokyo, Japan). Non-absorbed effluent was collected as pyroglutamly peptide fraction. Pyroglutamyl peptide fractions of 10% and 30% ACN were mixed. All pyroglutamyl fractions were freeze dried and used for animal experiments

Animal experiments

All the animals were treated and cared for in accordance with the guidelines of the National Institutes of Health (NIH) for the use of experimental animals. All experimental procedures were approved by the Animal Care Committee of Louis Pasteur Center for Medical Research (No. 20162 for *Experiment 1* and 20172 for *Experiment 2* and *3*). Five-week-old male Wistar/ST rats (120–140 g) were purchased from Japan SLC (Shizuoka, Japan). All rats were caged individually and housed at 24 ± 1°C and 40–70% relative humidity with a 12 h light/dark cycle. The rats were allowed free access to a normal diet

(solid type of certified diet MF; Oriental Yeast, Tokyo, Japan) and drinking water for one week. After acclimatization period, rats were received experimental diets for 5 weeks. Body weight, total food intake and total water intake were measured every two days.

Experiment 1

After the acclimatization period (1 week), the rats were divided into five groups (n=4 for each group); One group was fed on normal diets (Control; C). Other 4 groups were fed on a solid type of high fat diet (45% kcal/total kcal; D12451, Research Diets, New Brunswick, NJ). The high fat diet groups received vehicle (HF), crude water extract of miso (CE), pyroglutamyl peptide fraction of N-A fraction (N-A), and pyroglutamyl peptide fraction of mixture of 10% and 30% ACN fractions (ACN) via drinking water. The rats were allowed free access to either the normal or high fat diet, as well as drinking water. Doses of CE, N-A, and ACN corresponded to those in the soybean miso at 0.6 g/kg body weight/day. Drinking water containing CE, N-A, and ACN was prepared every week to administer above dose on the basis of consumption of drinking water in the previous week. After 5 weeks, all rats were sacrificed by puncturing the inferior vena cava that were anesthetized using isoflurane. Plasma was obtained from peripheral blood and stored at -80℃ until analysis. Blood biochemical parameters (alanine aminotransferase; ALT and aspartate aminotransferase; AST) were determined by outsourcing to Oriental Yeast.

Experiment 2

Pyroglutamyl peptides in ACN fraction were identified and determined by the methods as mentioned in ***Peptides determination***. Main pyroglutamyl peptides; pyroGlu-Pro, pyroGlu-Val, pyroGlu-Ile, and pyroGlu-Leu were synthesized and mixed in proportion of the contents in the ACN fraction. After the acclimatization period (1 week), the rats were divided into four groups (n=4 for each group). One group was fed on normal diet (Control; C). Other 3 groups were fed on a solid type of high fat diet (60% kcal/total kcal; D12492, Research Diets). The high fat diet groups received, vehicle (HF) and synthetic pyroglutamyl peptide mixture in ACN at doses corresponding to those in the

soybean miso at 0.6 and 6.0 g miso/kg body weight and referred to ×1 ACN-pep and ×10 ACN-pep, respectively. The synthetic pyroglutamyl peptide mixture was orally administered via drinking water. After 5 weeks, all rats were sacrificed by puncturing the inferior vena cava that were anesthetized using isoflurane. Weight of epididymal adipose tissue and liver were measured. Plasma was obtained from peripheral blood and stored at -80℃ until analysis. Blood biochemical parameters (ALT and AST) were determined by outsourcing to Oriental Yeast. Plasma leptin and ghrelin levels were determined by ELISA kit (leptin; Rat Leptin Assay Kit, Immuno-Biological Laboratories, Fujioka, Japan, and ghrelin; Rat Ghrelin ELISA Kit, MyBioSource, San Diego, USA) according to manufacture's instruction.

Experiment 3

After the acclimatization period (1 week), the rats were divided into four groups (n=4 for each group). Two groups were fed on normal diet and other two groups were fed on a solid type of high fat diet (60% kcal/total kcal; D12492, Research Diets). One group of normal diet and high fat diet groups were received pyroGlu-Leu or vehicle, respectively. They were referred to Control, C+pEL, HF, and HF+pEL. The rats were allowed free access to either the normal or high fat diet. Synthetic pyroGlu-Leu was orally administered via drinking water. Drinking water containing pyroGlu-Leu (3.6–8.3 mg/L) was prepared every week to administer pyroGlu-Leu at 1.0 mg/kg body weight on the basis of consumption of drinking water in the previous week. After 5 weeks, all rats were sacrificed by puncturing the inferior vena cava that were anesthetized using isoflurane. Weight of epididymal adipose tissue and liver were measured. Plasma was obtained from peripheral blood and stored at -80℃ until analysis. Blood biochemical parameters (ALT and AST) were determined by outsourcing to Oriental Yeast. Plasma leptin and ghrelin levels were determined by ELISA kit (leptin; Rat Leptin Assay Kit, Immuno-Biological Laboratories and ghrelin; Rat Ghrelin ELISA Kit, MyBioSource) according to manufacture's instruction.

Generation of stable cell line expressing GPR109A and 81

Stable cell lines, expressing vector only (pCDH), and vector inserted with human G-protein-coupled receptor (GPR) 109A (GPR109A-pCDH), and human GPR81 (GPR81-pCDH) were kindly prepared by Dr. Sathish Sivaprakasam (Texas Tech University Health Sciences Center), from normal human colon mucosal epithelium cell line, NCM460D (INCELL, San Antonio, TX, USA), by the methods as described previously.[18] They are referred to mock cells, GPR109A-expressing cells, and GPR81-expressing cells, respectively. The prepared cells were maintained in M3:BaseA medium (INCELL) with 10% FBS containing 0.5 μg/mL puromycin for western blotting and 5 μg/mL puromycin for preparation of membrane proteins for binding assay. The culture medium was replaced every 2 days a week. The cells were subcultured when the cells reached to 80-85% confluency.

Real-Time qPCR

Real-time qPCR was performed to determine the levels of humanGPR109A or humanGPR81 mRNA expression in mock cells, GPR109A-expressing cells, and GPR81-expressing cells. Total RNA were collected from the cells by using TRIzol reagents (Thermo Fisher Scientific, Waltham, MA, USA). cDNA was prepared by using a High capacity cDNA Reverse Transcription Kit (Thermo Fisher Scientific). qPCR was performed in triplicate on Applied Biosystems StepOnePlus Real-Time PCR System (Thermo Fisher Scientific) using iTaqTM Universal SYBR Green Supermix (Bio-Rad Laboratories). HPRT1 was used as internal control. The sequences of the primers used in the reactions are shown in Table 1-1.

Western blotting

Western blotting was performed triplicate. When mock cells, GPR109A-expressing cells, and GPR81-expressing cells reached to 80-85% confluency, cells were plated on 6-well plates at 1.5×10^6 cells/well. Next day, the cells were rinsed with FBS-free M3:BaseA medium and incubated for 24 h with same medium (2 mL/well). Thirty minutes before

treatment, the cells were rinsed with PBS and preincubated with PBS (2 mL/well). Before treatment, the cells were rinsed with fresh PBS (2 mL/well). After the rinse, the cells were treated with FBS-free M3:BaseA medium containing each pyroglutamyl peptide (pyroGlu-Pro, pyroGlu-Val, pyroGlu-Ile, and pyroGlu-Leu; 0, 3.16, 10, 31.6, 100, 316, 1000, and 3160 μM) for 5 minutes. After the treatment, the treat medium was removed and the cells were rinsed with cold PBS (2 mL/well) twice. Then, the cells were lysed with 250 μL of radioimmunoprecipitation assay (RIPA) buffer (Cell Signaling Technology, Danvers, MA, USA) containing 1% of protease inhibitor. After sonication, supernatant was collected for western blotting by the centrifugation at 12000 *g* for 15 min at 4°C. Western blotting was performed as described previously.[19] The protein content in the supernatant was determined by using Pierce BCA Protein Assay Kit (Thermo Fisher Scientific) with bovine serum albumin as a standard. The protein content was prepared at 1 μg/μL with 4×Laemmli sample buffer (Bio-Rad Laboratories) containing 10% of β-mercaptoethanol (Thermo Fisher Scientific) and RIPA buffer. The protein was denatured by heating at 95°C for 3 min. Then, 10 μL of samples were subjected to sodium dodecyl sulphate polyacrylamide gel electrophoresis (SDS-PAGE). The proteins in SDS-PAGE gels were transferred to polyvinylidene fluoride (PVDF) membranes (Bio-Rad Laboratories) using Mini-PROTEAN Tetra Vertical Electrophoresis Cell (Bio-Rad Laboratories) at 4°C for overnight. Next day, the blots were blocked in 5% skim milk in Tris-buffered saline (20 mM Tris, 137 mM NaCl, pH 7.6) containing 0.1% Tween 20 (TBS-T) at room temperature for 3 h. After blocking, the blots were probed with monoclonal anti-p44/42 MAPK (Erk1/2, 137F5, Rabbit, 1:1000 dilution) and monoclonal anti-phospho-p44/42 MAPK (Erk1/2, Thr202/Tyr204, D13.14.4E, VP Rabbit, 1:1000 dilution) (Cell Signaling Technology) at 4°C for 3 h. Monoclonal anti-β-Actin (1:4000 dilution) (Merck) were used as a control for protein loading. The blots were then washed with TBS-T for 10 min three times. Then the blots were probed with goat anti-rabbit IgG (H&L)-HRP conjugate or goat anti-mouse IgG (H+L)-HRP conjugate (1:2000 dilution, Bio-Rad Laboratories) at room temperature for 1 h. The blots were washed with TBS-T for 10 min three times. Pierce ECL Western Blotting Substrate (Thermo Fisher Scientific)

was used for protein detection to X-ray film in a dark room.

Binding assay

Binding assay was performed in mock cells and GPR109A-expressing cells (n=3). Nicotinate binding assay was performed as described before.[18,20] Mock cells and GPR109A-expressing cells were seeded in three 100-mm dishes (per one binding assay) and grown to be 80% confluency. Every following steps were done on ice. The cells were then collected by scrapping in binding buffer (50 mM Tris-HCl, pH7.4 and 2 mM $MgCl_2$) and centrifugation at 29,600 rpm for 30 min at 4°C. The pellet was resuspended in the binding buffer and passed through a 25G needle repeatedly. To collect membrane fraction, the suspension was ultracentrifuged at 60,000 × g for 30 min at 4°C by using a L8-70 ultracentrifuge (Beckman Coulter, Pasadena, CA, USA). The pellet was collected and resuspended in the binding buffer and passed through a 25G needle repeatedly. To obtain more pure membrane, the membrane fraction was resupended and centrifuged at 14000 rpm for 10 min at 4°C. Finally, the membrane fraction was added 100 μL of binding buffer to get 100-150 μg protein/assay. The final protein content was determined by using Pierce BCA Protein Assay Kit as described above. One hundred μL of membrane fraction, 50 μL of 50 nM (final conc.) of ^{3}H-labeled nicotinic acid (1 mCi/mL, 5Ci/mmol, [3H(G)], American Radiolabeled Chemicals, Saint Louis, MO, USA), and 50 μL of testing sample were mixed and incubated at room temperature for 4 h. As testing samples, binding buffer, 250 nM of cold nicotinic acid sodium salt (Merck), 1 and 10 mM of pyroGlu-Val, pyroGlu-ile, and pyroGlu-Leu were used (final conc.). All samples were dissolved in binding buffer. The membrane-bound form of ^{3}H-labeled nicotinic acid was recovered on the membrane by rapid filtration system using MF membrane filters (0.45 μm HA, Merck). The membrane was washed by 5 mL of ice-cold binding buffer twice. The filters were collected and mixed with 4 mL of liquid scintillation cocktail (Beckman Coulter). Tritium radioactivity was determined by using a scintillation counter (LS 6500 Multi-Purpose Scintillation Counter, Beckman Coulter).

Statistical analysis

The results were presented as the mean ± standard deviations (SD). In animal experiments 1 and 2, the significant differences compared with high fat diet group were evaluated by Dunnett's test. In animal experiments 3, the significant differences between each group were evaluated by *t*-test. The effect of peptides on phosphorylation of Erk was evaluated by Dunnett's test compared to control (no peptide treatment). The result of binding assay was also evaluated by Dunnett's test compared to control. Differences of $p < 0.05$ were considered significant. Statistical analysis was performed using GraphPad Prism version 6.04 (GraphPad Software, San Diego, CA, USA).

Results

Identification and determination of pyroglutamyl peptides in miso

Pyroglutamyl peptides in the soybean miso were analyzed by LC-MS and LC-MS/MS in precursor ion scan mode, targeting immonium ion of pyroglytamic acid residue (*m/z*=84.1). Mass chromatograms were obtained by scanning different *m/z* ranges (50-150, 150-200, 200-250, 250-300, and 300-500) as shown in Figure 1-1 A-E. The mass chromatograms by the LC-MS/MS (lower) were different from those by the LC-MS (upper). Precursor ions in peaks detected by the LC-MS/MS (Figure 1-1) were further analyzed by LC-MS/MS in product ion scan mode to obtain primary structure. The observed product ions including immonium ions are summarized in Table 1-2. On the basis of precursor and product ions, 13 pyroglutamyl di- and tri-peptides (pyroGlu-Gly, pyroGlu-Ser, pyroGlu-Thr, pyroGlu-Asp, pyroGlu-Ala, pyroGlu-Pro, pyroGlu-Val, pyroGlu-Ile/Leu, pyroGlu-Glu, pyroGlu-Gln, pyroGlu-Gly-Ser, and pyroGlu-Phe) were estimated (peaks a-m in Figure 1-1). Free pyroglutamic acid (peak x**)** and its methyl (peak y) and ethyl esters (peak z) were also observed. Adduct ions with acetonitrile and proton were observed (marked with *) for pyroglutamyl esters and pyroGlu-Ile/Leu. Adduct ions of two molecules of pyroglutamic acid, its esters, and pyroGlu-Pro with one proton were also observed (marked with **). Most of peaks by LC-MS/MS in precursor ion scan mode

targeting immonium ions of pyroglutamic acid residue can be assigned to pyroglutamyl peptides and its derivatives.

Presences of all pyroglutamyl peptides including pyroGlu-Ile and pyroGlu-Leu were confirmed by comparing retention time of synthetic peptides by LC-MS/MS in MRM mode. The contents of pyroglutamyl peptides in some commercial available miso are shown in Figure 1-2. Approximately 0.05 – 0.5 μmol/g of pyroglutamyl peptides were contained in miso. Short aging type of rice miso showed lower contents of pyroglutamyl peptides compared to long aging types. Contents of some hydrophilic pyroglutamyl peptides (pyroGlu-Asp, pyroGlu-Glu, and pyroGlu-Gln) were higher than those of hydrophobic ones (pyroGlu-Val, pyroGlu-Ile, and pyroGlu-Leu).

Effects of administration of miso extract

As shown in Figure 1-3, the feeding of high fat diet significantly increased the body weight gain compared to normal diet without increasing calorie intake. Administration of crude water extract of the soybean miso (CE) significantly suppressed the high fat diet-induced body weight gain with reduction of calorie intake. Administration of ACN fraction also significantly suppressed the high fat diet-induced body weight gain, however, no significant differences were observed in total calorie intake. Administration of N-A fraction did not significantly affect. These data suggest that hydrophobic pyroglutamyl peptides may be responsible for the suppression of high fat diet-induced body weight gain by administration of miso. There were no significant differences in plasma AST and ALT level between all groups (Supplemental Figure 1 A).

Effects of synthetic hydrophobic pyroglutamyl peptides

The contents of each pyroglutamyl peptide in CE, N-A, and ACN fractions were determined. As shown in Figure 1-4, ACN fraction was consisted of pyroGlu-Pro, pyroGlu-Val, pyroGlu-Ile, and pyroGlu-Leu, while pyroGlu-Pro was also distributed in N-A fraction. Mixtures of synthetic pyroGlu-Pro, pyroGlu-Val, pyroGlu-Ile, and pyroGlu-Leu (×1 ACN-pep and ×10 ACN-pep) were administered to high fat diet-fed rats

for five weeks. Dose of each peptides are shown in Table 1-3. As shown in Figure 1-5 A and B, administration of synthetic peptide mixtures tended to reduce high fat diet-induced body weight gain and total calorie intake (×10 ACN-pep; p=0.07 for body weight gain and p =0.05 for total calorie intake, respectively). However, administration of synthetic peptide mixtures did not significantly affect weight of epididymal adipose tissue and liver (Figure 1-5 C and D). As shown in Figure 1-5 E, plasma leptin level was significantly higher in high fat diet group compared to normal diet group. Administration of synthetic peptide mixtures (×1 ACN-pep) significantly decreased plasma leptin level, however, administration of ×10 ACN-pep did not affect this value. As shown in Figure 1-5 F, there were no significant differences in plasma ghrelin level between all groups. There were no significant differences in plasma AST and ALT level between all groups (Supplemental Figure 1 B).

Effects of synthetic pyroGlu-Leu in high fat diet-fed rats

Synthetic pyroGlu-Leu (1.0 mg/kg body weight) was administered to rats fed the normal diet and high fat diet for five weeks. As shown in Figure 1-6 A and B, administration of pyroGlu-Leu tended to suppress the high fat diet-induced body weight gain p=0.09) and significantly reduced total calorie intake, while administration of pyroGlu-Leu did not show significant effects on rat fed normal diet. Liver weight was significantly lower by administration of pyroGlu-Leu in high fat diet groups (Figure 1-6 D), however, there were no significant differences in the weight of epididymal adipose tissue (Figure 1-6 C). As shown in Figure 1-6 E, plasma leptin level was higher in high fat diet group compared to normal diet group, however, administration of pyroGlu-Leu did not affect this value in both normal and high fat diet groups. As shown in Figure 1-6 F, there were no significant differences in plasma ghrelin level between all groups. There were no significant differences in plasma AST and ALT level between all groups (Supplemental Figure 1 C).

Ligand activity of pyroglutamyl peptides

As shown in Figure 1-7, over expression of huGPR109A and huGPR81 in GPR109A-expressing cells, and GPR81-expressing cells compared to mock cells were confirmed by qPCR. Then, the effect of pyroglutamyl peptides on phosphorylation of Erk was examined. As shown in Figure 1-8, pyroGlu-Leu significantly increased phosphorylation of Erk of huGPR81 expressing cells compared to mock cells above 10 μM in dose dependent manner. On the other hand, it increased phosphorylation of Erk of GPR109A-expressing cells only at highest concentration (3.160 mM). PyroGlu-Val and pyroGlu-Ile increased phosphorylation of Erk of both cells at higher than 1 mM. PyroGlu-Pro increased phosphorylation of Erk of only GPR81-expressing cells above 10 μM, while dose dependency was not observed.

For only GPR109A, ^{3}H-labeled high affinity ligand (nicotinic acid) is available. Thus, competitive inhibition assay using ^{3}H-labeled nicotinate was performed. Cold nicotinate (positive control) significantly inhibited the binding of ^{3}H-labeled nicotinate to huGPR109A at 250 nM. PyroGlu-Val and pyroGlu-Ile significantly inhibited the binding of ^{3}H-labeled nicotinate to huGPR109A at 10 mM. PyroGlu-Leu significantly but slightly inhibited the binding of ^{3}H-labeled nicotinate to huGPR109A at 10 mM. These data are consistent with the phosphorylation of Erk of GPR109A-expressing cells (Figure 1-8). For GPR81, competitive assay was not done, as high affinity ligand is not available.

Discussion

Previous reports have demonstrated the presences of pyroglutamyl peptides in food protein hydrolysates[6–8] and sake (Japanese traditional fermented foods).[9] Pyroglutamyl peptides with known structure such as pyroGlu-Leu can be determined in some other fermented foods including miso by using LC-MS/MS in MRM mode.[10] However, it has been difficult to detect pyroglutamyl peptides with unknown structure in complex food matrix such as miso. To identify pyroglutamyl peptides in miso, pre-fractionation by using size exclusion chromatography (SEC) was used before LC-MS analysis. However,

LC-MS of SEC fractions still showed many peaks, majority of which could not be assigned to pyroglutamyl peptide. To solve this problem, precursor ion scan targeting immonium ion of pyroglutamic acid residue (*m/z*=84.1) was performed. In addition, precursor ions, which generated immonium ion of pyroglutamic acid residue, were detected in narrow scan ranges. As shown in Figure 1-1, all peaks by precursor ion scan were well resolved and could be assigned to pyroglutamyl peptides and related compounds (Table 1-2). Consequently, 13 pyroglutamyl peptides and 11 derivatives were identified without pre-fractionation by SEC. The precursor ion scan targeting immonium ion of pyroglutamic acid residue can be useful method to detect pyroglutamyl peptides with unknown structure from complex food matrix.

Administration of crude water extract (CE) from soybean miso (0.6 g/kg of body weight of rat) suppressed high diet-induced body weight gain, of which dose corresponded to 3 cups of miso soup/day (3×12 g miso/one cup/60 kg of body weight). These results suggest that daily intake of miso could impact on human health, which support results from epidemiological studies. The hydrophobic compounds without amino group in the ACN fraction were responsible for suppression of the high fat diet-induced body weight gain (Figure 1-3). The main pyroglutamyl peptides in ACN fraction (pyroGlu-Pro, pyroGlu-Val, pyroGlu-Ile, and pyroGlu-Leu) also suppressed body weight gain. Surprisingly, the administered dose was just 0.1-0.3 mg/kg B.W. The single administration of pyroGlu-Leu also tended to suppress the high fat diet-induced body weight gain, however, the dose was 1.0 mg/kg B.W. It has been shown that administration of hydrophobic pyroglutamyl peptide (pyroGlu-Leu) attenuates hepatitis[7] and colitis.[11,12] These findings suggest that hydrophobic pyroglutamyl peptide may be mainly responsible for health benefits by intake of miso. On the other hand, the significant effects of the administration of hydrophobic pyroglutamyl peptides on tissue weight (epididymal adipose tissue and liver) were not observed. Hence, target tissue and mechanism for potential anti-obesity effect by hydrophobic pyroglutamyl peptides should be further studied.

There are no reports demonstrating the administration of low dose (0.1-1.0 mg/kg

B.W) of food-derived peptides exert anti-obesity effect. To find the mechanism for potential anti-obesity effect by pyroglutamyl peptides, the effects of pyroglutamyl peptides on appetite and obesity-related molecules were evaluated. The administration of hydrophobic pyroglutamyl peptides suppressed total calorie intake in high fat diet-fed groups. Leptin and ghrelin are known to control food intake.[21] Leptin is a hormone mainly produced by adipose tissue,[21] which decreases appetite and body weight.[22,23] On the other hand, ghrelin is a hormone mainly produced by stomach,[21] which stimulates food intake and weight gain in rats,[24] and increases appetite of human.[25] Then, plasma leptin and ghrelin level were determined by ELISA, however, administration of hydrophobic pyroglutamyl peptides did not affect these hormone levels (Figure1-5 and 6 E and F). Therefore, it is unlikely that hydrophobic pyroglutamyl peptides control food intake by affecting leptin and ghrelin.

In addition to endocrine system, cell surface receptors, such as G Protein-coupled Receptor (GPR), have been demonstrated to be involved in suppression of inflammation in intestine and attenuation of lipid metabolism. GPR109A is expressed in colonic epithelium, adipose tissue and immune cells and suppresses inflammation.[18,20,26] On the other hand, GPR81 is highly homologous to GPR109A.[27] GPR81 is mainly expressed in adipose tissue and suppresses lipolysis in adipose tissue, as well as GPR109A.[27] GPR81 has been hypothesized to be a potential target for the treatment of dyslipidemia.[27] It is demonstrated that the expressions of GPR109A and GPR81 decrease in high fat diet-induced obesity.[28] GPR109A has hydrophobic ligands, such as 3-hydroxy-butyrate, butyrate and nicotinate.[20,27] Then, ligand activity of hydrophobic pyroglutamyl peptides were examined, however, they did not affect intracellular signaling via GPR109A at physiological concentration (μM level). On the other hand, lactate has been demonstrated to be a ligand of GPR81. However, its affinity is low (EC_{50} of 1~5 mM).[29,30] Then, competition binding assay using radiolabeled ligand cannot be used. In the present study, pyroGlu-Leu significantly activated intracellular signaling of GPR81 at 10 μM. Therefore, pyroGlu-Leu could be a ligand of GPR81 with higher affinity than lactate and involved in anti-obesity via affecting fat metabolism.

Previous reports have demonstrated that the administration of low doses (1.0 mg/kg B.W.) of pyroGlu-Leu attenuates colitis-induced increase of one of major phylum; *Firmicutes* in mice.[11,12] Recently, the relationship between the increase of *Firmicutes* and obesity has been demonstrated.[31,32] Therefore, it is likely that the administration of hydrophobic pyroglutamly peptides including pyroGlu-Leu exerts potential anti-obesity effect via attenuation of high fat diet-induced increase of *Firmicutes*. In Chapter 2, the effect of pyroGlu-Leu in miso on gut microbiota in high fat diet-fed rats is described.

Tables and Figures

Table 1-1. Primer sequences used for qPCR

Gene name	Gene ID	Primer sequence	Product size (bp)
Human GPR109A	NM_177551.3	F: ACTATGTGAGGCGTTGGGAC R: TGGAGATCTTGTTCAGGGCG	165
Human GPR81	NM_032554.3	F: TGGAGAACCATCTCTGCGTG R: TGATGCCGAGGGGCATAAAG	120
HPRT1	NM_000194.2	F: GCGTCGTGATTAGCGATGATGAAC R: CCTCCCATCTCCTTCATGACATCT	157

Primer sequences used for qPCR are listed. F and R represent forward and reverse of the primer.

Table 1-2. Estimated sequences of pyroglutamyl peptides and related peptides in miso

Peaks	Estimated structures	Precursor ions (*m/z*)	Product ions (*m/z*)
a	pyroGlu-Gly	187.1	30.8 (immonium ion of Gly), 168.3 (b2)
b	pyroGlu-Ser	217.1	60.4 (immonium ion of Ser), 88.2 (z1), 106.1 (y1)
c	pyroGlu-Thr	231.2	74.2 (immonium ion of Thr), 102.4 (z1), 120.6 (y1)
d	pyroGlu-Asp	245.3	70.0 (related ion of Asp), 88.4 (immonium ion of Asp), 116.4 (z1), 134.1 (y1)
e	pyroGlu-Ala	201.2	44.3 (immonium ion of Ala), 72.9 (z1), 90.1 (y1), 155.8 (a2)
f	pyroGlu-Pro	227.2	70.7 (immonium ion of Pro), 116.7 (y1), 181.5 (a2)
g	pyroGlu-Val	229.2	72.4 (immonium ion of Val), 41.4 (related ion of Val)
h	pyroGlu-Ile	243.2	86.8 (immonium ion of Ile), 132.2 (y1)
i	pyroGlu-Leu	243.2	43.9 (related ion of Leu), 86.8 (immonium ion of Leu), 132.2 (y1)
j	pyroGlu-Glu	259.2	130.7 (z1)
k	pyroGlu-Gln	258.2	56.3 (immonium ion of Gln), 130.2 (z1)
l	pyroGlu-Gly-Ser	274.2	106.1 (y1), 256.7 (b3)
m	pyroGlu-Phe	277.2	120.1 (immonium ion of Phe), 162.2 (y1)
x	pyroglutamic acid	130.1	130.1 (y1)
y	pyroglutamic acid methyl ester	144.1	144.0 (y1)
y*	pyroglutamic acid methyl ester+CH_3CN	185.1	144.0 (y1)
z	pyroglutamic acid ethyl ester	158.1	158.0 (y1)
z*	pyroglutamic acid ethyl ester+CH_3CN	199.1	158.0 (y1)
x**	Two pyroglutamic acid	259.2	129.9 (y1)
y**	dimer of pyroglutamic acid methyl ester	287.3	144.0 (y1)
h*	pyroGlu-Ile+CH_3CN	284.2	86.3 (immonium ion of Ile), 132.8 (y1), 243.2 (pyroGlu-Ile)
i*	pyroGlu-Leu+CH_3CN	284.2	86.3 (immonium ion of Leu), 132.8 (y1), 243.2 (pyroGlu-Leu)
f**	Two pyroGlu-Pro	453.3	70.2 (immonium ion of Pro), 115.9 (y1), 226.9 (pyroGlu-Pro)
z**	Two pyroglutamic acid ethyl ester	315.2	158.0 (y1)

Pyroglutamyl peptides in the soybean miso were analyzed by LC-MS and LC-MS/MS. Peak name, estimated structure, precursor ions, and observed product ions are summarized. Pyroglutamic acid residue is represented as pyroGlu. Adduct ions with acetonitrile and proton are marked with *. Adduct ions of two molecules with proton are marked with **.

Table 1-3. Content of pyroglutamyl peptides, orally administered in animal experiment 2

Groups	miso (g/kg BW)	pyroGlu-Pro [mg/kg BW]	pyroGlu-Val [mg/kg BW]	pyroGlu-Ile [mg/kg BW]	pyroGlu-Leu [mg/kg BW]
× 1 ACN-pep	0.6	0.0276	0.0113	0.00884	0.0166
× 10 ACN-pep	6	0.276	0.113	0.0884	0.166

The content of four pyroglutamyl peptides which were orally administered to rats in experiment 2 is shown. The mixture of synthetic pEP, pEV, pEI, and pEL in ACN, whose doses are corresponded to those in the miso at 0.6 and 6.0 g miso/kg body weight, were referred to ×1 ACN-pep and ×10 ACN-pep, respectively.

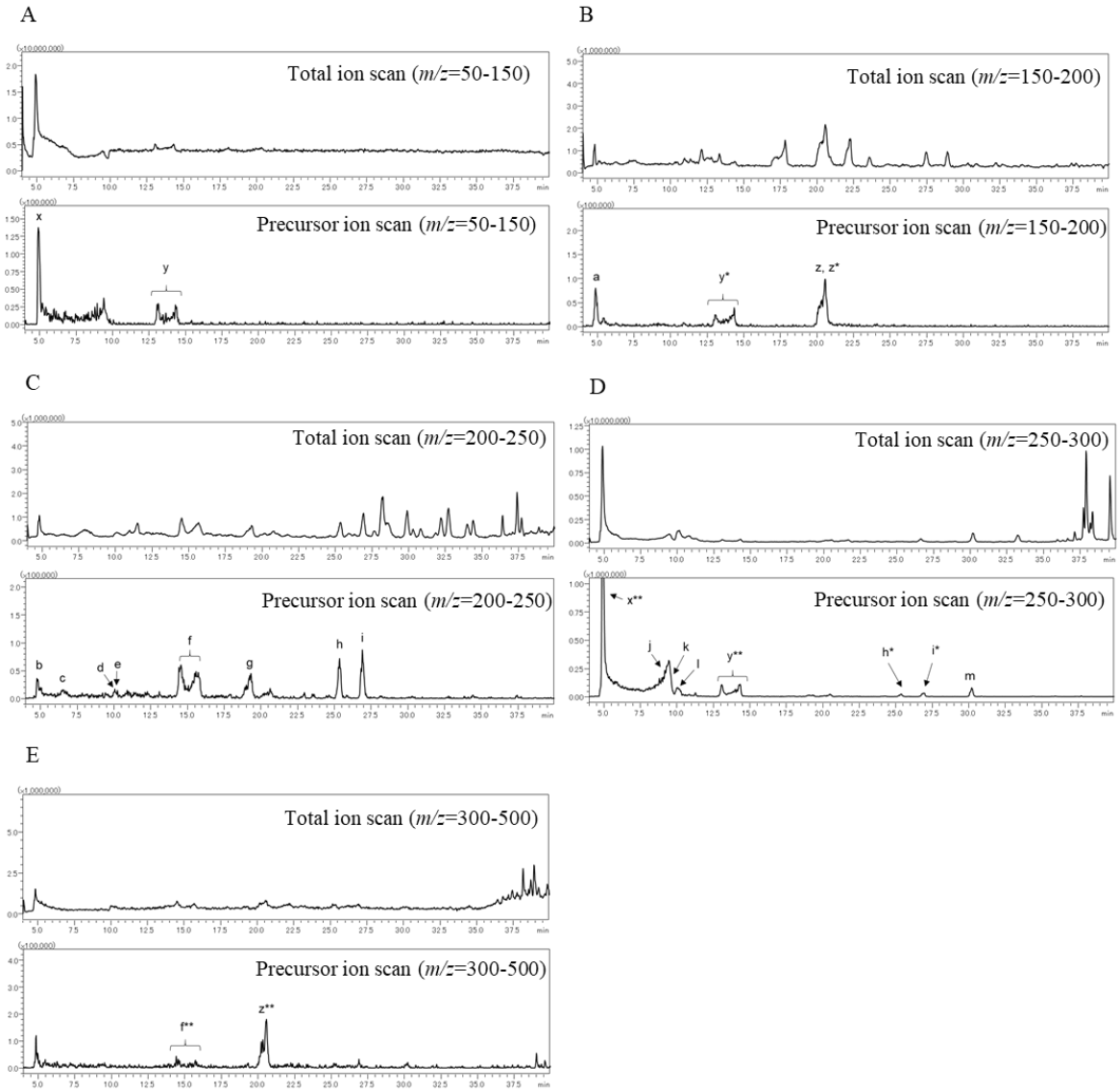

Figure 1-1. Mass spectrometry chromatograms of total ion scan (upper) and precursor ion scan (lower).

Total ion intensity was monitored at a positive mode in the scan range of *m/z* =50-150, 150-200, 250-300 and 300-500 (total ion scan). Pyroglutamyl peptides were specifically detected by selecting precursor ions, which generated immonium ion of pyroglutamic acid residue (*m/z*=84.1) at a positive mode in the same scan range with total ion scan (precursor ion scan). Peaks which could be assigned to pyroglutamyl peptides were marked with alphabets (peak a-m). Peak x, y, and z represent pyroglutamic acid, pyroglutamic acid methyl ester, and

pyroglutamic acid ethyl ester, respectively. Adduct ions with acetonitrile and proton are marked with *. Adduct ions of two molecules with proton are marked with **.

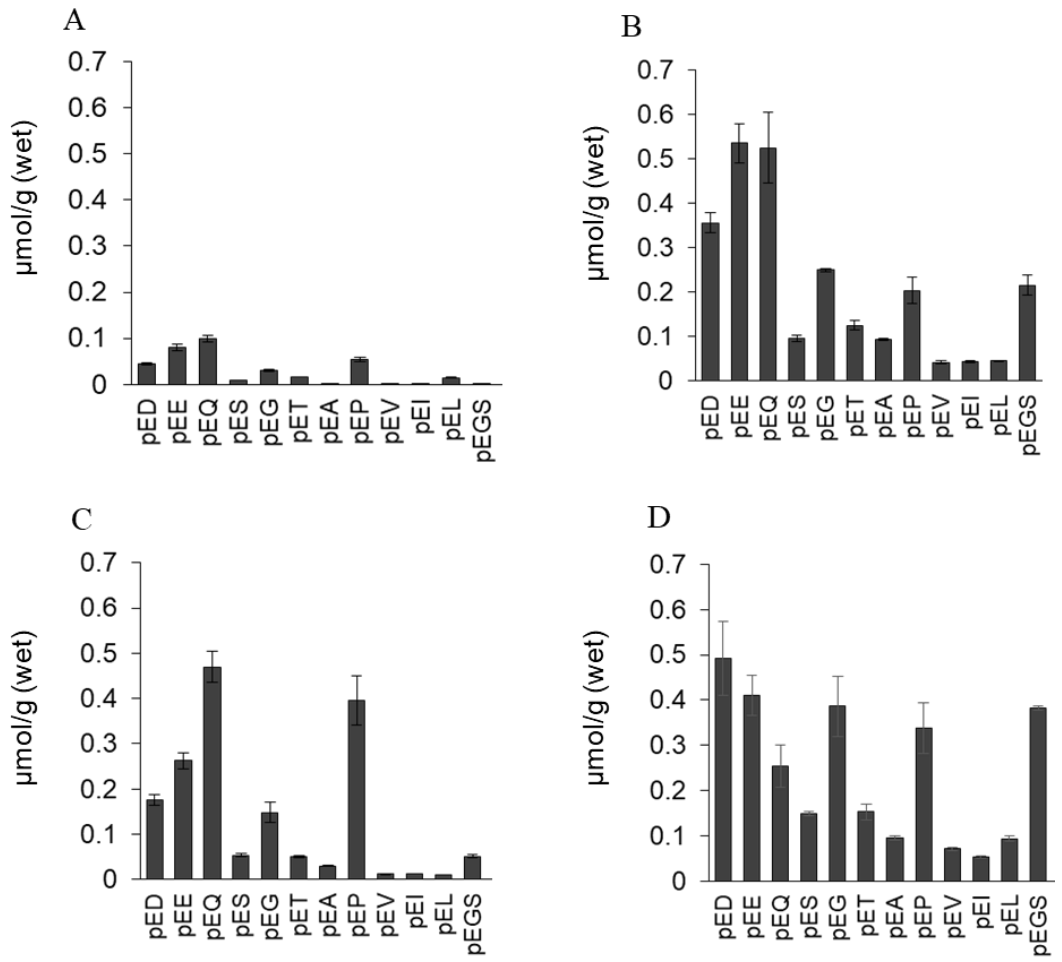

Figure 1-2. The content of pyroglutamyl peptides in miso.

Rice miso (short aging type) (A), rice miso (long aging type) (B), barley miso (C), and soybean miso (D), respectively (n=3-6). pE represents pyroglutamic acid (pE) residue. One-letter abbreviations are used for amino acid residues.

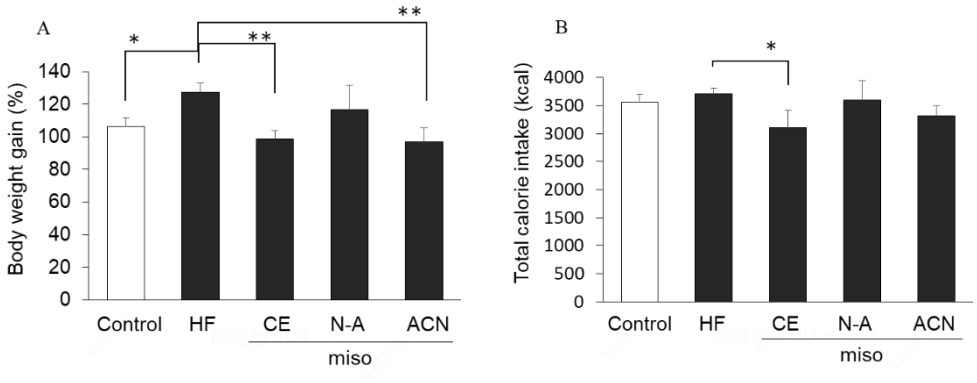

Figure 1-3. The effect of miso extraction on body weight gain and total calorie intake.

Body weight gain (A) and total calorie intake (B). Data are shown in mean ± SD (n=4). * and ** represent significant differences of $p<0.05$ and $p<0.01$, respectively, by Dunnett's test vs HF.

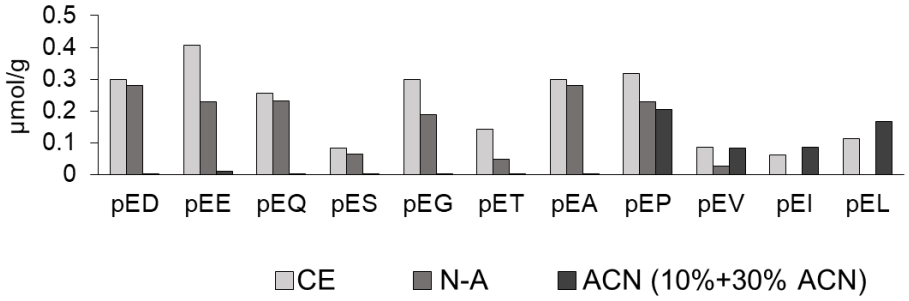

Figure 1-4. The contents of pyroglutamyl peptides in miso extract.

The contents of purpglutamyl peptides in crude water extract of miso (CE), non-absorbed (N-A), mixture of 10% ACN and 30% ACN (ACN) are shown. The content of pyroglutamyl peptide in each fraction was determined by LC-MS/MS in MRM mode.

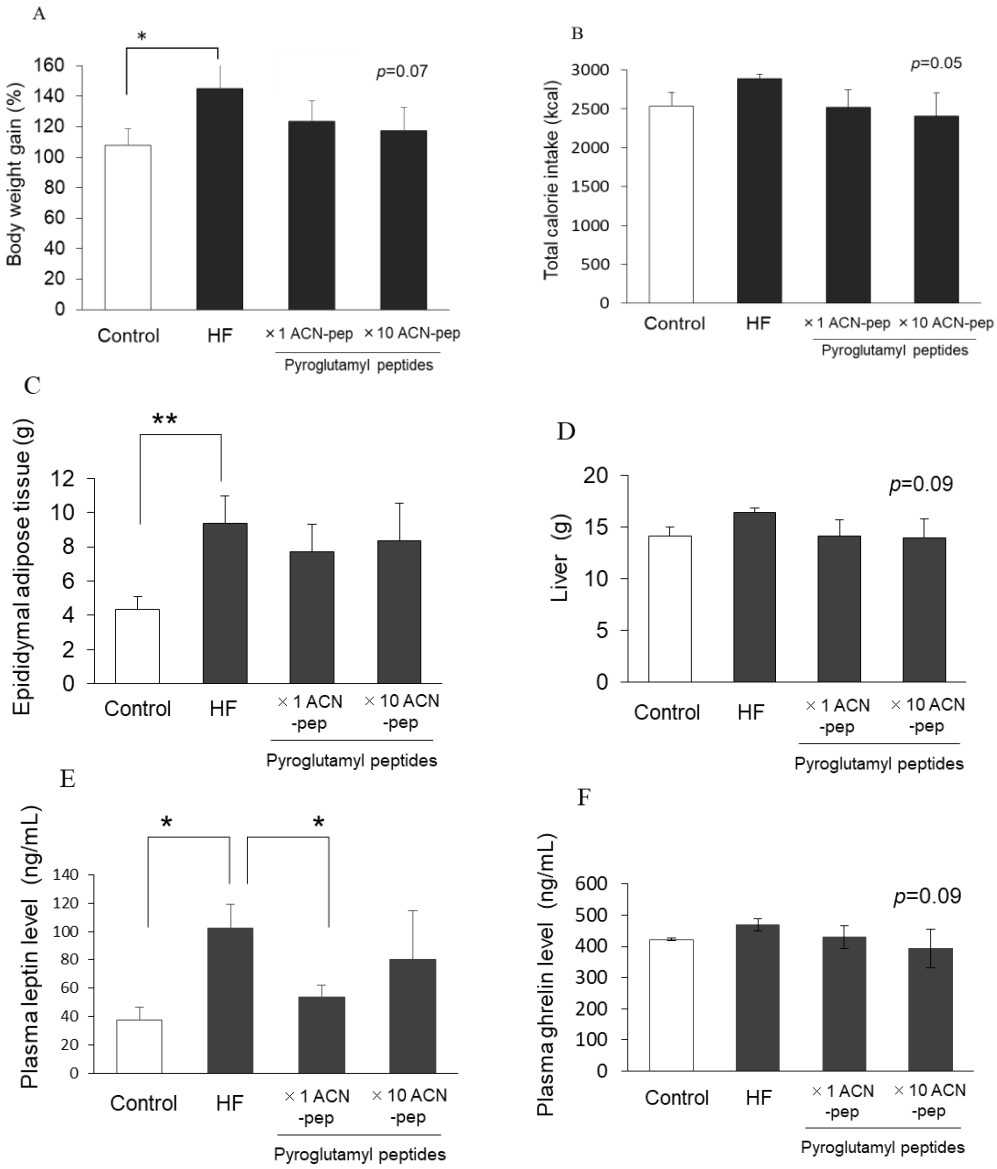

Figure 1-5. The effect of pyroglutamyl peptides in high fat diet-fed rats.

Body weight gain (A), total calorie intake (B), weight of epididymal adipose tissue (C) and liver (D), plasma leptin (E), and ghrelin level (F). Data are shown in mean ± SD (n=4). * represents significant differences of $p<0.05$ by Dunnett's test vs HF.

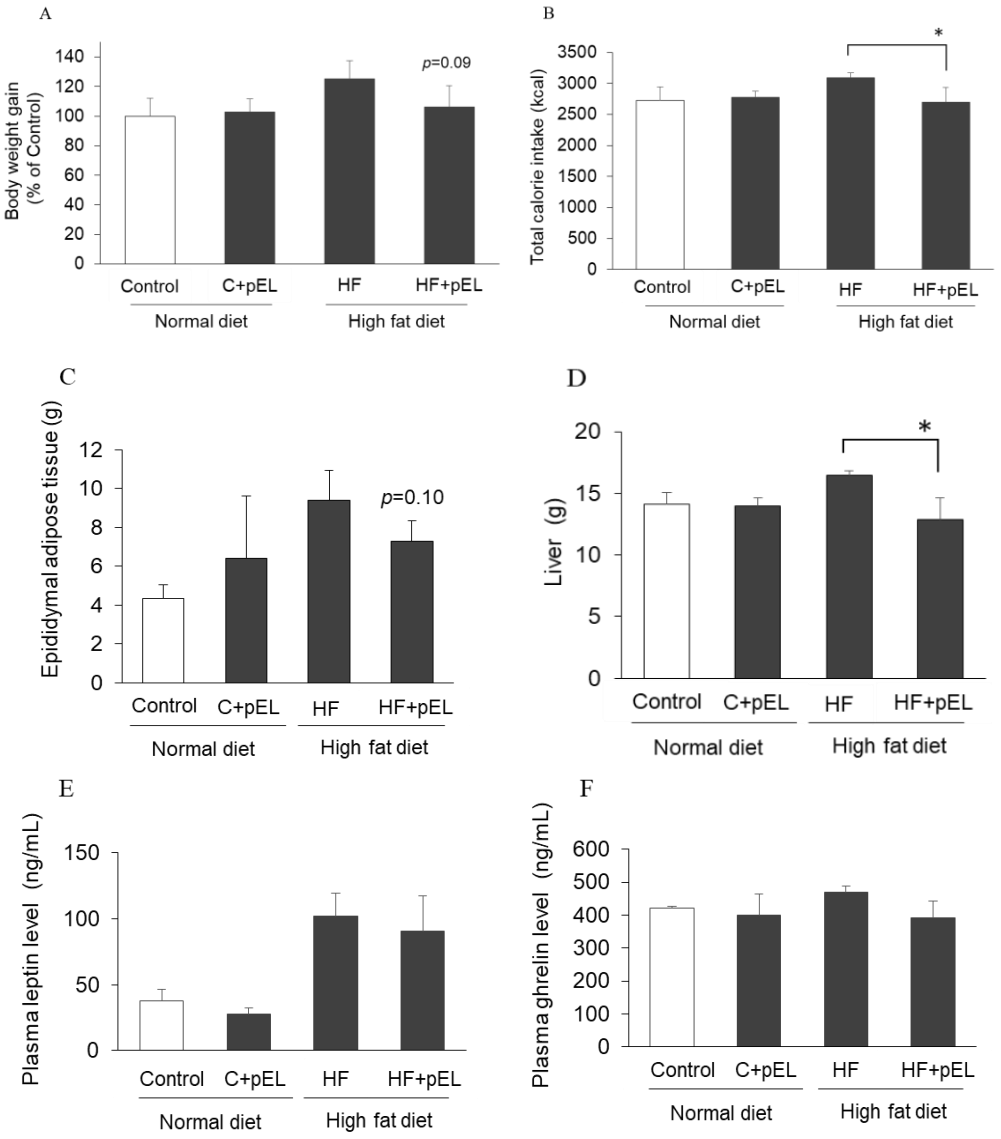

Figure 1-6. The effect of pyroglutamyl leucine in high fat diet-fed rats.

Body weight gain (A), total calorie intake (B), weight of epididymal adipose tissue (C) and liver (D), plasma leptin (E), and ghrelin level (F). Data are shown in mean ± SD (n=4). * represents significant differences of $p<0.05$ by *t*-test between each diet group.

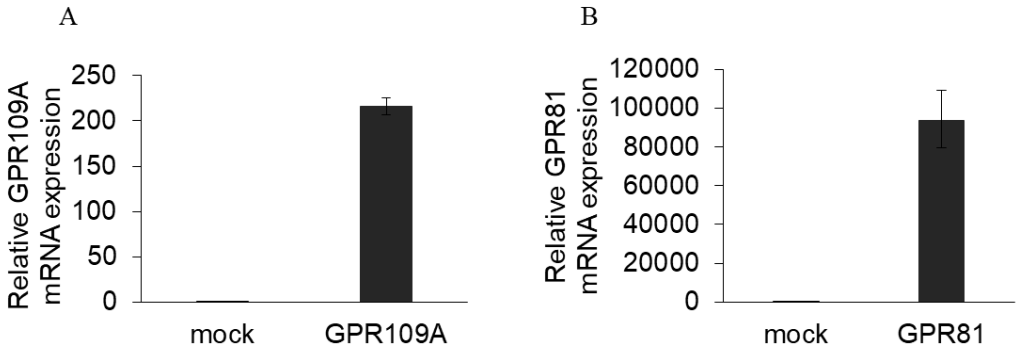

Figure 1-7. Expression of huGPR109A and huGPR81 in transfected NCM460D cell lines. Expression of huGPR109A (A) and huGPR81 (B) in mock cells, GPR109A-expressing cells, and GPR81-expressing cells were confirmed by qPCR. HPRT was used as house-keeping gene. Data are shown in mean ± SD (n=3).

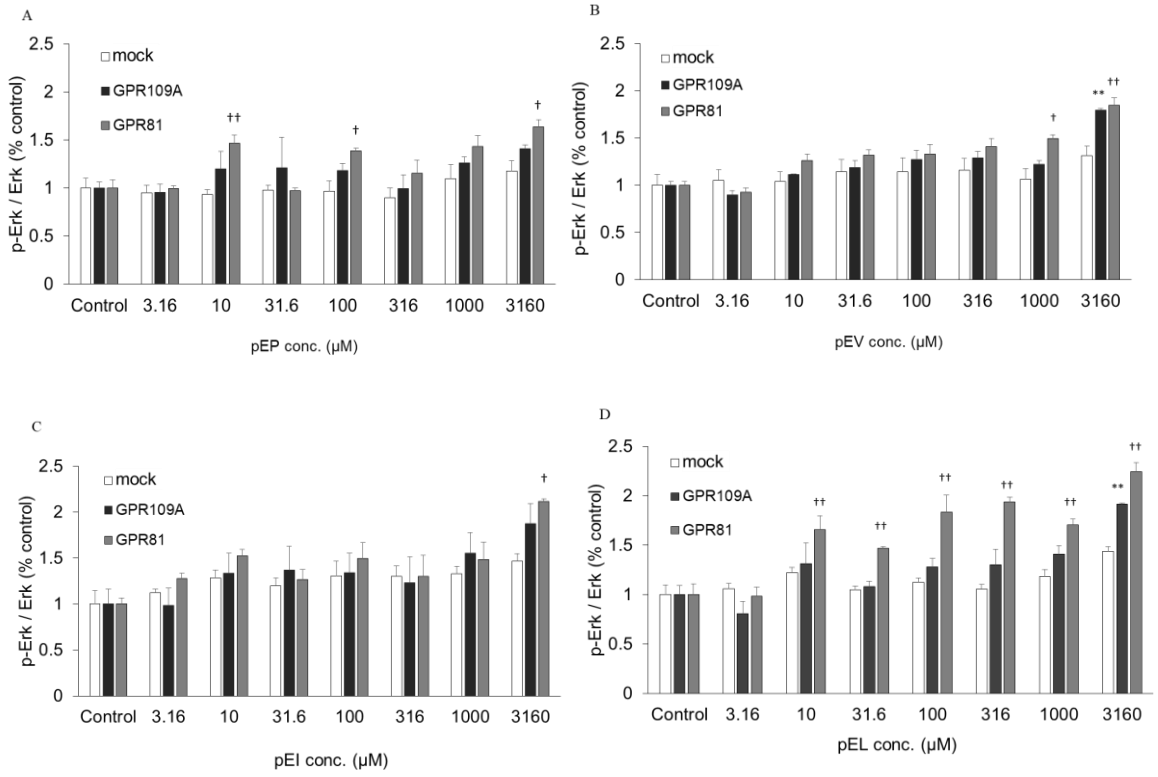

Figure 1-8. The effect of pyroglutamyl peptides on phosphorylation of Erk.

Protein level of Erk and p-Erk in mock cells, GPR109A-expressing cells, and GPR81-expressing cells were evaluated by western blotting. pEP (A), pEV (B), pEI (C), and pEL (D) were treated at 0 (control), 3.16, 10, 31.6, 100, 316, 1000, and 3160 μM onto the cells. Data are shown in mean ± SD (n=3). * and ** represent significant differences of $p<0.05$ and $p<0.01$,respectively, by Dunnett's test vs control in GPR109A. † and †† represent significant differences of $p<0.05$ and $p<0.01$,respectively, by Dunnett's test vs control in GPR81.

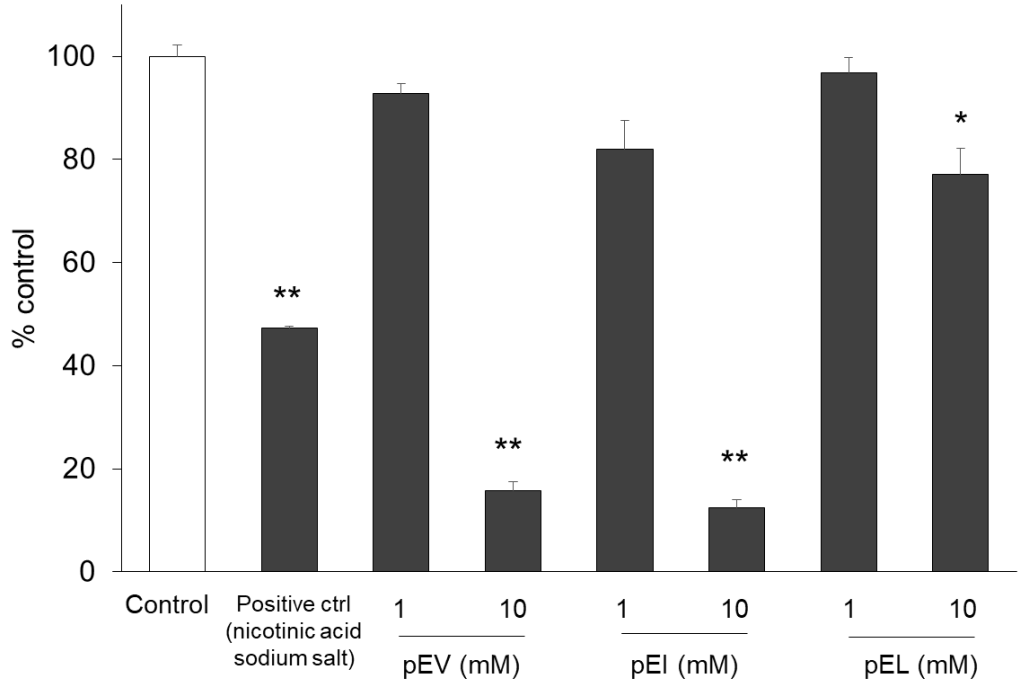

Figure 1-9. Ligand activities of pyroglutamyl peptides.

Ligand activities of pEV, pEI, and pEL were evaluated based on inhibition of binding of ^{3}H-labeled nicotinate to huGPR109A. Data are shown in mean ± SD (n=3). Data are shown based on the % control; {(GPR109A-mock)/mock}×100. * and ** represent significant differences of $p<0.05$ and $p<0.01$, respectively, by Dunnett's test vs control.

Supplemental Figure 1

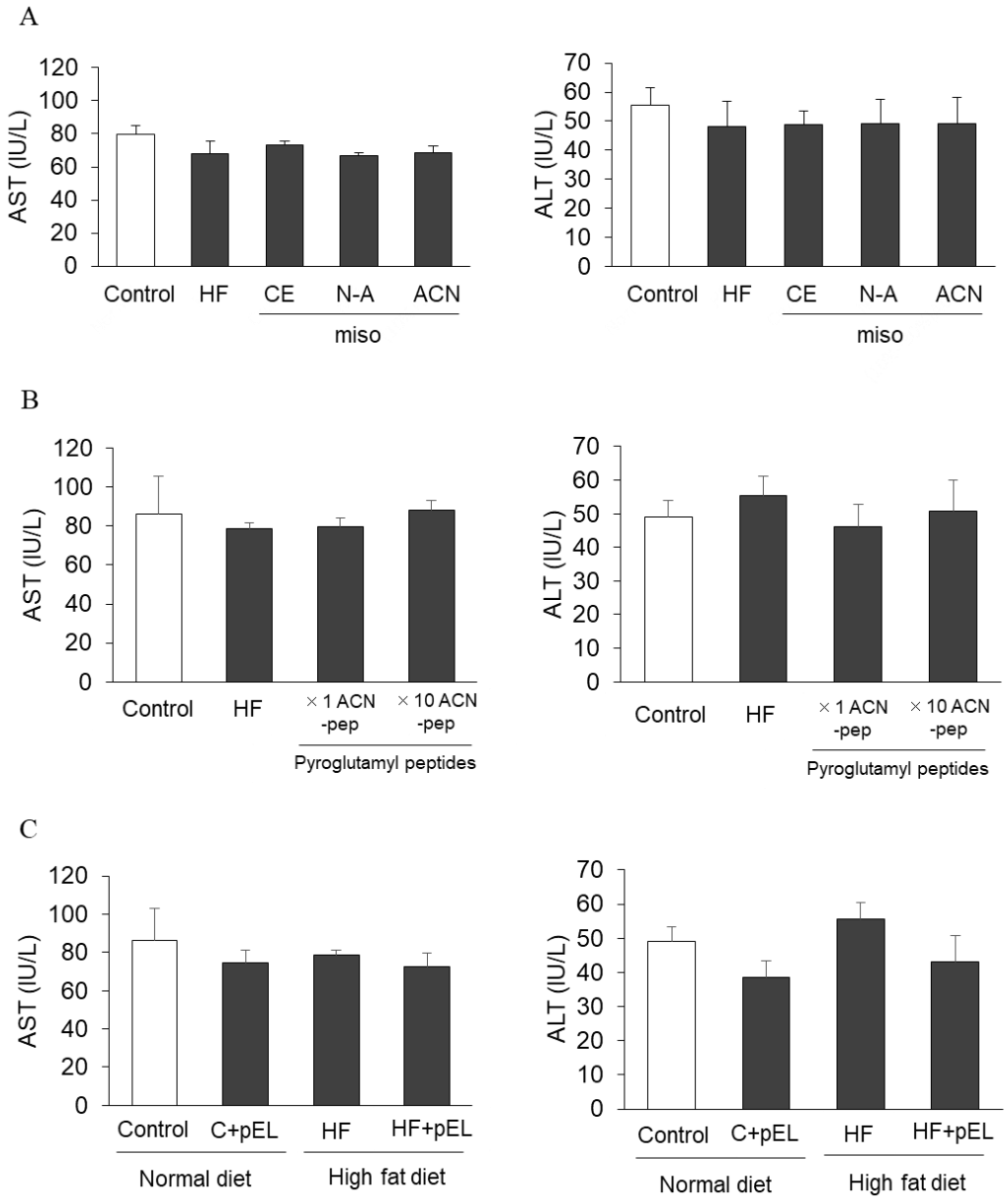

Supplemental Figure 1. The effect of miso extract and pyroglutamyl peptides on plasma AST and ALT level.

Plasma AST level (left graphs) and ALT level (right graphs) in rats administered miso extract (Experiment 1; A), synthetic hydrophobic pyroglutamyl peptides (Experiment 2; B), and pyroglutamyl leuine (pEL) (Experiment 3; C). Data are shown in mean ± SD (n=4). There were no significant differences between all groups.

References for Chapter 1

1. Kumazawa, K., Kaneko, S. & Nishimura, O. Identification and characterization of volatile components causing the characteristic flavor in miso (Japanese fermented soybean paste) and heat-processed miso products. *J. Agric. Food Chem.* **61**, 11968–11973 (2013).
2. Ito, K., Miyata, K., Mohri, M., Origuchi, H. & Yamamoto, H. The effects of the habitual consumption of miso soup on the blood pressure and heart rate of Japanese adults: A cross-sectional study of a health examination. *Intern. Med.* **56**, 23–29 (2017).
3. Ikeda, K. *et al.* Dietary habits associated with reduced insulin resistance: The Nagahama study. *Diabetes Res. Clin. Pract.* **141**, 26–34 (2018).
4. Kondo, H. *et al.* Long-term intake of miso soup decreases nighttime blood pressure in subjects with high-normal blood pressure or stage I hypertension. *Hypertens. Res.* **42**, 1757–1767 (2019).
5. Okouchi, R., Sakanoi, Y. & Tsuduki, T. Miso (fermented soybean paste) suppresses visceral fat accumulation in mice, especially in combination with exercise. *Nutrients* **11**, 560 (2019).
6. Sato, K. *et al.* Occurrence of indigestible pyroglutamyl peptides in an enzymatic hydrolysate of wheat gluten prepared on an industrial scale. *J. Agric. Food Chem.* **46**, 3403–3405 (1998).
7. Sato, K. *et al.* Identification of a hepatoprotective peptide in wheat gluten hydrolysate against D-galactosamine-induced acute hepatitis in rats. *J. Agric. Food Chem.* **61**, 6304–6310 (2013).
8. Ejima, A., Nakamura, M., Suzuki, Y. A. & Sato, K. Identification of food-derived peptides in human blood after ingestion of corn and wheat gluten hydrolysates. *J. Food Bioact.* **2**, 104–111 (2018).
9. Kiyono, T. *et al.* Identification of pyroglutamyl peptides in Japanese rice wine (sake): Presence of hepatoprotective pyroGlu-Leu. *J. Agric. Food Chem.* **61**, 11660–11667 (2013).

10. Sato, K. & Kiyono, T. Modified peptides in foods; Structure and function of pyroglutamyl peptides. *FFI J.* **222**, 216–222 (2017).
11. Wada, S. *et al.* Ingestion of Low dose pyroglutamyl leucine improves dextran sulfate sodium-induced colitis and intestinal microbiota in mice. *J. Agric. Food Chem.* **61**, 8807–8813 (2013).
12. Kiyono, T. *et al.* Identification of pyroglutamyl peptides with anti-colitic activity in Japanese rice wine, sake, by oral administration in a mouse model. *J. Funct. Foods* **27**, 612–621 (2016).
13. Hirai, S. *et al.* Anti-inflammatory effect of pyroglutamyl-leucine on lipopolysaccharide-stimulated RAW 264.7 macrophages. *Life Sci.* **117**, 1–6 (2014).
14. Oishi, M. *et al.* pyroGlu-Leu inhibits the induction of inducible nitric oxide synthase in interleukin-1β-stimulated primary cultured rat hepatocytes. *Nitric Oxide* **44**, 81–87 (2015).
15. Yamamoto, Y. *et al.* Antidepressant-like effect of food-derived pyroglutamyl peptides in mice. *Neuropeptides* **51**, 25–29 (2015).
16. Higaki-Sato, N. *et al.* Occurrence of the free and peptide forms of pyroglutamic acid in plasma from the portal blood of rats that had ingested a wheat gluten hydrolysate containing pyroglutamyl peptides. *J. Agric. Food Chem.* **54**, 6984–6988 (2006).
17. Bidlingmeyer, B. A., Cohen, S. A. & Tarvin, T. L. Rapid analysis of amino acids using pre-column derivatization. *J. Chromatogr. B Biomed. Sci. Appl.* **336**, 93–104 (1984).
18. Elangovan, S. *et al.* The niacin/butyrate receptor GPR109A suppresses mammary tumorigenesis by inhibiting cell survival. *Cancer Res.* **74**, 1166–1178 (2014).
19. Ogura, J. *et al.* Transport mechanisms for the nutritional supplement β-hydroxy-β-methylbutyrate (HMB) in mammalian cells. *Pharm. Res.* **36**, 84 (2019).
20. Thangaraju, M. *et al.* GPR109A is a G-protein-coupled receptor for the bacterial fermentation product butyrate and functions as a tumor suppressor in colon.

Cancer Res. **69**, 2826–2832 (2009).

21. Klok, M. D., Jakobsdottir, S. & Drent, M. L. The role of leptin and ghrelin in the regulation of food intake and body weight in humans: a review. *Obes. Rev.* **8**, 21–34 (2007).
22. Farooqi, I. S. *et al.* Partial leptin deficiency and human adiposity. *Nature* **414**, 34–35 (2001).
23. Licinio, J. *et al.* Phenotypic effects of leptin replacement on morbid obesity, diabetes mellitus, hypogonadism, and behavior in leptin-deficient adults. *Proc. Natl. Acad. Sci.* **101**, 4531–4536 (2004).
24. Nakazato, M. *et al.* A role for ghrelin in the central regulation of feeding. *Nature* **409**, 194–198 (2001).
25. Wren, A. M. *et al.* The novel hypothalamic peptide ghrelin stimulates food intake and growth hormone secretion. *Endocrinology* **141**, 4325–4328 (2000).
26. Singh, N. *et al.* Activation of Gpr109a, receptor for niacin and the commensal metabolite butyrate, suppresses colonic inflammation and carcinogenesis. *Immunity* **40**, 128–139 (2014).
27. Ahmed, K., Tunaru, S. & Offermanns, S. GPR109A, GPR109B and GPR81, a family of hydroxy-carboxylic acid receptors. *Trends Pharmacol. Sci.* **30**, 557–562 (2009).
28. Wanders, D., Graff, E. C. & Judd, R. L. Effects of high fat diet on GPR109A and GPR81 gene expression. *Biochem. Biophys. Res. Commun.* **425**, 278–283 (2012).
29. Cai, T.-Q. *et al.* Role of GPR81 in lactate-mediated reduction of adipose lipolysis. *Biochem. Biophys. Res. Commun.* **377**, 987–991 (2008).
30. Liu, C. *et al.* Lactate inhibits lipolysis in fat cells through activation of an orphan G-protein-coupled receptor, GPR81. *J. Biol. Chem.* **284**, 2811–2822 (2009).
31. Ley, R. E., Turnbaugh, P. J., Klein, S. & Gordon, J. I. Human gut microbes associated with obesity. *Nature* **444**, 1022–1023 (2006).
32. Turnbaugh, P. J. *et al.* An obesity-associated gut microbiome with increased capacity for energy harvest. *Nature* **444**, 1027–1031 (2006).

Chapter 2

Pyroglutamyl leucine, a peptide in fermented foods and food protein hydrolysates, attenuates dysbiosis by increasing host antimicrobial peptide

Introduction

In Chapter 1, it was demonstrated that the administration of hydrophobic pyroglutamyl peptides (pyroGlu-Val, pyroGlu-Ile, and pyroGlu-Leu) suppressed high fat diet-induced body weight gain. To elucidate how hydrophobic pyroglutamyl peptides exert potential anti-obesity effect, the effect on appetite and G Protein-coupled Receptor (GPR) was evaluated in Chapter 1. However, it is unlikely that hydrophobic pyroglutamyl peptides affect appetite-related hormones; leptin and ghrelin and GPRs; GPR109A and GPR81.

On the other hand, the relationship between the disturbance of gut microbiota and obesity and other diseases has been demonstrated.[1,2] In addition, previous reports have demonstrated that the oral administration of very low doses (0.1-1.0 mg/kg body weight) of one of hydrophobic pyroglutamyl peptides; pyroGlu-Leu can normalize the disturbances of colonic microbiota in mice with dextran sulfate sodium (DSS)-induced colitis.[3] The pathological disturbance of gut microbiota is referred to as dysbiosis.[4] It was seen that another related pyroglutamyl peptide, pyroGlu-Asn-Ile, also ameliorated DSS-induced dysbiosis in mice at 1.0 mg/kg body weight.[5] It has been previously reported that certain foods and food components can improve the gut microbiota.[6,7] In many cases, foods containing live microorganisms that have beneficial effects on the host or those with nutrients that are beneficial for the gut microorganisms, referred to as probiotics and prebiotics, respectively, are used for their health benefits as they directly target microorganisms found in the gut. An effective dose of pro- and prebiotics is around 100 mg–1.0 g/kg body weight.[6,7] Alternatively, the oral administration of lactoferrin, which produces naturally-occurring antimicrobial peptides, such as lactoferricin, by peptic digestion, has been demonstrated to modulate the gut microbiota.[8] However, previous study has demonstrated that pyroGlu-Leu attenuates DSS-induced dysbiosis at a dose of

0.1 mg/kg body weight without increasing the level of pyroGlu-Leu in the colon. Therefore, it is unlikely that pyroGlu-Leu, at such small doses, can directly enhance and suppress the growth of microorganisms in the colon.

On the other hand, the epithelial surfaces of tissues from organs such as the intestine, skin, and respiratory and reproductive tracts, secrete antimicrobial peptides.[9] These antimicrobial peptides exert their bactericidal activity mainly by damaging the cell wall of the bacteria.[9] Peptides such as α-defensins, rattusin (α-defensin-related peptide), lysozyme, REG3, and cathelicidins are secreted into the lumen from the intestine to suppress the growth of bacteria in the small intestine.[9] Guo *et al.* have shown that the expression of intestinal antimicrobial peptides in mice with high fat diet-induced colonic dysbiosis is lower than that in normal mice.[10] Furthermore, it has been shown that the secretion of α-defensin 5 in the small intestine is relatively suppressed in obese human subjects with dysbiosis compared to normal subjects.[11] Based on these findings, it is speculated that intestinal antimicrobial peptides might control colonic microbiota; hence, a decrease in the intestinal antimicrobial peptides can induce dysbiosis. Indeed, the oral administration of mouse α-defensin (cryptdin-4) improves graft-versus-host disease-mediated dysbiosis.[12] Therefore, food components capable of enhancing the production of host antimicrobial peptides in the intestine can also improve colonic microbiota.

These data suggest that the administration of low doses of pyroGlu-Leu may attenuate dysbiosis by enhancing the production of host antimicrobial peptides. In Chapter 2, the relationship between dysbiosis and one of hydrophobic pyroglutamyl peptides; pyroGlu-Leu was evaluated, focusing on host antimicrobial peptides. The objective was to elucidate the effects of pyroGlu-Leu on the production of intestinal antimicrobial peptides in rats with high fat diet-induced dysbiosis.

Methods

Reagents

Acetonitrile (HPLC grade) was purchased from Nacalai Tesque. PyBOP, HOBt,

Boc-Pyr-OH), H-Leu-OtBu・HCl, *N*-α-(9-Fluorenylmethoxycarbonyl)-*N*-ω-(2,2,4,6,7-pentamethyldihydrobenzofuran-5-sulfonyl)-L-arginine *p*-methoxybenzyl alcohol resin (Fmoc-Arg(Pbf)-Alko Resin), Fmoc-L-Leu-OH, Fmoc-L-Val-OH, Fmoc-O-(*t*-butyl)-L-serine (Fmoc-Ser(*t*Bu)-OH), Fmoc-L-Ile-OH, and Fmoc-L-Trp-OH were purchased from Watanabe Chemical Industries. Fmoc-*N*-ω-(*t*-butyloxycarbonyl)-L-lysine (Fmoc-Lsy(Boc)-Resin), Fmoc-L-Pro-OH, and Fmoc-L-glutamic acid γ-*t*-butyl ester (Fmoc-Glu(OtBu)-OH) were purchased from HiPep Laboratories (Kyoto, Japan).

Peptides synthesis

PyroGlu-Leu (pEL) was synthesized in liquid phase through Boc strategy as described previously.[13] Tryptic digested peptides potentially released from the active form of rattusin (Leu-Arg, Val-Arg, and Leu-Ser-Arg) and defensin alpha 9 (Leu-Glu-Ile-Arg and Trp-Pro-Trp-Lys), except for the cysteine-containing peptides, were synthesized by the Fmoc strategy using an automatic peptide synthesizer (PSSM-8, Shimadzu). The synthesized peptides were purified by RP-HPLC using a Cosmosil MS-II (10 mm i.d. × 250 mm; Nacalai Tesque) as described in Chapter 1.

Animal experiments

Five-week-old male Wistar/ST rats (120–140 g) were purchased from Japan SLC. A total of 12 rats were caged individually in a room, and housed at 22–24°C and 40–70% relative humidity, with a 12 h light/dark cycle. The rats were allowed free access to a control diet (solid type of certified diet MF; Oriental Yeast) and drinking water for an acclimatization period of one week. All the animals were treated and cared for in accordance with the guidelines of the National Institutes of Health (NIH) for the use of experimental animals. All experimental procedures were approved by the Animal Care Committee of Kyoto Prefectural University (KPU280609). After the acclimatization period, the rats were divided into four groups (n=3 for each group); control diet (C), control diet + pyroGlu-Leu (C+pEL), high fat diet (HF), and high fat diet + pyroGlu-Leu (HF+pEL). Rats in all groups received experimental diets for five weeks. The rats in the

HF and HF+pEL groups were fed a solid type of high fat diet (60% kcal/total kcal; D12492, Research Diets). The rats were allowed free access to either the control or high fat diet as well as drinking water. PyroGlu-Leu was orally administered via drinking water. Drinking water containing pyroGlu-Leu (3.6–8.3 mg/L) was prepared every week to administer pyroGlu-Leu at 1.0 mg/kg body weight on the basis of consumption of drinking water in the previous week. The feces were collected from each rat on the final day and stored at –80°C until the microbiota analysis. The rats were sacrificed after five weeks from beginning of the experiment by puncturing the inferior vena cava of the rats that were anesthetized using pentobarbital sodium (40–50 mg/kg). The small intestines were dissected. The inner content of intestines were flushed with 15 mL of physiological saline. The washed intestines (duodenum, ileum, and colon) and the inner contents of small intestines were collected and stored at –80°C until use.

Microbiota analysis

The copies of two major phyla of rat microbiota, *Firmicutes* and *Bacteroidetes*, were evaluated by qPCR, as described previously.[3] Briefly, DNA was extracted from 0.5 g of each feces using a QIAmp DNA StoolMini Kit (Qiagen, Venlo, Netherlands), according to the manufacturer's instructions. qPCR analysis was outsourced to the Primary Cell Division of Cosmo Bio (Sapporo, Japan).

Peptides extraction from the intestines

The duodenum, ileum, and colon were cut into small pieces using scissors. The pieces (100 mg) were homogenized with 100 μL of PBS in a BioMasher II (Nippi, Tokyo, Japan). The homogenates were further mixed with 200 μL of 60% acetic acid and homogenized again. These homogenates were centrifuged at 13,000 × g for 10 min and the supernatants were collected. This solvent (30% acetic acid) has been used to preferentially extract animal antimicrobial peptides.[14]

Size exclusion chromatography (SEC)

The 30% acetic acid extracts of ileums were purified by passing through Ultrafree-MC (pore size 5 µm; Merck) packed with Sephadex G-25 (fine grade; GE Healthcare). Samples were eluted by spinning the column at 815 × g for 1 min. The clarified samples (200 µL) were subjected to SEC using a Superdex peptide 10/300 (GE Healthcare) equilibrated with 0.1% formic acid containing 10% acetonitrile at a flow rate of 0.5 mL/min. Fractions were collected every 1 min.

Liquid chromatography mass spectrometry (LC-MS)

The aliquots of SEC fractions 14-35 of ileums were clarified by passing through a filter W (pore size 0.45 µm, 4 mm i.d.; Nacalai Tesque). The peptides in the SEC fractions (10 µL) were resolved by RP-HPLC using a Cosmosil Protein-R (5 µm, 2.0 mm i.d. × 150 mm; Nacalai Tesque). The column was equilibrated with 0.1% formic acid (solvent A). The elution was performed using a binary linear gradient of solvent A and 0.1% formic acid containing 80% acetonitrile (solvent B) at a flow rate of 0.2 mL/min. The gradient program was as follows: 0-10 min; B 0-50%, 10-10.1 min; B 50-100%, 10.1-20 min; B 100%, 20-20.1 min; B 100-0%, 20.1-30 min; B 0%. The column was maintained at 40°C. The peptides were detected by ESI-MS using LCMS 8040 (Shimadzu) in total ion monitoring mode at positive ion mode. The molecular weights of the peptides in peaks were estimated on the basis of the *m/z* ratio of the multivalent ions. The *m/z* ratio of the adjacent multivalent ions were designated to X_n and X_{n-1}, where n is the charge number. Assuming that all ions were generated by coupling with protons, the following simultaneous equations were formularized: $X_n=(Y+n)/n$ and $X_{n-1}=(Y+n-1)/(n-1)$, where Y is the molecular weight of the target peptide. The total ion chromatogram of SEC fraction 32 of the HF+pEL group is shown in Figure 2-1 panel A (upper). The MS spectrum of the peak is denoted by an arrow in Figure 2-1 panel A (lower). Multivalent ions, with an *m/z* of 621.4, 710.0, 828.1, and 993.5, were observed. All two adjacent ions were used for the estimation of molecular weights using the aforementioned equation. Consequently, the molecular weight was estimated to be 4962 Da, where the charges for

the ions were 8, 7, 6, and 5, respectively. The peptides whose molecular weight could be estimated were detected by LC-MS in SIM mode for the highest 2 or 3 multivalent ions. For example, 3 ions (*m/z*=710.0, 828.1, and 993.5) were selected for the peak marked with an arrow (Figure 2-1 panel A). The 30% acetic acid extracts were diluted with 100 times its volume of 0.1% formic acid containing 10% acetonitrile, and the diluents were then directly subjected to LC-MS analysis. The total ion chromatogram of SIM targeting *m/z*=710, 828.1, and 993.5 is shown in Figure 2-1 panel B (upper). If all the ions used for SIM were observed as shown in Figure 2-1 panel B (lower), the peak area was recorded. In some cases, the molecular weights of the peptide was also evaluated by MALDI-TOFMS using an AXIMA Performance (Shimadzu). Sinapinic acid (10 mg/mL) was used as the matrix. Insulin and apomyoglobin were used for calibration. Peptides were purified by RP-HPLC using Protein-R by the same condition as described above. Aliquots of the peptide solution (5-20 ng/0.5 μL) and the matrix (0.5 μL) were added to the sample plate. The mass range was set from *m/z* 1000 to 20000, the pulsed extraction was optimized at 7000 Da, the ion gate was set at 1000 Da, and the laser application power was started from 80.

Peptide sequence

The amino acid sequences of the purified peptides were estimated by Edman degradation using a PPSQ-21 (Shimadzu). The amino acid sequences were assigned to protein using Basic Local Alignment Search Tool (BLAST).

Detection of tryptic peptides of rattusin and defensin alpha 9

The presence of active form of rattusin and defensin alpha 9 in the inner contents of the small intestines was determined by detecting the tryptic peptides that are potentially derived from them. The suspension of the inner contents in PBS was centrifuged at 12,000 × g for 10 min. The peptide concentration in the supernatant was evaluated by determining the absorbance at 280 nm using a Nanodrop Lite (Thermo Fisher Scientific). The concentration was adjusted to 1 mg/mL. The sample solution (48 μL) was mixed with 2

μL of 500 mM DTT and kept at 60°C for 1 h. Thereafter, 4 μL of 500 mM 2-iodoacetamide (IAA) was added the solution and allowed to stand for 30 min in the dark. To terminate the alkylation process, 1 μL of 500 mM DTT was added. The alkylated peptides were digested with 1 μg of trypsin (1 μL) (MS grade, Thermo Fisher Scientific) at 37°C for 24 h. The reaction was terminated by cooling at -30°C. The contents of LR, VR, LSR, LEIR, and WPWK in the tryptic digests of the inner contents were evaluated by LC-MS/MS in MRM mode. The MRM conditions were optimized using synthetic peptides, which were pretreated with DTT and IAA, by LabSolutions Version 5.65. The tryptic digests were clarified by passing them through a filter, as described above, and then aliquots (10 μL) were injected into an Inertsil ODS-3 (5 μm, 2.1 mm i.d. × 150 mm; GL Sciences) equilibrated with 0.1% formic acid (solvent A). An elution was performed using a binary linear gradient of solvent A and 0.1% formic acid containing 80% acetonitrile (solvent B) at a flow rate of 0.2 mL/min. The gradient program was as follows; 0-15 min; B 0-50%, 15-20 min; B 50-100%, 20-25 min; B 100%, 25-25.1 min; B 100-0%, 25.1-35 min; B 0%. The column was maintained at 40°C.

Statistical analysis

All analyses were performed for every rat (n=3). The results were presented as the mean ± standard deviations (SD). For microbiota analysis and comparison of the effect of pyroGlu-Leu on rattusin propeptide between duodenum, ileum, and colon, the significant differences between the groups were evaluated by Tukey's test. For other analyses, the significant differences between each diet (C vs C+pEL or HF vs HF+pEL) were evaluated by Student's *t*-test. Differences of $p<0.05$ were considered significant. Statistical analysis was performed using GraphPad Prism version 6.04 (GraphPad Software).

Results

Effect of pyroGlu-Leu on high fat diet-induced dysbiosis

As shown in Figure 2-2, rats on a high fat diet (HF) without pyroGlu-Leu administration displayed increased *Firmicutes/Bacteroidetes* ratio in their feces compared to the rats in the control diet groups (C and C+pEL; p=0.003 by Tukey's test, n=3), which indicates that dysbiosis was induced by a high fat diet. The administration of pyroGlu-Leu (1.0 mg/kg body weight) significantly attenuated high fat diet-induced dysbiosis (HF+pEL; p=0.035 by Tukey's test, n=3). The administration of pyroGlu-Leu did not affect the *Firmicutes/Bacteroidetes* ratio in the control diet groups (C and C+pEL; p>0.99 by Tukey's test, n=3).

Comprehensive analysis of peptides in 30% acetic acid extracts

The peptides extracted using 30% acetic acid from the ileums of rats (n=3) from 4 experimental groups (C, C+pEL, HF, and HF+pEL) were fractionated using size exclusion chromatography (SEC). The peptides in the SEC fractions were resolved by reversed phase-HPLC (RP-HPLC). The elution of peptides by RP-HPLC was monitored by electron spray ionization mass spectrometry (ESI-MS) in total ion monitoring (TIM) mode. Sixty-nine peaks were observed in the total ion chromatograms of RP-HPLC of the SEC fractions from the rats (n=3) in each group (Supplemental Figure 2-1 A-D). Table 2-1 summarizes the retention time and observed *m/z*. The first peak (peak 1) appeared in SEC fractions 14-26 and 30-35, respectively. The peptides in the former and latter SEC fractions showed the same retention time and mass spectrum pattern in RP-HPLC-MS, which suggests that the peptide in peak 1 in the former SEC fraction forms an oligomer via non-covalent bonding. Based on the *m/z* of the multivalent ions, the molecular weights of 57 peptides were estimated (Table 2-1).

The peptides in the 30% acetic acid extracts were directly detected using RP-HPLC-MS in selected ion monitoring (SIM) mode, as described in the Methods section. Forty-four peptides were detected. The level of 9 peptides were significantly changed after pyroGlu-Leu administration, as shown in Figure 2-3 (p<0.05 by t-test, n=3). Other

peptides, which did not significantly change after pyroGlu-Leu administration, were shown in Supplemental Figure 2-2. Among the control diet groups, the peptides in peaks 11 (estimated molecular weight; 13289 Da), 16 (2086 Da), 29 (18330 Da), 36 (14013 Da), 41 (2791 Da), and 58 (697 Da) significantly increased after the administration of pyroGlu-Leu (p=0.02, 0.01, 0.04, 0.01, 0.01 and 0.02, respectively by t-test, n=3). Among the high fat diet groups, the peptides in peaks 20 (4962 Da), 30 (9872 Da), and 39 (2590 Da) significantly increased after the administration of pyroGlu-Leu (p=0.01, 0.04 and 0.03, respectively by t-test, n=3). Among these three peptides, the peptide in peak 20 (4962 Da) showed the highest ion intensity. Further, the exact same molecular weight for the peptide in peak 20 was identified using matrix assisted laser desorption/ionization time of flight mass spectrometry (MALDI-TOFMS) analysis (Figure 2-4). This peptide was purified by RP-HPLC and subjected to amino acid sequence analysis. The resulting sequence (DPIEEAEEETKTE) correlated with the amino terminal region of the precursor form of the rat α-defensin-related peptide (rattusin) or defensin alpha 9 ($_{20}$DPIQEAEEETKTE$_{32}$), which are generated after the cleavage of the signaling peptide. These two antimicrobial peptides share the same propeptide amino terminal sequence, while the active regions differ in sequence. On the basis of the molecular weight, this peptide was identified as a propeptide of rattusin or defensin alpha 9 that is released after the conversion of its inactive precursor into the active form.

Detection of peptides derived from the active form of rattusin and defensin alpha 9

To detect the secretion of the active form of these antimicrobial peptides from the lumen, peptides from the inner contents of the small intestine were subjected to SEC and RP-HPLC-MS, as described in the Methods section. RP-HPLC-MS showed large broad peaks and mass spectra analysis revealed the presence of numerous compounds in these peaks. Therefore, it was difficult to identify the peptides in such complicated matrix based on sequence analysis. Alternatively, the peptides that were potentially released from the active form of rattusin and defensin alpha 9 via trypsin digestion were detected by LC-MS/MS in the MRM mode. The levels of rattusin-related peptides, LR, VR, and LSR,

were found to be higher after pyroGlu-Leu administration in the high fat diet groups (Figure 2-5, panel A and B), while this was not the case with the defensin alpha 9-related peptides, LEIR and WPWK, both in the control and high fat diet groups (Figure 2-5, panel A and C).

Discussion

Although antimicrobial peptides are usually detected by ELISA assay using specific antibodies, many types of antimicrobial peptides are present in the ileum. In addition, most of these antimicrobial peptides are synthesized in the precursor form and converted into their active form by the proteolytic removal of propeptides. To observe all the changes in the antimicrobial peptides in tissues, several kinds of ELISA systems are necessary. Antimicrobial peptides in the intestine can be extracted using a high concentration of acetic acid (final concentration of 30%).[14] In the present study, a comprehensive analysis of peptides in 30% acetic acid extracts from the ileum was carried out. Using SEC and RP-HPLC in series along with ESI-MS analyses, 57 peptides with different molecular weights were detected. The administration of pyroGlu-Leu was found to significantly enhance the levels of the propeptide of rattusin or defensin alpha 9 in the rats fed with a high fat diet, suggesting that the oral administration of pyroGlu-Leu increases the production of the active form of rattusin or defensin alpha 9. However, any increases in these peptides in their active forms either directly in the ileum extracts or the lumen were not observed using the same method. The active forms of antimicrobial peptides, such as α-defensins, exert their antimicrobial activity by perforating the cell walls of bacteria and can also potentially damage the host cells.[9] To achieve this, these active peptides should be immediately excreted into the lumen in order to target the bacteria without damaging the host cells. Indeed, tryptic fragment peptides of rattusin were found in the lumen. In addition, no significant decreases in the other peptides in the 30% acetic acid extract, which includes most of the antimicrobial peptides, were observed to compensate for the increase of rattusin. These findings indicate that the oral

administration of pyroGlu-Leu increases the secretion of the active form of rattusin into the lumen, which consequently suppresses excess proliferation of *Firmicute*s (Gram-positive bacteria) due to high fat diet as *Firmicutes* are more susceptible to certain antimicrobial peptides.[9]

Although the propeptide of rattusin, whose molecular weight is 4962 Da, could be detected in the 30% acetic acid extract from the ileum by direct injection to LC-MS in SIM mode, it was difficult to detect the active form of rattusin. Therefore, the propeptide of rattusin (4962 Da) can be used to monitor the activation of rattusin in rats to screen for food components that can enhance the production of rattusin.

The mechanism underlying the enhancement of rattusin activation by pyroGlu-Leu remains to be elucidated. Intestinal α-defensins are known to be produced by the Paneth cells in the ileum.[15] It has also been suggested that rattusin, which belongs to a defensin subfamily, is produced by Paneth cells.[16] The level of rattusin propeptide in the ileum was found to be higher than that in duodenum and colon (Supplemental Figure 2-3). Therefore, pyroGlu-Leu may interact directly with the Paneth cells in the ileum to produce rattusin. However, there is a possibility that pyroGlu-Leu interacts with other cells as well, such as macrophages and neutrophils, to enhance or suppress certain active substances that affect Paneth cells. To solve this problem, target tissue of hydrophobic pyroglutamyl peptides including pyroGlu-Leu was evaluated in Chapter 3.

However, there is no study demonstrating the enhancement of the production of host antimicrobial peptides by the oral administration of a single food component. It has been shown that pyroGlu-Leu is widely distributed in food protein hydrolysates, such as wheat gluten and corn gluten hydrolysates,[13,17,18] as well as in Japanese fermented foods produced by *Asperigillus oryzae*, such as miso, shoyu, and sake, relatively at high concentration.[19,20] Therefore, significant amounts of pyroGlu-Leu can be obtained by the consumption of Japanese diet resulting in the improvement of the gut microbiota due to the increased production of host antimicrobial peptides. Previous studies have suggested that the consumption of Japanese fermented foods may improve gastrointestinal conditions.[21] The fiber and live microorganisms found in these fermented foods are

thought to be responsible for their beneficial effect on the gut. In conclusion, the present study proposes the concept that peptides produced during fermentation can improve the gut conditions by enhancing the host antimicrobial peptides. Attenuation of dysbiosis by increasing host antimicrobial peptide might be one of the mechanisms of suppression of high fat diet-induced body weight gain, as demonstrated in Chapter 1. This initial findings are need to be further validated by epidemiological studies and then confirmed by well-designed human clinical trials.

Table and Figures

Table 2-1. Summary of the peaks obtained by the LC-MS of the SEC fractions

Peak No.	SEC Fr.	RT	observed *m/z*	estimated molecular weight	SIM
1	14-20, 32-34 (C), 14-21, 32-33 (CP), 14-26, 31-34 (HF), 14-26, 30-35 (HP)	11.2	723.7, 761.8, 804.0, 851.2, 904.4, 964.6, 1033.4, 1112.9, 1205.4, 1315.0, 1446.4, 1607.0	14453	○
2	17-18 (C)	11.8	775.7, 816.6, 861.8, 912.5, 969.4, 1034.0, 1107.7, 1192.9, 1292.2	15493	○
3	17-18 (C), 15-19, 27-29 (HF), 14-19, 26-29 (HP)	11.7	796.2, 843.0, 895.6, 955.2, 1023.4, 1102.1, 1193.8, 1302.3, 1432.3, 1591.5	14312	○
4	22-27 (C), 21-25 (CP), 21-24 (HF), 21-24 (HP)	10.5	879.9, 932.6, 989.7, 1055.6, 1131.0, 1217.7, 1319.2	15825	○
5	14-16 (CP)	14.6	532.4, 576.4, 620.5	—	—
6	20, 23 (CP)	12.8	787.2, 847.5, 885.5, 917.8, 972.0	—	—
7	14-19 (HF), 14-20 (HP)	12.3	752.7, 792.2, 836.2, 885.3, 940.7, 1003.2, 1074.8, 1157.4, 1253.9, 1367.6, 1504.5, 1671.5	15033	○
8	30-32 (C), 29-31 (CP), 29-32 (HF), 29-31 (HP)	10.7	739.9, 778.5, 821.9, 870.2, 924.5, 986.1, 1056.5, 1137.7	14779	○
9	30-33 (C), 29-31 (CP), 29-31 (HF), 29-31 (HP)	11.4	721.8, 773.3, 832.6, 902.0, 983.9	10812	○
10	30-31 (C), 29-31 (CP), 28-31 (HF), 28-30 (HP)	11.1	814.5, 862.3, 916.1, 977.1, 1046.9	14644	○
11	31 (C)	11.3	782.4, 831.2, 886.5, 949.8, 1022.7	13289	○
12	33-35 (C), 34-35 (CP), 33-35 (HF), 33-35 (HP)	10.9	765.5, 829.1, 904.4, 994.7, 1105.2, 1243.1	9941	○
13	31 (C), 25-27 (CP), 26 (HF)	12.5	846.1, 890.2, 937.1, 989.0	17535	○
14	31-32 (C), 30-32 (CP), 30-32 (HF), 29-32 (HP)	12.2	807.5, 846.0, 888.1, 934.8, 986.7, 1044.6	17748	○
15	26-27 (C), 25-27 (CP), 25-27 (HF), 25-26 (HP)	9.2	973.7, 1459.8	2919	○
16	29-30 (C), 29-30 (CP), 28 (HF), 29-30 (HP)	7.8	696.9, 1045.1	2086	○
17	29-30 (C), 29-30 (CP), 29-30 (HF), 28-30 (HP)	8.7	749.3, 998.9	2991	○
18	28-30 (C), 28 (HF)	9.5	564.3, 868.1, 1166.8	—	—
19	30-33 (C), 29-33 (CP), 29-33 (HF), 28-33 (HP)	12.4	724.6, 760.8, 800.8, 845.3, 894.9, 950.8	15191	○
20	31-33 (C), 31-33 (CP), 31-33 (HF), 30-33 (HP)	8.3	621.3, 710.0, 828.1, 993.5	4962	○
21	31 (C), 29-31 (CP), 30-31 (HF)	7.5	555.1, 739.6	2218	○
22	31 (C), 31 (CP), 31 (HF)	7.2	537.0, 715.5, 1032.6	2234	○
23	31 (C)	8.5	536.9, 716.0	2139	N.D.
24	31-34 (C), 31-34 (CP), 30-34 (HF), 30-34 (HP)	13.3	754.9, 792.6, 834.3, 880.6, 932.4	15823	○
25	32-34 (C), 32-33 (CP), 32-33 (HF), 32-33 (HP)	12.0	726.0, 766.3, 811.3, 861.9	13777	○
26	32-33 (C), 32 (CP), 32 (HF), 31-32 (HP)	8.0	712.3, 830.8, 996.9	4978	○
27	33-34 (C), 33-34 (CP), 33 (HF), 33 (HP)	10.1	717.5, 789.2, 876.8, 986.3	7878	○
28	33-34 (C), 33-34 (CP), 33-34 (HF), 32-33 (HP)	6.1	771.4, 841.8, 925.7, 1028.7, 1156.9	9239	○
29	33-34 (C), 32-33 (CP)	10.1	706.3, 734.5, 765.2, 798.4, 834.7, 874.3, 918.0	18330	○
30	33 (C), 33 (CP), 33 (HF), 33 (HP)	8.5	706.1, 759.9, 823.6	9872	○
31	34 (C)	13.4	895.3, 995.2, 1119.6, 1279.3	8931	○
32	34-35 (C), 35 (HF)	8.7	577.8, 720.6, 957.0, 1063.1, 1196.1	—	—
33	34-35 (C), 34-35 (CP), 33-35 (HF), 34-35 (HP)	7.4	566.9, 708.4, 944.0	2830	○
34	34 (C)	9.2	636.0, 684.2, 739.0, 769.7, 839.4, 923.4	—	—
35	34-35 (C), 34-35 (CP)	9.5	712.1, 745.8, 783.2, 824.3, 870.0	15653	N.D.
36	34-35 (C), 34-35 (CP), 34-35 (HF), 34 (HP)	12.2	701.3, 738.2, 779.1, 824.8	14013	○
37	35 (C)	9.8	736.1, 809.6, 899.4, 1011.6, 1156.0	8087	N.D.
38	25-26 (CP), 24-26 (HF), 25-27 (HP)	8.6	1019.1, 1273.4	5094	○
39	27 (CP)	8.9	674.9, 911.8	2590	○
40	28 (CP)	8.3	654.3, 980.9	1960	○
41	30-31 (CP), 30 (HF)	8.4	699.3, 932.3	2791	○
42	30 (CP)	10.1	644.3, 664.3, 685.7, 708.6, 732.9, 759.1	21240	N.D.
43	31 (CP), 31 (HF), 31 (HP)	6.8	695.6, 834.5	4168	○
44	31 (CP), 30 (HP)	10.4	942.1, 1046.7, 1177.4, 1345.5, 1569.1	9414	N.D.
45	32 (CP), 32 (HP)	9.0	681.8, 749.7, 833.0, 936.9, 1070.4, 1248.7	7491	○
46	33 (CP), 28 (HP)	9.5	672.6, 691.9, 712.2, 733.8, 756.7	24138	N.D.
47	32 (CP)	10.3	828.5, 887.5, 935.2, 1168.9, 1335.9, 1580.0	—	—
48	33 (CP)	10.9	726.0, 760.7, 798.7, 840.6	15934	N.D.
49	34 (CP)	7.6	607.6, 708.8, 850.5, 1062.9	4244	○
50	34 (CP)	8.8	664.6, 691.4, 720.1, 751.4, 785.5, 822.8, 864.0	17232	N.D.
51	34 (CP)	7.7	626.4, 730.7, 876.8, 1095.4	4377	N.D.
52	34 (CP)	11.1	761.8, 821.4, 851.3, 904.4, 964.6, 1058.6, 1164.3, 1293.7	—	—
53	35 (CP), 35 (HF)	7.9	617.0, 649.7, 685.7, 725.8, 771.2, 822.4, 881.2	12314	N.D.
54	34-35 (CP), 35 (HF), 34-35 (HP)	13.5	841.9, 912.1, 994.9, 1094.2, 1215.7	10930	○
55	35 (CP), 35 (HF), 35 (HP)	12.9	889.2, 957.6, 1037.3, 1131.7, 1244.6, 1382.7	12433	○
56	28 (HF), 28 (HP)	9.2	520.3	520	○
57	29 (HF)	7.5	672.9, 779.5	4906	○
58	29-30 (HF)	7.8	697.0	697	○
59	29 (HF)	7.0	819.7, 983.8	4903	○
60	35 (HF)	8.1	524.9, 655.9, 1454.1, 1595.4, 1963.1	—	—
61	35 (HF), 35 (HP)	12.3	703.2, 739.4, 781.3, 827.1, 878.9, 937.4, 1003.3, 1157.3, 1671.6	—	—
62	29 (HP)	8.8	504.3, 1276.1	—	—
63	28 (HP)	14.5	532.4, 576.3, 620.4, 664.5, 708.4, 1425.5, 1613.9, 1828.1	—	—
64	29 (HP)	8.8	504.3, 648.9	2255	○
65	32 (HP)	10.6	765.0, 834.5, 917.9, 1019.7, 1147.1, 1310.8	9167	N.D.
66	33-34 (HP)	8.7	761.8, 888.5	5329	N.D.
67	34 (HP)	9.8	904.4, 1033.7, 1205.6	7225	N.D.
68	35 (HP)	6.4	549.7, 584.0, 603.0, 667.3, 718.8, 778.7, 849.2	—	—
69	35 (HP)	8.1	599.0, 718.4, 897.9	3588	○

The aliquots of the size exclusion chromatography fractions (SEC Fr.) were subjected to LC-MS. RT=retention time of LC-MS. The molecular weights were calculated using the observed multivalent ions. "—" represents Molecular weight could not be calculated. "○" represents Peak was observed by selected ion monitoring (SIM) for the top 2 or 3 divalent ions. "N.D." represents Peak could not be detected by SIM analysis.

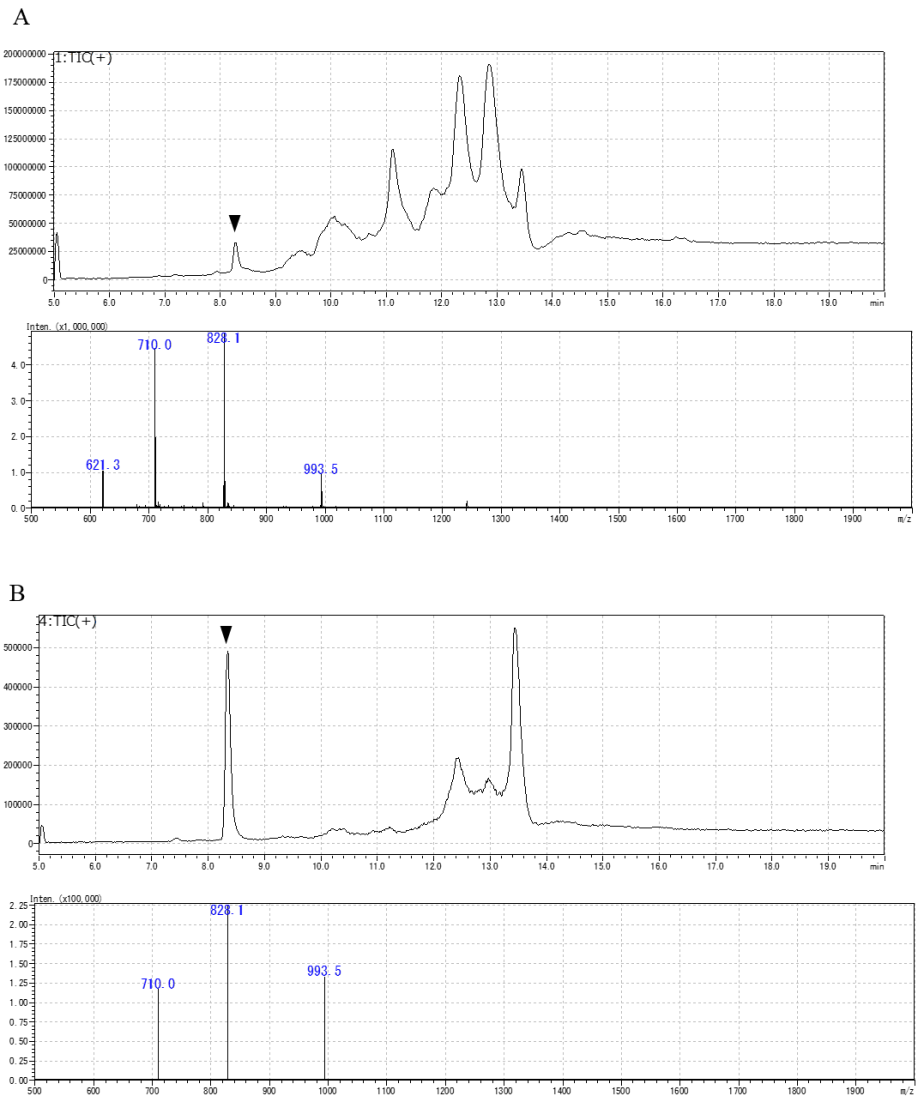

Figure 2-1. Mass chromatograms of RP-HPLC-MS of SEC Fr. 32 of HF+pEL group and mass spectra of the peak marked with arrowhead.

Total ion monitoring mode (A) and selected (m/z=710.0, 828.1, 993.5) ion monitoring mode (B), respectively. The peptides whose molecular weight could be estimated were detected by LC-MS in SIM mode for the highest 2 or 3 multivalent ions. The Y axis represents ion intensity

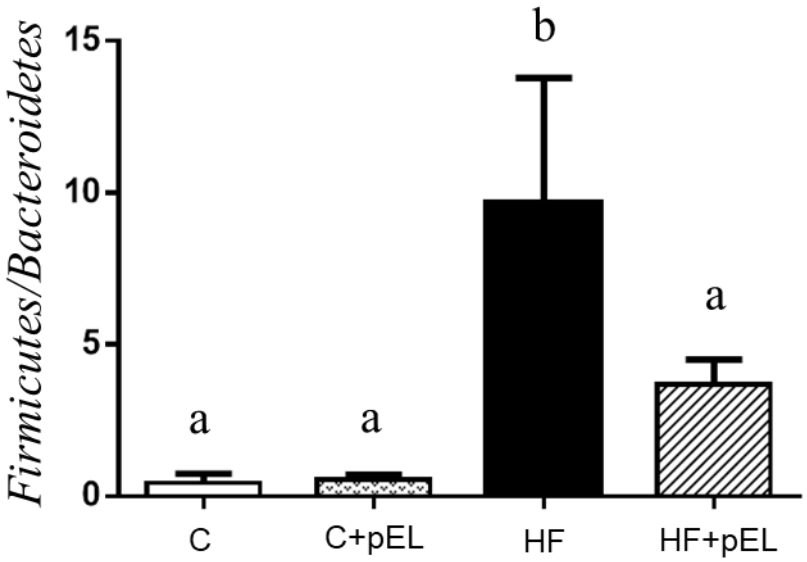

Figure 2-2. Effect of administration of pyroGlu-Leu (pEL) on the ratio of *Firmicutes* to *Bacteroidetes* in the feces.

Control group (C), control+ pEL group (C+pEL), high fat diet group (HF), high fat diet+pEL group (HF+pEL), respectively. The Y axis represents the ratio of *Firmicutes*/*Bacteroidetes*. Different letters indicate significant differences ($p<0.05$) by Tukey's test ($n=3$). The results are presented as the mean ± SD.

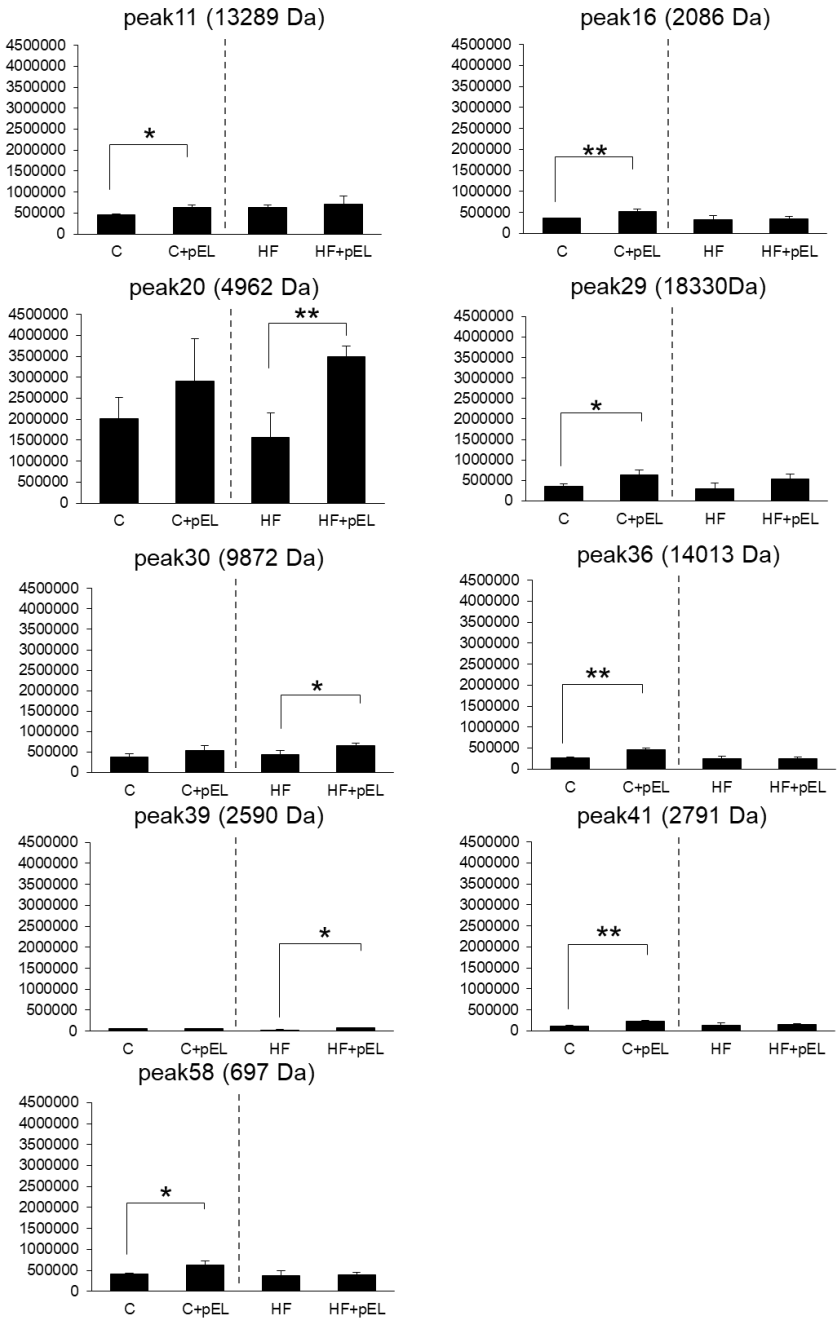

Figure 2- 3. Effect of pyroGlu-Leu on the peak area of the peptides in the 30% acetic acid extract of ileum.

Refer the figure legend of Figure 2-1 for affiliation of animal groups. The Y axis represents peak area of LC-MS. * and ** represent $p<0.05$ and $p<0.01$, respectively, compared with the vehicle (C vs. C+pEL, HF vs. HF+pEL, respectively) by Student's *t*-test (n=3). The results are presented as the mean ± SD.

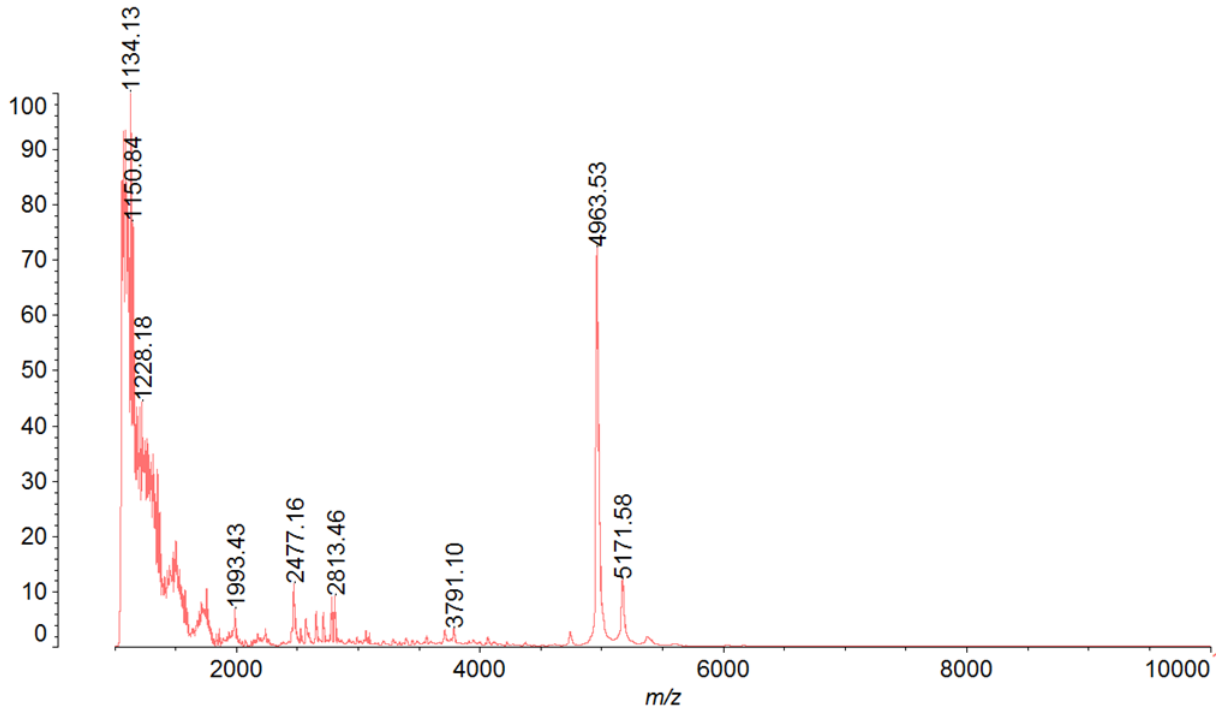

Figure 2- 4. Confirmation of m/z of peptides in peak 20 using MALDI-TOFMS.

The molecular weight of the peptide in peak 20 was evaluated by MALDI-TOFMS. As estimated on the basis of multivalent ions of MS spectrum by LC-MS, *m/z*=4963.53 was also observed by using MALDI-TOFMS.

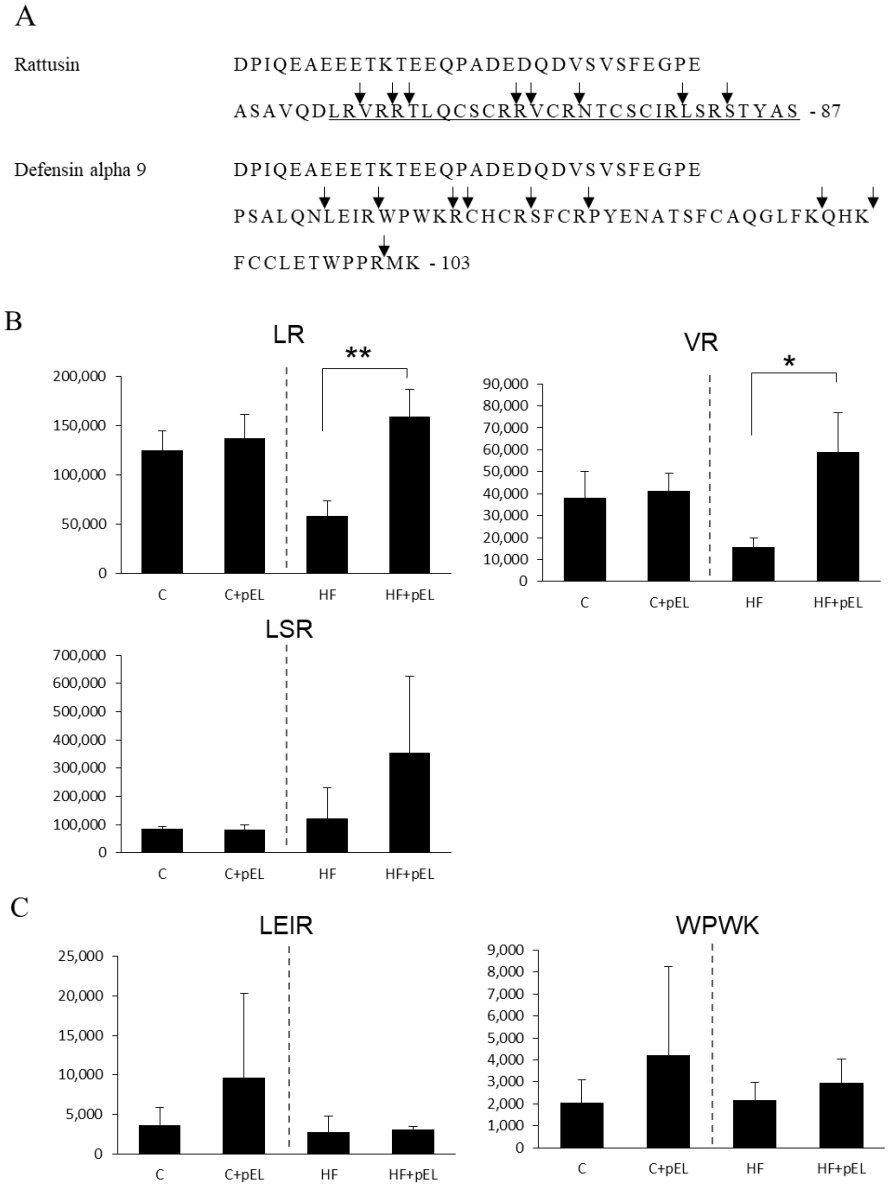

Figure 2-5. Detection of tryptic peptides from the active form of rattusin and defensin alpha 9.

Refer the figure legend of Figure 2-1 for affiliation of animal groups. The amino acid sequence of rattusin and defensin alpha 9 precursors, respectively. The sequence of known active form is underlined. Arrows indicate the trypsin cleavage sites (A). Comparison of peak area of fragment peptides–rattusin (B) and defensin alpha 9 (C). The Y axis represents peak area of LC-MS/MS. * and ** represent $p<0.05$ and $p<0.01$, respectively, compared with the vehicle (C vs. C+pEL, HF vs. HF+pEL, respectively) by Student's *t*-test (n=3). The results are presented as the mean ± SD.

Supplemental Figure 2

A

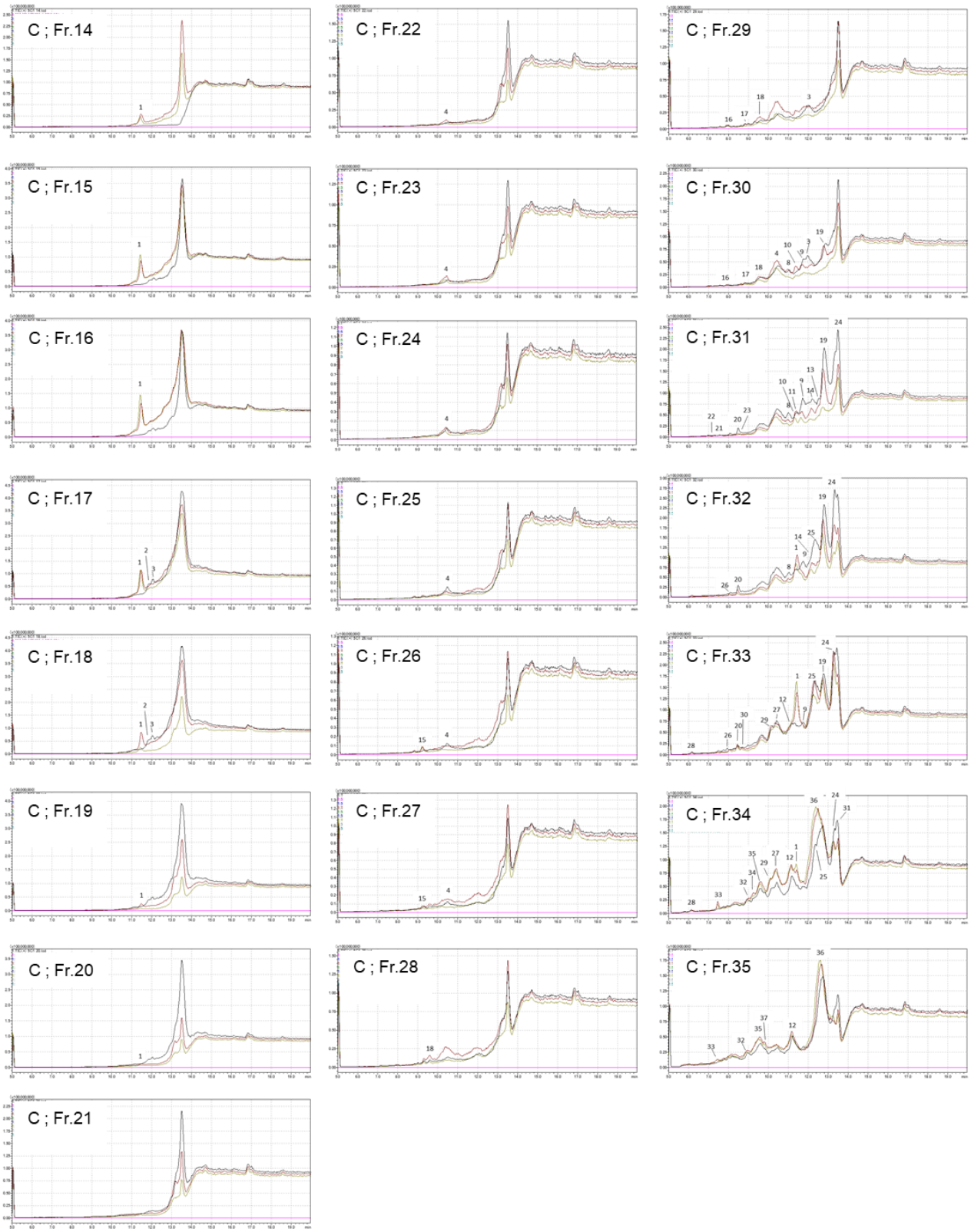

B

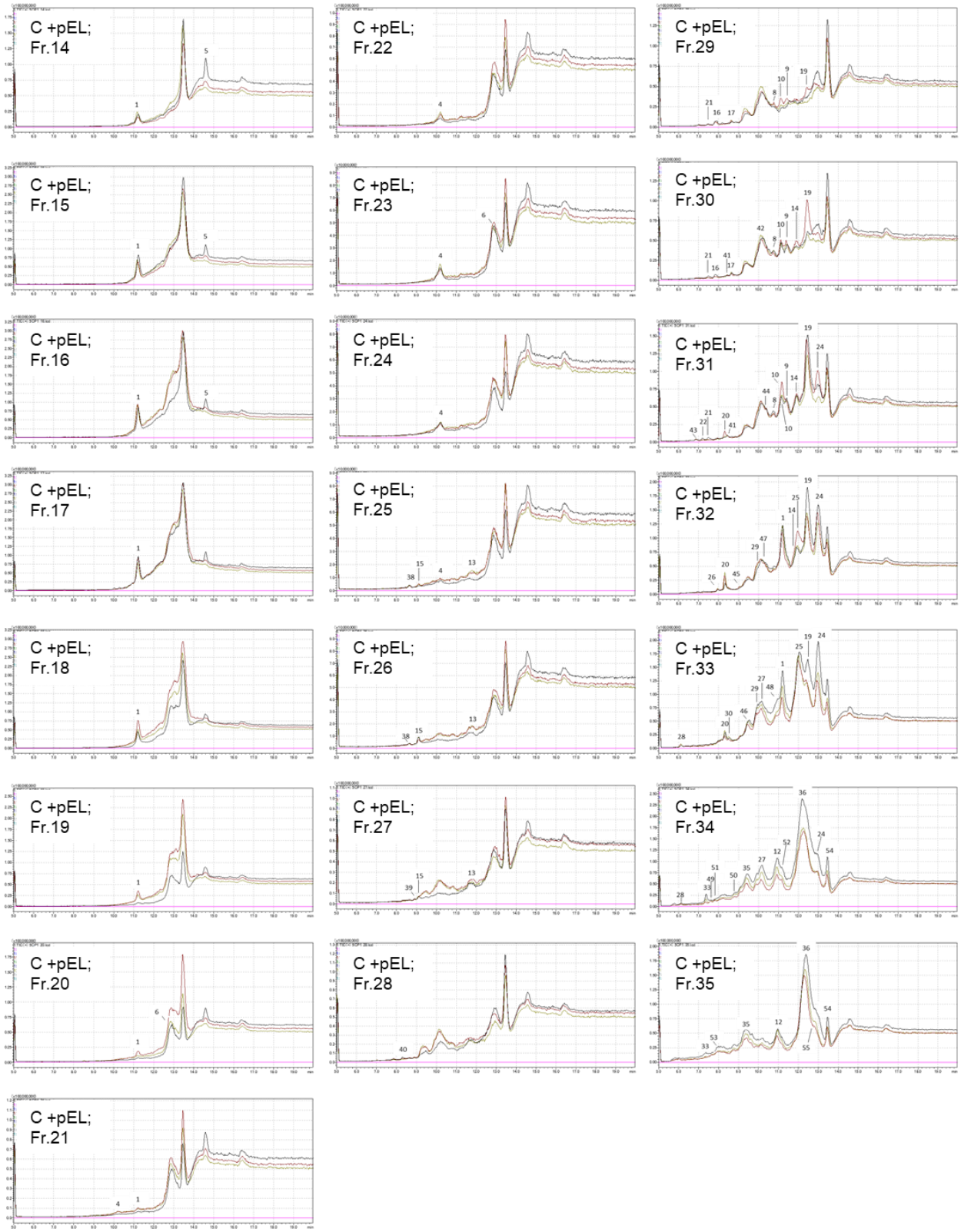
C +pEL;
Fr.14
C +pEL;
Fr.22
C +pEL;
Fr.29
C +pEL;
Fr.15
C +pEL;
Fr.23
C +pEL;
Fr.30
C +pEL;
Fr.16
C +pEL;
Fr.24
C +pEL;
Fr.31
C +pEL;
Fr.17
C +pEL;
Fr.25
C +pEL;
Fr.32
C +pEL;
Fr.18
C +pEL;
Fr.26
C +pEL;
Fr.33
C +pEL;
Fr.19
C +pEL;
Fr.27
C +pEL;
Fr.34
C +pEL;
Fr.20
C +pEL;
Fr.28
C +pEL;
Fr.35
C +pEL;
Fr.21

C

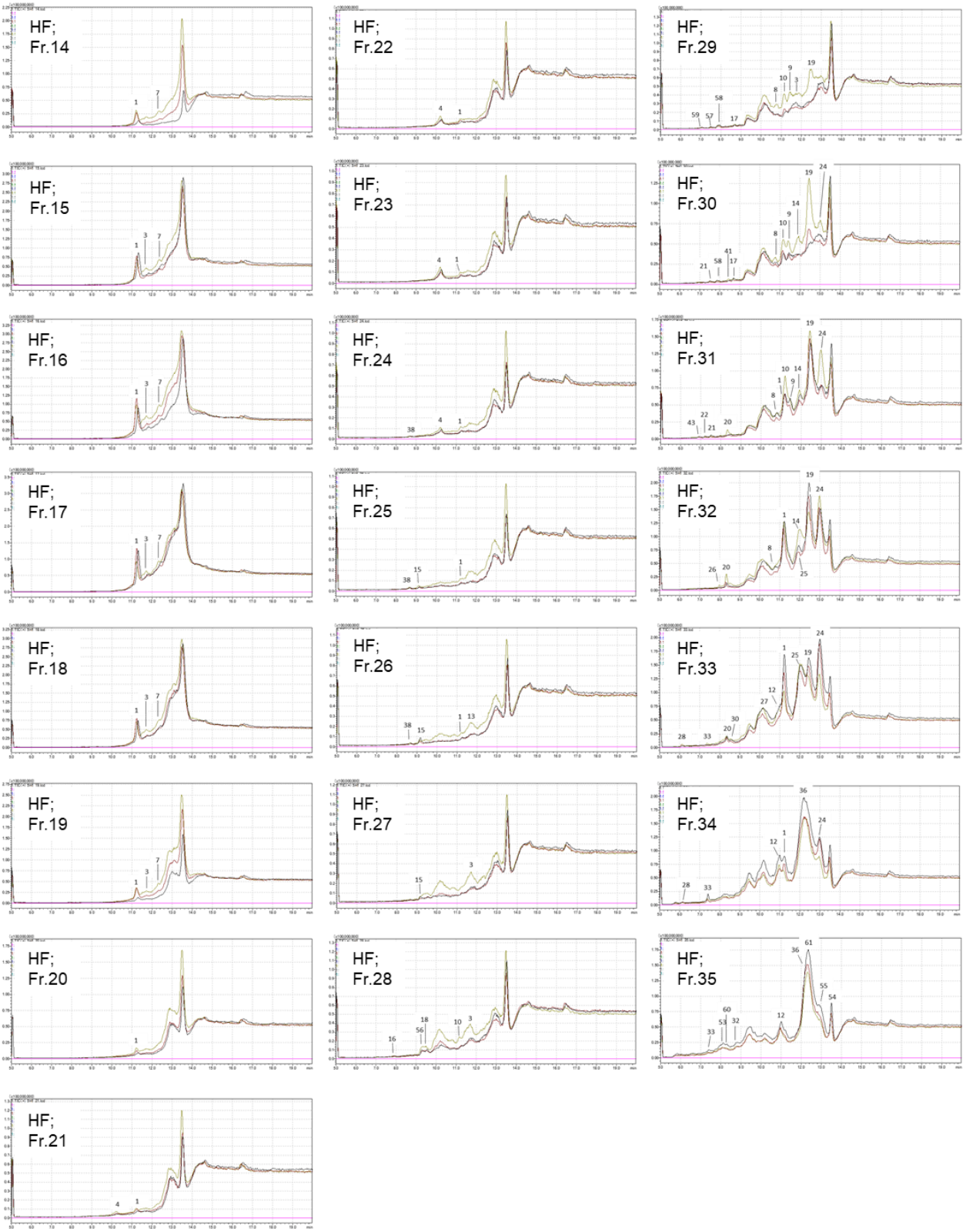
HF;
Fr.14
HF;
Fr.22
HF;
Fr.29
HF;
Fr.15
HF;
Fr.23
HF;
Fr.30
HF;
Fr.16
HF;
Fr.24
HF;
Fr.31
HF;
Fr.17
HF;
Fr.25
HF;
Fr.32
HF;
Fr.18
HF;
Fr.26
HF;
Fr.33
HF;
Fr.19
HF;
Fr.27
HF;
Fr.34
HF;
Fr.20
HF;
Fr.28
HF;
Fr.35
HF;
Fr.21

D

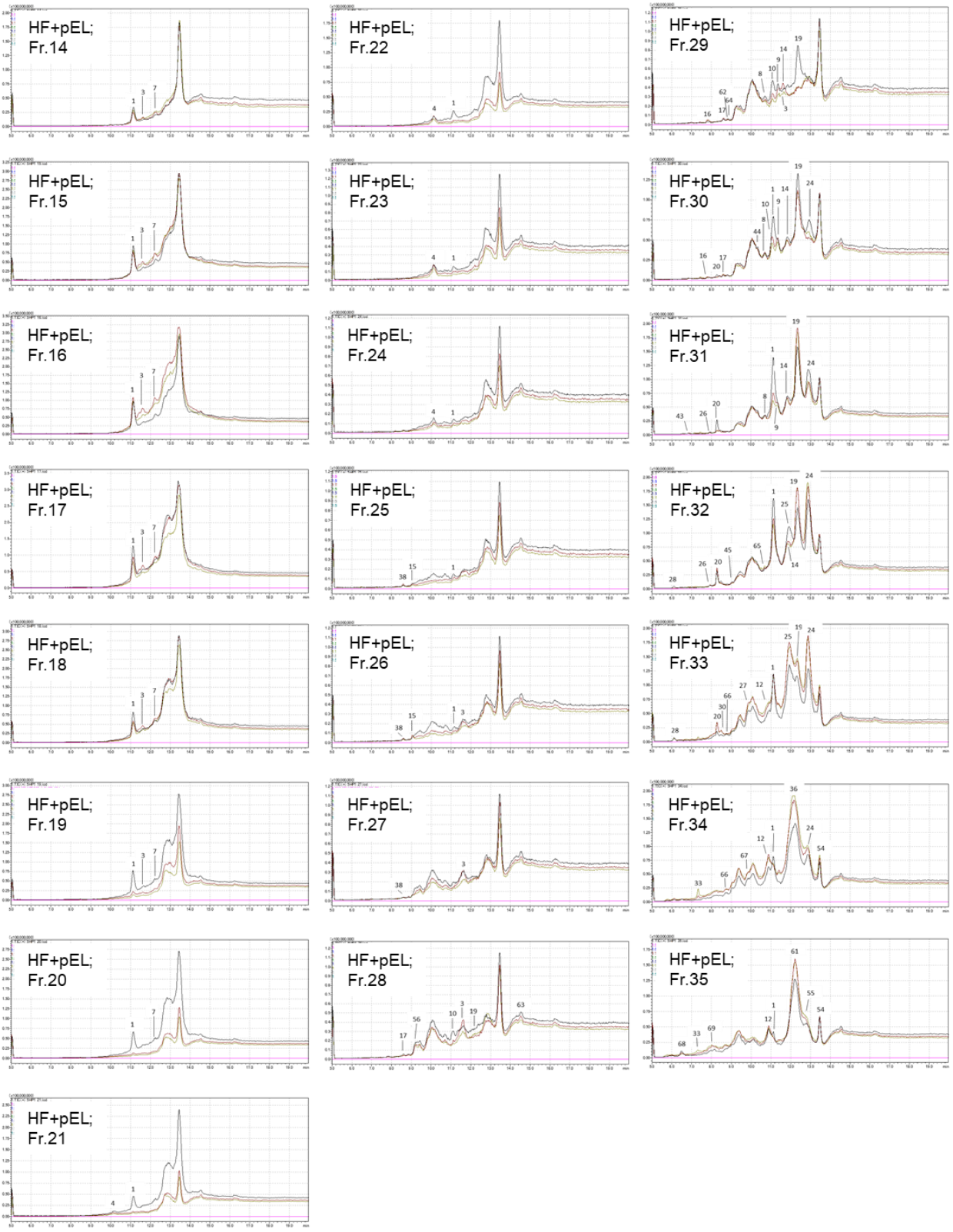
HF+pEL;
Fr.14
HF+pEL;
Fr.22
HF+pEL;
Fr.29
HF+pEL;
Fr.15
HF+pEL;
Fr.23
HF+pEL;
Fr.30
HF+pEL;
Fr.16
HF+pEL;
Fr.24
HF+pEL;
Fr.31
HF+pEL;
Fr.17
HF+pEL;
Fr.25
HF+pEL;
Fr.32
HF+pEL;
Fr.18
HF+pEL;
Fr.26
HF+pEL;
Fr.33
HF+pEL;
Fr.19
HF+pEL;
Fr.27
HF+pEL;
Fr.34
HF+pEL;
Fr.20
HF+pEL;
Fr.28
HF+pEL;
Fr.35
HF+pEL;
Fr.21

Supplemental Figure 2-1. Total ion chromatogram of RP-HPLC-MS of SEC Fr. 14-35.

Peaks were numbered. The Y axis of the chromatogram represents ion intensity. Three chromatograms represent of 3 samples from same animal group. A; control group (C), B; control + pEL group (C + pEL), C; high fat group (HF), and D; high fat + pEL group (HF + pEL), respectively.

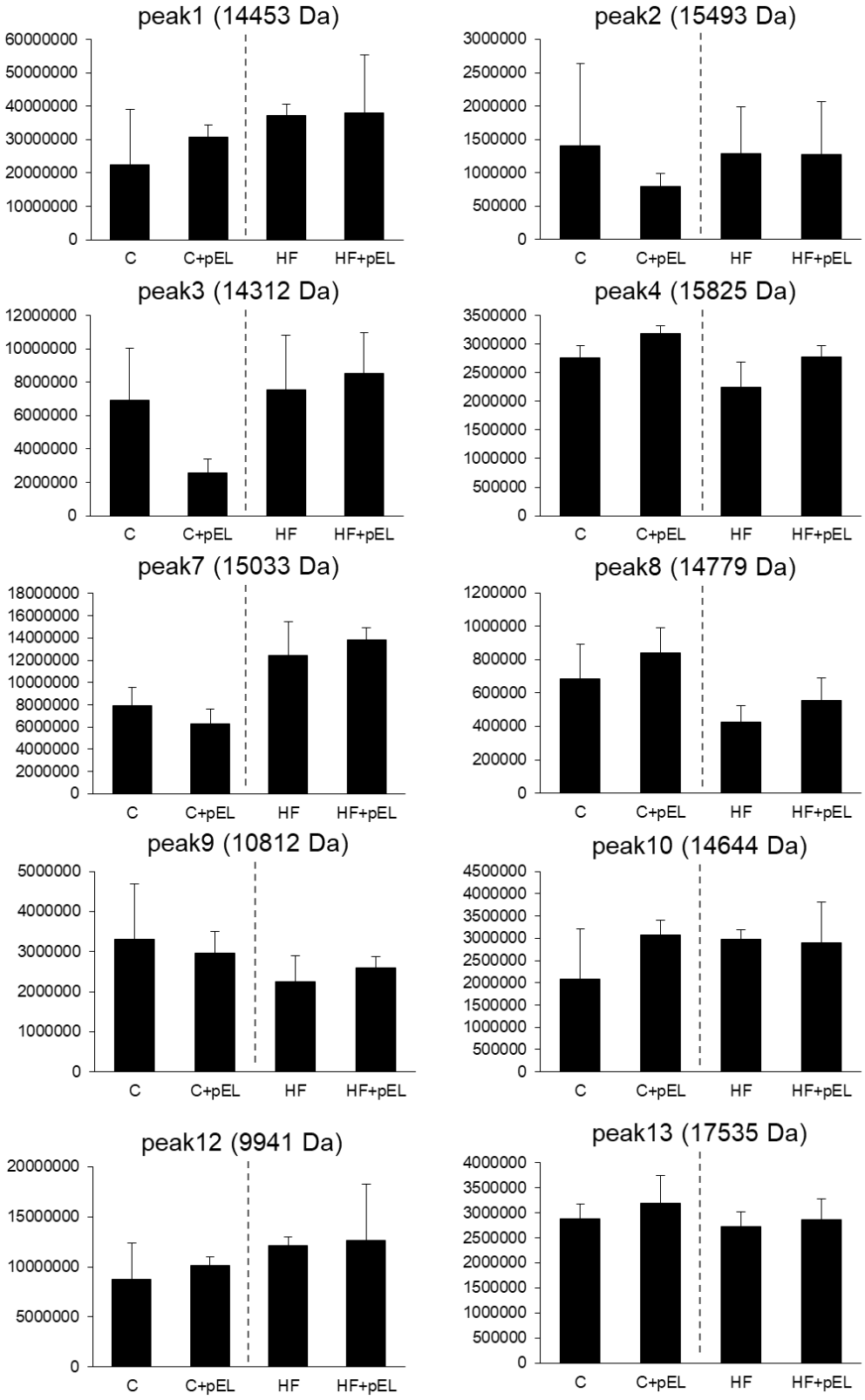
peak1 (14453 Da)
60000000
50000000
40000000
30000000
20000000
10000000
0
C
C+pEL
HF
HF+pEL
peak2 (15493 Da)
3000000
2500000
2000000
1500000
1000000
500000
0
C
C+pEL
HF
HF+pEL
peak3 (14312 Da)
12000000
10000000
8000000
6000000
4000000
2000000
0
C
C+pEL
HF
HF+pEL
peak4 (15825 Da)
3500000
3000000
2500000
2000000
1500000
1000000
500000
0
C
C+pEL
HF
HF+pEL
peak7 (15033 Da)
18000000
16000000
14000000
12000000
10000000
8000000
6000000
4000000
2000000
0
C
C+pEL
HF
HF+pEL
peak8 (14779 Da)
1200000
1000000
800000
600000
400000
200000
0
C
C+pEL
HF
HF+pEL
peak9 (10812 Da)
5000000
4000000
3000000
2000000
1000000
0
C
C+pEL
HF
HF+pEL
peak10 (14644 Da)
4500000
4000000
3500000
3000000
2500000
2000000
1500000
1000000
500000
0
C
C+pEL
HF
HF+pEL
peak12 (9941 Da)
20000000
15000000
10000000
5000000
0
C
C+pEL
HF
HF+pEL
peak13 (17535 Da)
4000000
3500000
3000000
2500000
2000000
1500000
1000000
500000
0
C
C+pEL
HF
HF+pEL

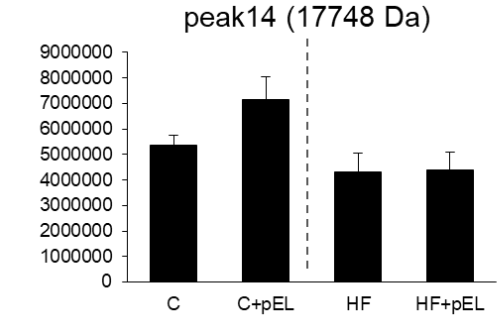
peak14 (17748 Da)
9000000
8000000
7000000
6000000
5000000
4000000
3000000
2000000
1000000
0
C
C+pEL
HF
HF+pEL

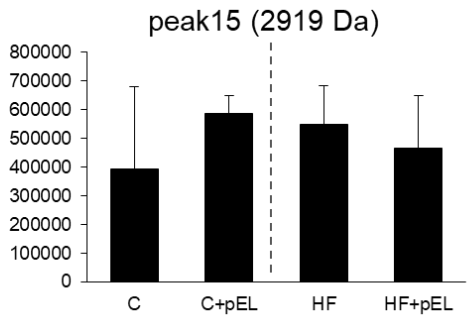
peak15 (2919 Da)
800000
700000
600000
500000
400000
300000
200000
100000
0
C
C+pEL
HF
HF+pEL

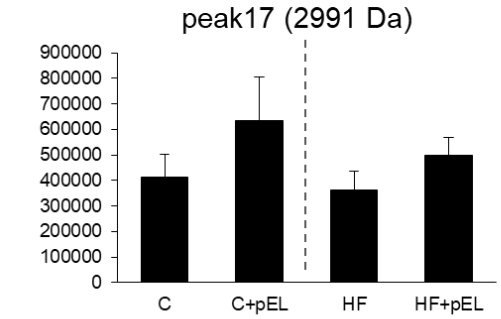
peak17 (2991 Da)
900000
800000
700000
600000
500000
400000
300000
200000
100000
0
C
C+pEL
HF
HF+pEL

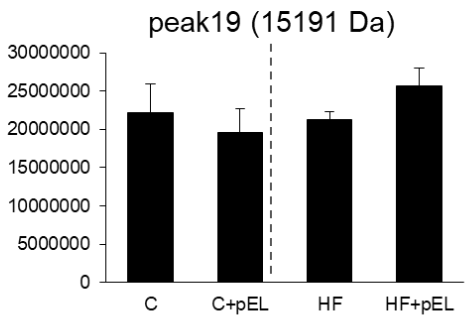
peak19 (15191 Da)
30000000
25000000
20000000
15000000
10000000
5000000
0
C
C+pEL
HF
HF+pEL

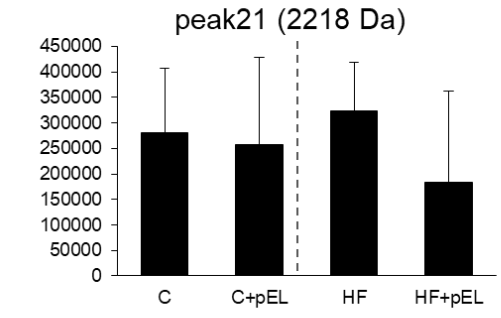
peak21 (2218 Da)
450000
400000
350000
300000
250000
200000
150000
100000
50000
0
C
C+pEL
HF
HF+pEL

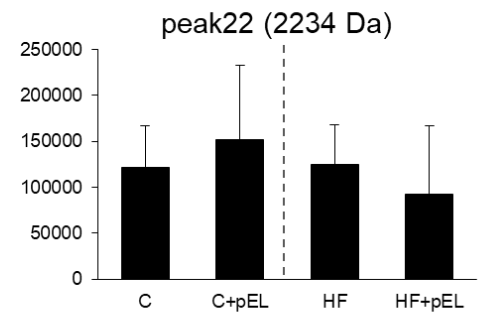
peak22 (2234 Da)
250000
200000
150000
100000
50000
0
C
C+pEL
HF
HF+pEL

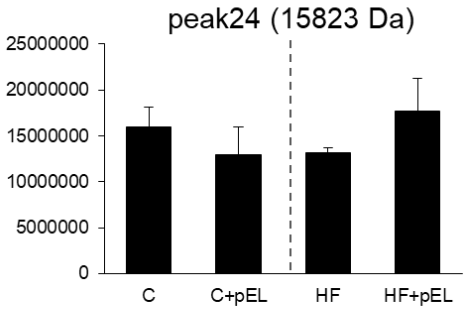
peak24 (15823 Da)
25000000
20000000
15000000
10000000
5000000
0
C
C+pEL
HF
HF+pEL

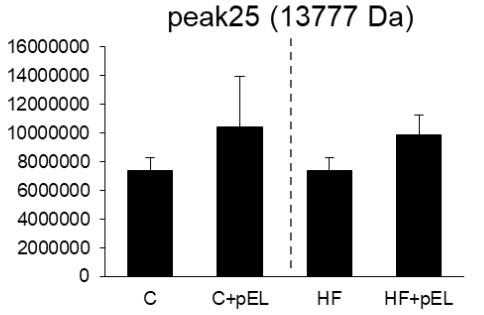
peak25 (13777 Da)
16000000
14000000
12000000
10000000
8000000
6000000
4000000
2000000
0
C
C+pEL
HF
HF+pEL

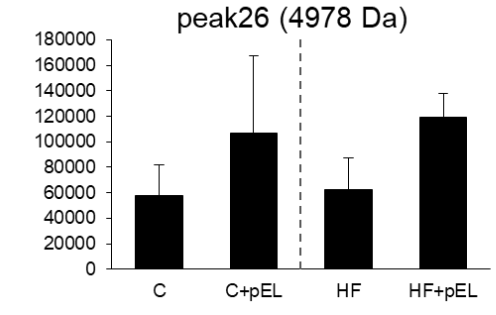
peak26 (4978 Da)
180000
160000
140000
120000
100000
80000
60000
40000
20000
0
C
C+pEL
HF
HF+pEL

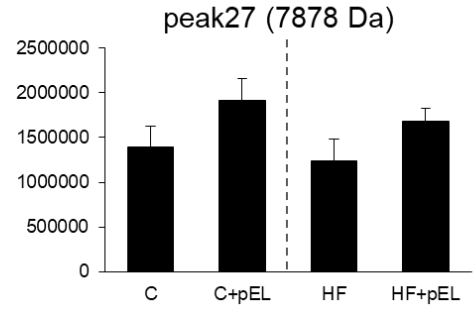
peak27 (7878 Da)
2500000
2000000
1500000
1000000
500000
0
C
C+pEL
HF
HF+pEL

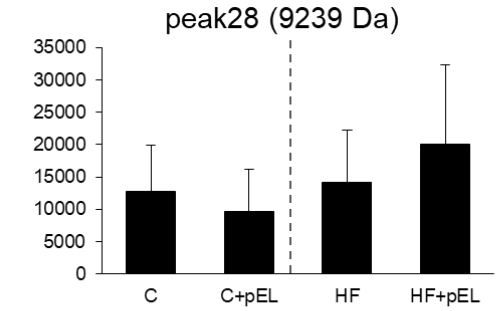
peak28 (9239 Da)
35000
30000
25000
20000
15000
10000
5000
0
C
C+pEL
HF
HF+pEL

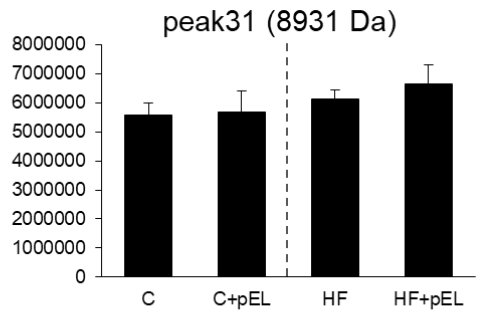
peak31 (8931 Da)
8000000
7000000
6000000
5000000
4000000
3000000
2000000
1000000
0
C
C+pEL
HF
HF+pEL

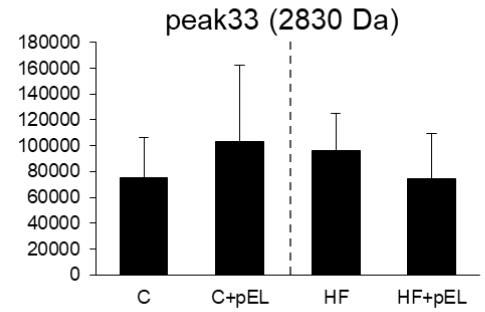
peak33 (2830 Da)
180000
160000
140000
120000
100000
80000
60000
40000
20000
0
C
C+pEL
HF
HF+pEL

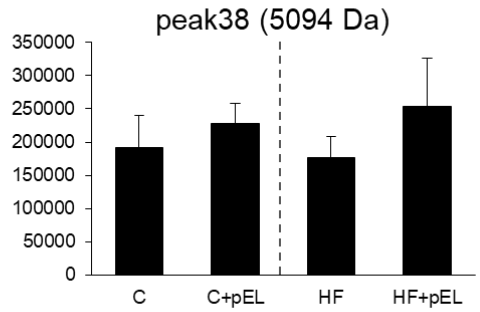
peak38 (5094 Da)
350000
300000
250000
200000
150000
100000
50000
0
C
C+pEL
HF
HF+pEL

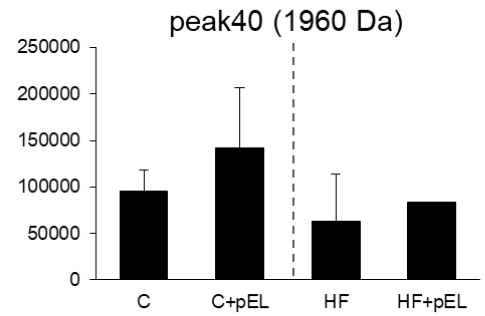
peak40 (1960 Da)
250000
200000
150000
100000
50000
0
C
C+pEL
HF
HF+pEL

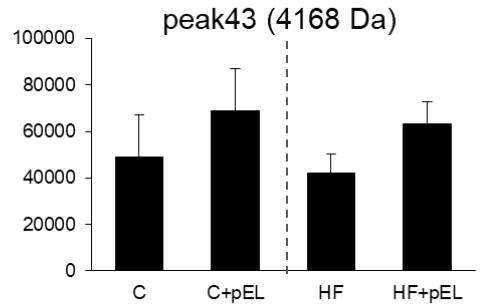
peak43 (4168 Da)
100000
80000
60000
40000
20000
0
C
C+pEL
HF
HF+pEL

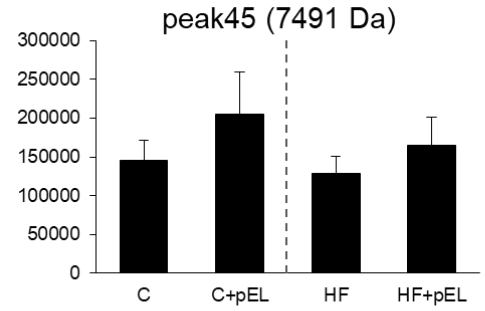
peak45 (7491 Da)
300000
250000
200000
150000
100000
50000
0
C
C+pEL
HF
HF+pEL

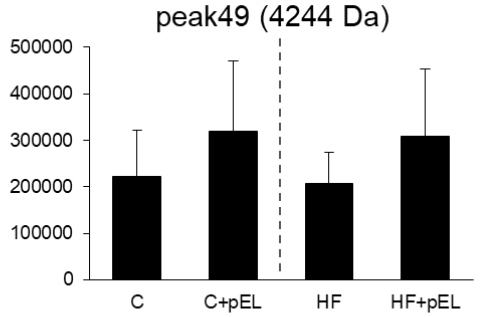
peak49 (4244 Da)
500000
400000
300000
200000
100000
0
C
C+pEL
HF
HF+pEL

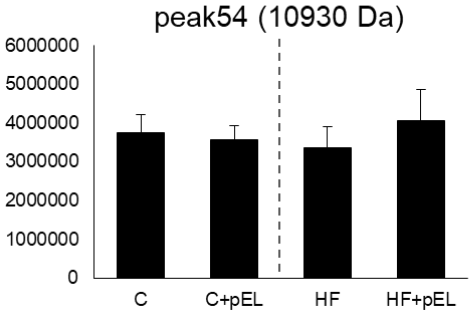
peak54 (10930 Da)
6000000
5000000
4000000
3000000
2000000
1000000
0
C
C+pEL
HF
HF+pEL

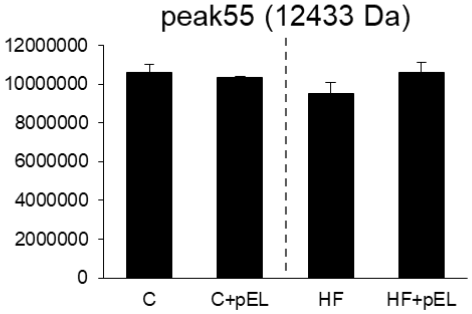
peak55 (12433 Da)
12000000
10000000
8000000
6000000
4000000
2000000
0
C
C+pEL
HF
HF+pEL

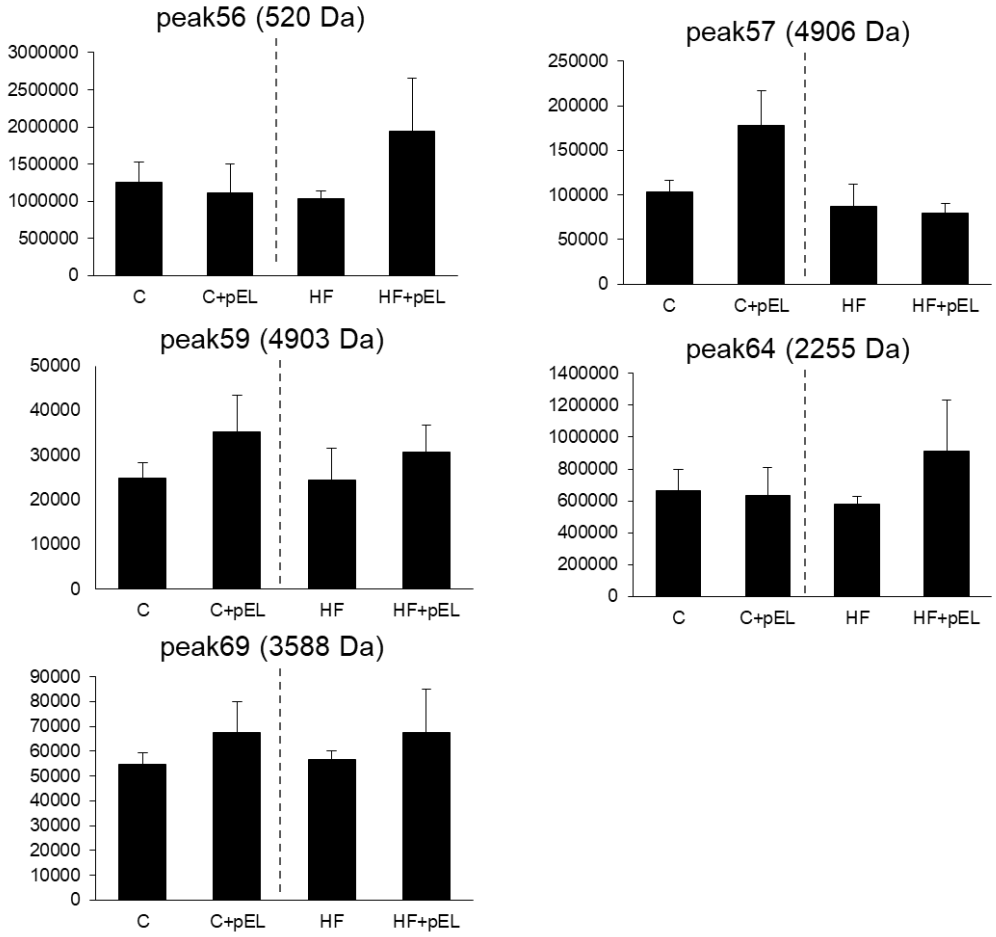

Supplemental Figure 2-2. Effect of pyroGlu-Leu on the peak area of the peptides in the 30% acetic acid extract of ileum, which did not significantly change by pyroGlu-Leu.

Refer the figure legend of Figure 2-1 for affiliation of animal groups. The Y axis represents peak area of LC-MS. The peptides which did not significantly change after pyroGlu-Leu administration are shown (n=3).

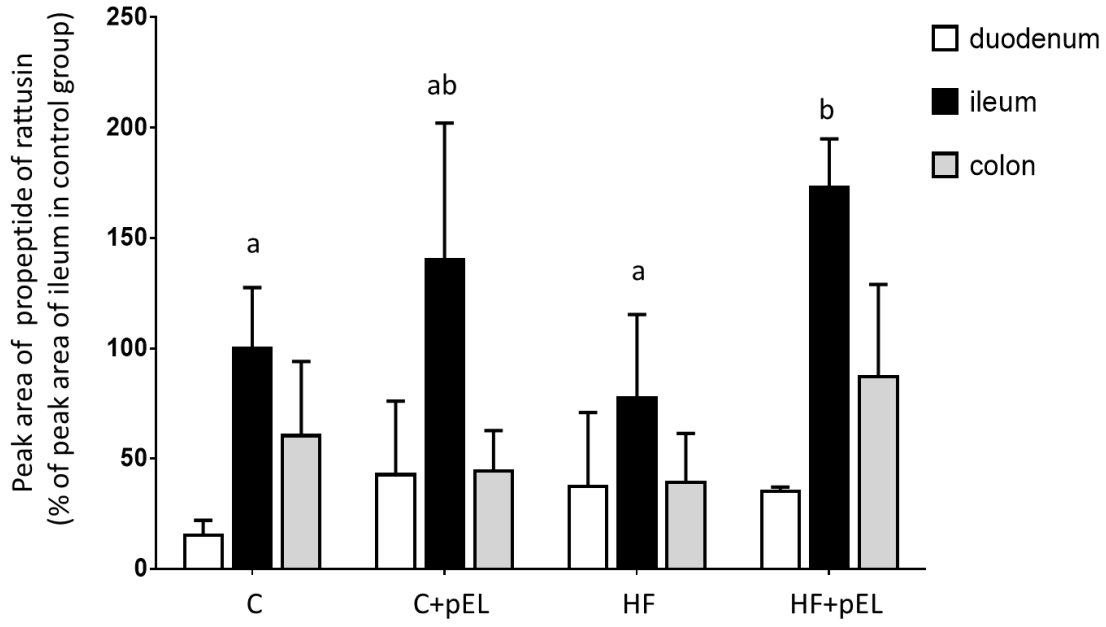

Supplemental Figure 2-3. Comparison of effect of pyroGlu-Leu on contents of rattusin propeptide in 30% acetic acid extracts between duodenum, ileum, and colon.

Refer the figure legend of Figure 2-1 for affiliation of animal groups. The propeptide of rattusin in the duodenum, ileum, and colon was detected in LC-MS in SIM mode. Peak area was collected (n=3 for each tissue) and shown as % of that in ileum in control group. Different letters indicate significant differences ($p<0.05$) by Tukey's test.

References for Chapter 2

1. Ley, R. E., Turnbaugh, P. J., Klein, S. & Gordon, J. I. Human gut microbes associated with obesity. *Nature* **444**, 1022–1023 (2006).
2. Turnbaugh, P. J. *et al.* An obesity-associated gut microbiome with increased capacity for energy harvest. *Nature* **444**, 1027–1031 (2006).
3. Wada, S. *et al.* Ingestion of low dose pyroglutamyl leucine improves dextran sulfate sodium-induced colitis and intestinal microbiota in mice. *J. Agric. Food Chem.* **61**, 8807–8813 (2013).
4. Matsuoka, K. & Kanai, T. The gut microbiota and inflammatory bowel disease. *Semin. Immunopathol.* **37**, 47–55 (2015).
5. Kiyono, T. *et al.* Identification of pyroglutamyl peptides with anti-colitic activity in Japanese rice wine, sake, by oral administration in a mouse model. *J. Funct. Foods* **27**, 612–621 (2016).
6. Huang, H., Krishnan, H. B., Pham, Q., Yu, L. L. & Wang, T. T. Y. Soy and gut microbiota: Interaction and implication for human health. *J. Agric. Food Chem.* **64**, 8695–8709 (2016).
7. Danneskiold-Samsøe, N. B. *et al.* Interplay between food and gut microbiota in health and disease. *Food Res. Int.* **115**, 23–31 (2019).
8. Wen, Y. *et al.* An intact gut microbiota may be required for lactoferrin-driven immunomodulation in rats. *J. Funct. Foods* **39**, 268–278 (2017).
9. Mukherjee, S. & Hooper, L. V. Antimicrobial defense of the intestine. *Immunity* **42**, 28–39 (2015).
10. Guo, X. *et al.* High fat diet alters gut microbiota and the expression of Paneth cell-antimicrobial peptides preceding changes of circulating inflammatory cytokines. *Mediators Inflamm.* **2017**, 1–9 (2017).
11. Hodin, C. M. *et al.* Reduced Paneth cell antimicrobial protein levels correlate with activation of the unfolded protein response in the gut of obese individuals. *J. Pathol.* **225**, 276–284 (2011).
12. Hayase, E. *et al.* R-Spondin1 expands Paneth cells and prevents dysbiosis

induced by graft-versus-host disease. *J. Exp. Med.* **214**, 3507–3518 (2017).

13. Sato, K. *et al.* Identification of a hepatoprotective peptide in wheat gluten hydrolysate against D-galactosamine-induced acute hepatitis in rats. *J. Agric. Food Chem.* **61**, 6304–6310 (2013).
14. Ayabe, T. *et al.* Activation of Paneth cell α-defensins in mouse small intestine. *J. Biol. Chem.* **277**, 5219–5228 (2002).
15. Ayabe, T. *et al.* Secretion of microbicidal alpha-defensins by intestinal Paneth cells in response to bacteria. *Nat. Immunol.* **1**, 113–8 (2000).
16. Patil, A. A., Ouellette, A. J., Lu, W. & Zhang, G. Rattusin, an intestinal α-defensin-related peptide in rats with a unique cysteine spacing pattern and salt-insensitive antibacterial activities. *Antimicrob. Agents Chemother.* **57**, 1823–1831 (2013).
17. Sato, K. *et al.* Occurrence of indigestible pyroglutamyl peptides in an enzymatic hydrolysate of wheat gluten prepared on an industrial scale. *J. Agric. Food Chem.* **46**, 3403–3405 (1998).
18. Ejima, A., Nakamura, M., Suzuki, Y. A. & Sato, K. Identification of food-derived peptides in human blood after ingestion of corn and wheat gluten hydrolysates. *J. Food Bioact.* **2**, 104–111 (2018).
19. Kiyono, T. *et al.* Identification of pyroglutamyl peptides in Japanese rice wine (sake): Presence of hepatoprotective pyroGlu-Leu. *J. Agric. Food Chem.* **61**, 11660–11667 (2013).
20. Sato, K. & Kiyono, T. Modified peptides in foods; Structure and function of pyroglutamyl peptides. *FFI J.* **222**, 216–222 (2017).
21. Kanai, T., Matsuoka, K., Naganuma, M., Hayashi, A. & Hisamatsu, T. Diet, microbiota, and inflammatory bowel disease: lessons from Japanese foods. *Korean J. Intern. Med.* **29**, 409 (2014).

Chapter 3

Generation of a novel leucine-derivative, propionyl leucine, in ileum after oral administration of pyroglutamyl peptides

Introduction

The studies in Chapter 1 and 2 have shown that hydrophobic pyroglutamyl peptides (pyroGlu-Val, pyroGlu-Ile, and pyroGlu-Leu) exert potential anti-obesity effect and pyroGlu-Leu attenuates high fat diet-induced dysbiosis by increasing host antimicrobial peptide. However, target tissues of hydrophobic pyroglutamyl peptides still remained unknown. Previous reports have mentioned that food-derived bioactive peptides have to be absorbed into blood circulation system and delivered to targets to exert *in vivo* biological activities after oral administration.[1,2] In a previous study, it has been demonstrated that content of pyroGlu-Leu increases in small intestine, but not in colon, after the administration of low dose (1.0 mg/kg B.W.).[3] Thus, it is expected that one of target tissues of pyroglutamyl peptides is small intestine. In addition, pyroGlu-Leu has demonstrated to be absorbed into portal vein in μM level in rat after 30-60 min of the high dose (20 mg/kg B.W.) of administration.[4] However, there are no comprehensive data on absorption of hydrophobic pyroglutamyl peptides after administration of practical dose (1.0 mg/kg B.W.). From these facts, the tissue distribution and metabolic fate of hydrophobic pyroglutamyl peptides at a practical dose (1.0 mg/kg B.W.) were examined.

Methods

Reagents

Acetonitrile (HPLC grade) and acetic acid were purchased from Nacalai Tesque. Propionic acid and butyric acid were purchased from Wako Pure Chemical (Kyoto, Japan). PyBOP, HOBt, Fmoc-Val, Ile, and Leu derivatives, Boc-Pyr-OH, H-Val-OtBu・HCl, H-Ile-OtBu・HCl, and H-Leu-OtBu・HCl were purchased from Watanabe Chemical

Industries.

Peptides synthesis

Pyroglutamyl peptides (pyroGlu-Val, pyroGlu-Ile, and pyroGlu-Leu) for animal experiment were synthesized through Boc strategy as described previously.[4] Acetyl-, propionyl-, and butyl-Val, Ile, and Leu were synthesized through Fmoc strategy using a PSSM-8 peptide synthesizer (Shimadzu). All synthetic peptides were purified via RP-HPLC using a Cosmosil 5C18-MS-II column (10 mm i.d. × 150 mm, Nacalai Tesque) as described in Chapter 1.

Animal experiment

Animals were treated and cared for in accordance with the guidelines of the National Institutes of Health (NIH) for the use of experimental animals. All experimental procedures were approved by the Animal Care Committee of Louis Pasteur Center for Medical Research (No. 20191). Four-week-old male Wistar/ST rats (80–100 g) were purchased from Japan SLC (Shizuoka, Japan). Every four rat was caged together and housed at 24 ± 1°C and 40–70% relative humidity with a 12 h light/dark cycle. The rats were allowed free access to a normal diet (solid type of certified diet MF; Oriental Yeast) and drinking water for two weeks. After acclimatization period, the rats were fasted for 16 h. Then, rats were orally administered 0.5 mL of PBS or 0.5 mL of PBS containing the mixture of pyroglutamyl peptides (pyroGlu-Val, pyroGlu-Ile, and pyroGlu-Leu; 1 mg/kg body weight/each peptide) (n=4). Rats, which were administered PBS, were sacrificed by puncturing the inferior vena cava under anesthetization using isoflurane as soon as after administration, and referred to control (Ctrl). Rats, which were administered the mixture of pyroglutamyl peptides, were sacrificed in the same manner 1, 3, 6, and 15 h after the administration. Blood (portal and inferior vena cava), duodenum, jejunum, ileum, colon, liver, kidney, and muscle (gastrocnemius) were collected and kept in -80℃ until analyses. The inner contents of intestines were flushed with 10 mL of PBS and kept in -80℃ until analyses. Blood was centrifuged at 800 × g for 10 min at 4°C and plasma was collected.

Plasma was added 3-volume of ethanol and kept in -30℃ until analyses.

Preparation of tissue sample

Ten mL of PBS suspension of inner contents of small intestines and colon were centrifuged at 200 × g for 10 min at room temperature. The supernatant was added 3-volume of ethanol and centrifuged at 12,000 × g for 10 min at 4°C. The ethanol-soluble fractions were collected and used for analyses. Plasma with 3-volume of ethanol was centrifuged at 12,000 × g for 10 min at 4°C. The ethanol-soluble fractions were collected and used for analyses. Collected tissues were cut into small pieces using scissors on ice. The pieces (100 mg) of tissue samples were homogenized with 100 μL of PBS in a BioMasher II (Nippi). The homogenates were further mixed with 600 μL of ethanol. These homogenates were centrifuged at 12,000 × g for 10 min and the ethanol-soluble fractions were collected.

Determination of pyroglutamyl peptides in rats

The ethanol-soluble fractions of inner contents of small intestines and colon (200 μL respectively), plasma from portal vein (100 μL) and peripheral vein (300 μL), and tissues (100 μL) were dried under vacuum. The dried samples were then added same volumes of Pico-Tag buffer (5 mM NaH_2PO_4 containing 5% of acetonitrile) and clarified by passing through a filter W (pore size 0.45 μm, 4 mm i.d.; Nacalai Tesque). Aliquots (10 μL) of the filtrates were subjected to a LC-MS/MS (LCMS 8040, Shimadzu) in MRM mode using Inertsil ODS-3 column (5 μm, 2.1 mm i.d. × 250 mm, GL Science). The synthetic peptides were used as standard for optimization of MRM condition. A binary liner gradient was used with 0.1% formic acid (solvent A) and 0.1% formic acid containing 80% acetonitrile (solvent B) at a flow rate of 0.2 mL/min. The gradient program was as follows: 0–15 min, 0–50% B; 15–20 min, 50–100% B; 20–25 min, 100% B; 25–25.1 min, 100–0% B; 25.1–35 min, 0% B. The column was maintained at 40°C.

Identification of amino acid derivatives in ileum of rats orally administered the mixture of pyroglutamyl peptides

The ethanol-soluble fractions of ileums of control (Ctrl) and 1 h after the administration of the mixture of pyroglutamyl peptides (1 h) were used for analysis. Three hundred μL of the ethanol-soluble fractions were dried under vacuum, added with 75 μL of Pico-Tag buffer, and clarified by passing through a filter W (pore size 0.45 μm, 4 mm i.d.; Nacalai Tesque). Aliquots (10 μL) of the filtrates were subjected to a LC-MS/MS in total ion scan mode and precursor ion scan mode using Inertsil ODS-3 column (5 μm, 2.1 mm i.d. × 250 mm, GL Science). Solvents, flow rate, gradient program, and column temperature were same as described in ***Determination of pyroglutamyl peptides in rats***. Total ion intensity was monitored at a positive mode in the scan range of *m/z* =100-150, 150-175, 175-200, 200-225, 225-250, and 250-500 (total ion scan). Valine derivatives were specifically detected by targeting immonium ion of valine (*m/z*=72.05) at collision energy -35 V in a positive mode in the same scan range of total ion scan above (precursor ion scan). Isoleucine or leucine derivatives were specifically detected by targeting that of isoleucine or leucine (*m/z*=86.05) at collision energy -35 V in a positive mode in the same scan range of total ion scan above (precursor ion scan). The *m/z* of peaks, which increased in 1 h after the administration, were selected and used for product ion scanning to estimate the peptides structure at collision energies -15, -25, and -35 V (product ion scan).

Determination of propionyl-Leu and related peptides

The ethanol-soluble fractions of inner contents of small intestines and colon (200 μL), duodenum, jejunum, ileum, and colon (100 μL) were dried under vacuum. The dried samples were redissolved in the same volumes of Pico-Tag buffer and clarified by passing through a filter W (pore size 0.45 μm, 4 mm i.d.; Nacalai Tesque). Aliquots (10 μL) of the filtrates were subjected to a LC-MS/MS in MRM mode using Inertsil ODS-3 column (5 μm, 2.1 mm i.d. × 250 mm, GL Science). The synthetic propionyl-Leu and other related peptides (acetyl-Val, Ile, and Leu, propionyl-Val, butyl-Val, Ile, and Leu) were used as standard for optimization of MRM condition. Solvents, flow rate, gradient program, and

column temperature were same as described in ***Determination of pyroglutamyl peptides in rats***.

Statistical analysis

The results were presented as the mean ± standard deviations (SD). The significant differences compared with control (PBS group) in pyroglutamyl peptides and propionyl-Leu were evaluated by Dunnett's test. Differences of $p < 0.05$ were considered significant. Statistical analysis was performed using GraphPad Prism version 6.04 (GraphPad Software).

Results

Tissue distribution of pyroglutamyl peptides in rats after the oral administration

As shown in Figure 3-1 A and B, the contents of pyroGlu-Val, pyroGlu-Ile, and pyroGlu-Leu in inner contents of small intestines were significantly increased 1 h after the administration of the mixture of pyroglutamyl peptides. That in inner content of colon did not increase. In plasma from portal vein, pyroGlu-Val and pyroGlu-Ile were significantly increased 1 h after the administration, however, pyroGlu-Leu did not significantly increase (Figure 3-1 C). The contents of the all peptides in plasma from peripheral vein, liver, kidney, and muscle did not significantly increase after the administration (Figure 3-1 D and Figure 3-2). As shown in Figure 3-3, the contents in duodenum, jejunum, and ileum significantly increased 1 h after the administration, while, that in colon did not increase. One hour after the administration, contents of all pyroglutamyl peptides in ileum were higher than other parts of intestine.

Identification and determination of propionyl-Leu after the oral administration of pyroglutamyl peptides

As shown in Figure 3-4 A, precursor ion scan mode (*m/z*=86.05; targeting immonium ion of isoleucine or leucine) revealed the presences of pyroGlu-Ile and pyroGlu-Leu in

the scan range of *m/z*=225-250 in ileum 1 h after the administration of the mixture of pyroglutamyl peptides. The presence of pyroGlu-Val was also observed in ileum in the scan range of *m/z*=200-225>72.05; targeting immonium ion of valine (data not shown). In scan range of *m/z*=175-200, the compound with *m/z*=188.1 was increased in 1 h after the administration, as shown in Figure 3-4 B. The compound was further evaluated by LC-MS/MS in product ion scan mode. The MS spectrum obtained from product ion scan are shown in Figure 3-5 A. From the MS spectrum, the compound was estimated to consist of propionic acid and isoleucine (propiony-Ile) or leucine (propionyl-Leu). As shown in Figure 3-5 B, by comparing the elution pattern of standard, the compound with *m/z*=188.1 was identified as propionyl-Leu. Contents of pripionyl-Leu in inner contents of small intestines and colon, duodenum, jejunum, ileum, and colon were determined by LC-MS/MS in MRM mode. As shown in Figure 3-6, propionyl-Leu was not observed in inner contents of small intestines and colon, duodenum, and jejunum. Interestingly, propionyl-Leu was observed and significantly increased only in ileum 1 h after the administration of the mixture of pyroglutamyl peptides. Other propionyl-Leu-related peptides standards (acetyl-Val, Ile, and Leu, propionyl-Val, Ile, and butyl-Val, Ile, and Leu) were successfully detected by LC-MS/MS in MRM mode (Supplemental Figure 3), however, they were not observed or increased in ileum after the administration of the mixture of pyroglutamyl peptides (Figure 3- 7).

Discussion

As emphasized by Foltz *et al*, it is important to know the absorption, distribution, metabolism, and excretion (ADME) profiles of orally administered peptides for evaluation of bioactivity of bioactive peptides.[5] The present study showed that hydrophobic pyroglutamyl peptides (pyroGlu-Val, pyroGlu-Ile, and pyroGlu-Leu) were absorbed into small intestine, especially into ileum, 1 h after the administration. Approximately 15% of pyroglutamyl peptides, which existed in lumen, were absorbed into ileum. The increase levels of the pyroglutamyl peptides in ileum returned to initial

levels 3 h after the administration. These facts suggest that pyroglutamyl peptides might be absorbed into blood circulation system or metabolized in ileum after 1 h. However, the significant increase of pyroglutamyl peptides in blood circulation system was not observed by the administration of low dose (1.0 mg/kg B.W.) of pyroglutamyl peptides in the present study. Therefore, it is likely that pyroglutamyl peptides are metabolized in ileum.

To detect potential metabolites of pyroglutamyl peptides in ileum, precursor ion scan, targeting immonium ion of Val, Ile, and Leu, was used. As a result, the increase of novel peptide, propionyl-leucine (propionyl-Leu), was detected in ileum, while no significant increase was observed in other tissues. It is known that acetate, propionate, and butyrate are the most abundant short-chain fatty acids in the gut lumen in humans and rodents.[6] Therefore, all combination of propionyl-Leu-related peptides were synthesized. However, the presences or increase of other related peptides (acetyl-Val, Ile, and Leu, propionyl-Val, butyl-Val, Ile, and Leu) in ileum were not observed by LC-MS/MS analysis. These data indicates that propionyl-Leu is specifically generated especially in ileum. In addition, it is suggested that significant amounts of generated propionyl-Leu in ileum is not secreted into lumen and blood circulation system. However, there are no reports demonstrating that food-derived peptides stimulate the generation of another compound. Therefore, biological activity of propionyl-Leu in ileum should be further studied.

On the other hand, the biological activities of propionate regarding with anti-obesity effect have been shown.[6,7] Propionate is known to regulate appetite.[8] The authors have demonstrated that propionate increases the release of peptide YY (PYY) and glucagon-like peptide-1 (GLP-1) from human colonic cells.[8] Other papers have also reported that the treatment of propionate increases the expression of leptin in adipocytes.[9–11] Higashimura *et al* have demonstrated that propionate (5 mM) induces the expression of peroxisome proliferator-activated receptor α (PPARα) in a mouse intestinal epithelial cell line.[12] They indicate that modulation of the expression of intestinal PPARα by propionate might be responsible for suppression of TG accumulation and prevention of obesity. As propionyl-Leu is not secreted into lumen after the generation, it is unlikely that propionyl-

Leu bind to membrane surface receptors. There is a possibility that propionyl-Leu induces the expression of nuclear receptor; PPARα in intestine at a lower level (μM level) than propionate (mM level).

Thus, the effects of propionyl-Leu on appetite related hormones and nuclear receptors will be investigated. Finding of propionyl-Leu might provide breakthrough for elucidating the mechanism for biological activities of hydrophobic short chain pyroglutamyl peptides.

Figures

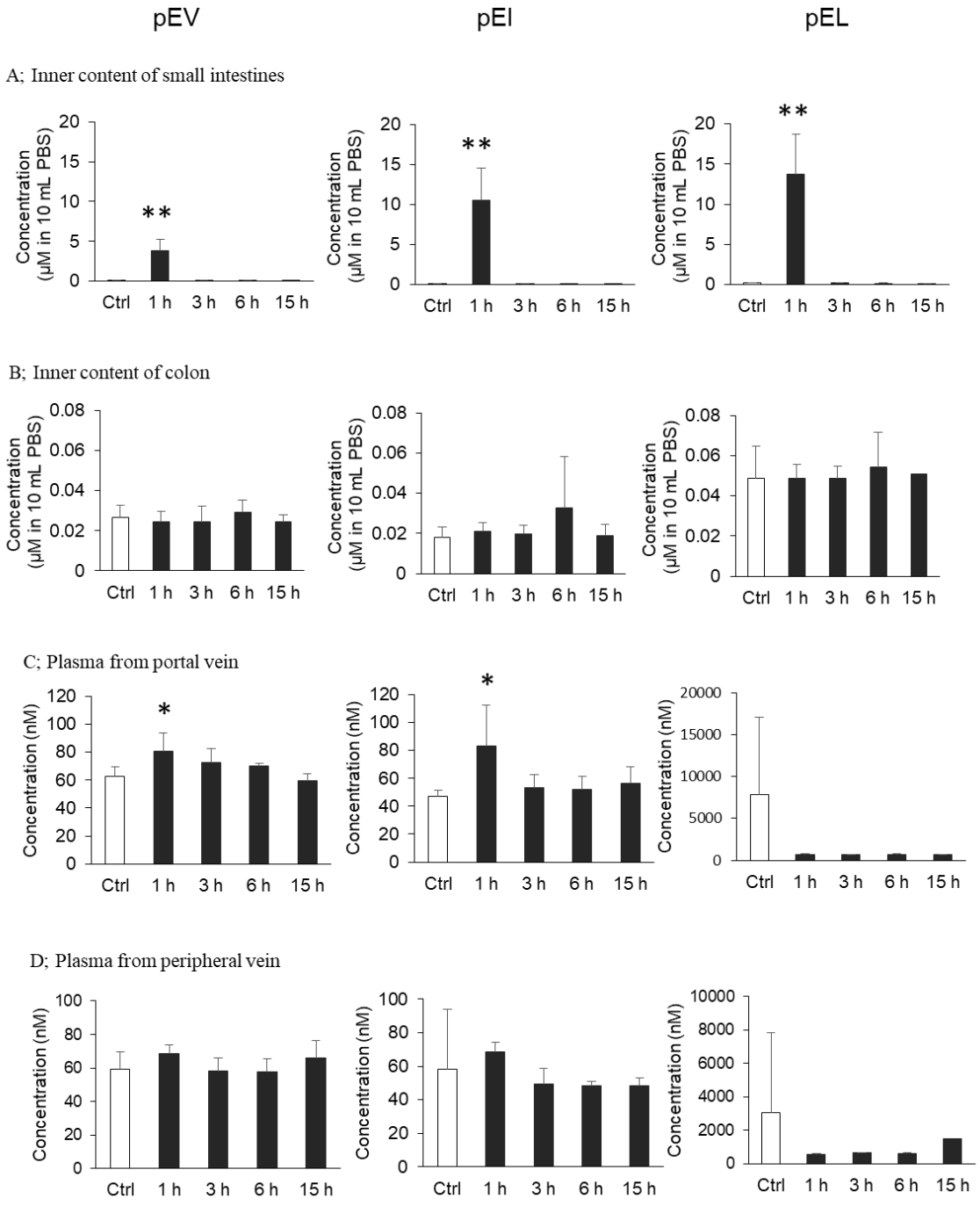

Figure 3-1. Contents of pyroglutamyl peptides after oral administration of mixture of pyroglutamyl peptides.

Ctrl; samples were collected from rats sacrificed as soon as after administration of PBS. Samples

were also collected from rats sacrificed 1, 3, 6, and 15 h after administration of the mixture of pyroglutamyl peptides (pEV, pEI, and pEL; 1.0 mg/kg B.W./each peptide). Contents of each pyroglutamyl peptide in inner content of small intestines (A), inner content of colon (B), plasma from portal vein (C), and peripheral vein (D) were determined by LC-MS/MS. Data are shown in mean ± SD (n=4). ** represents significant differences of $p<0.01$ by Dunnett's test vs Ctrl.

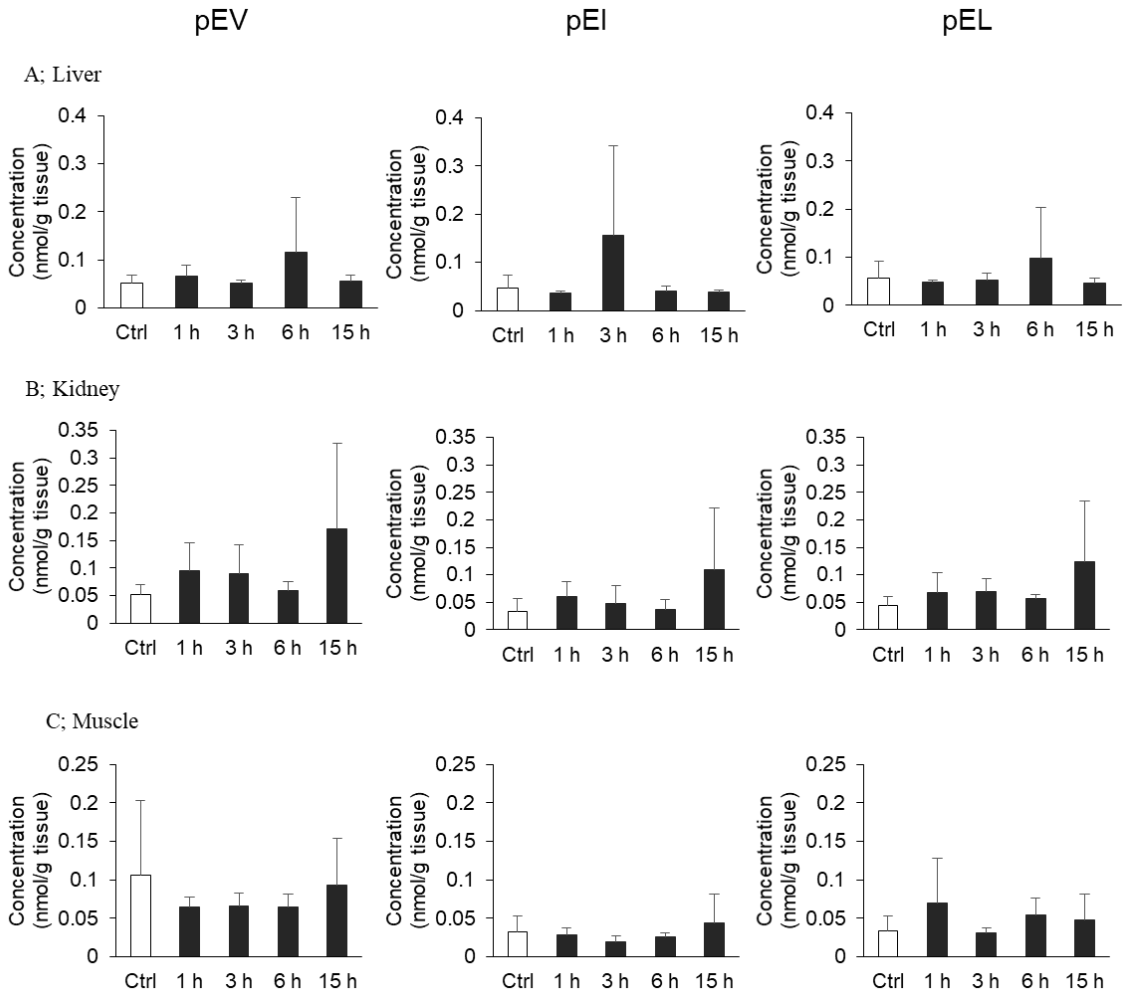

Figure 3-2. Contents of pyroglutamyl peptides after oral administration of mixture of pyroglutamyl peptides.

Refer the figure legend of Figure 3-1 for affiliation of animal groups. Contents of each pyroglutamyl peptide in liver (A), kidney (B), and muscle (C) were determined by LC-MS/MS. Data are shown in mean ± SD (n=4). No significant differences were observed by Dunnett's test vs Ctrl.

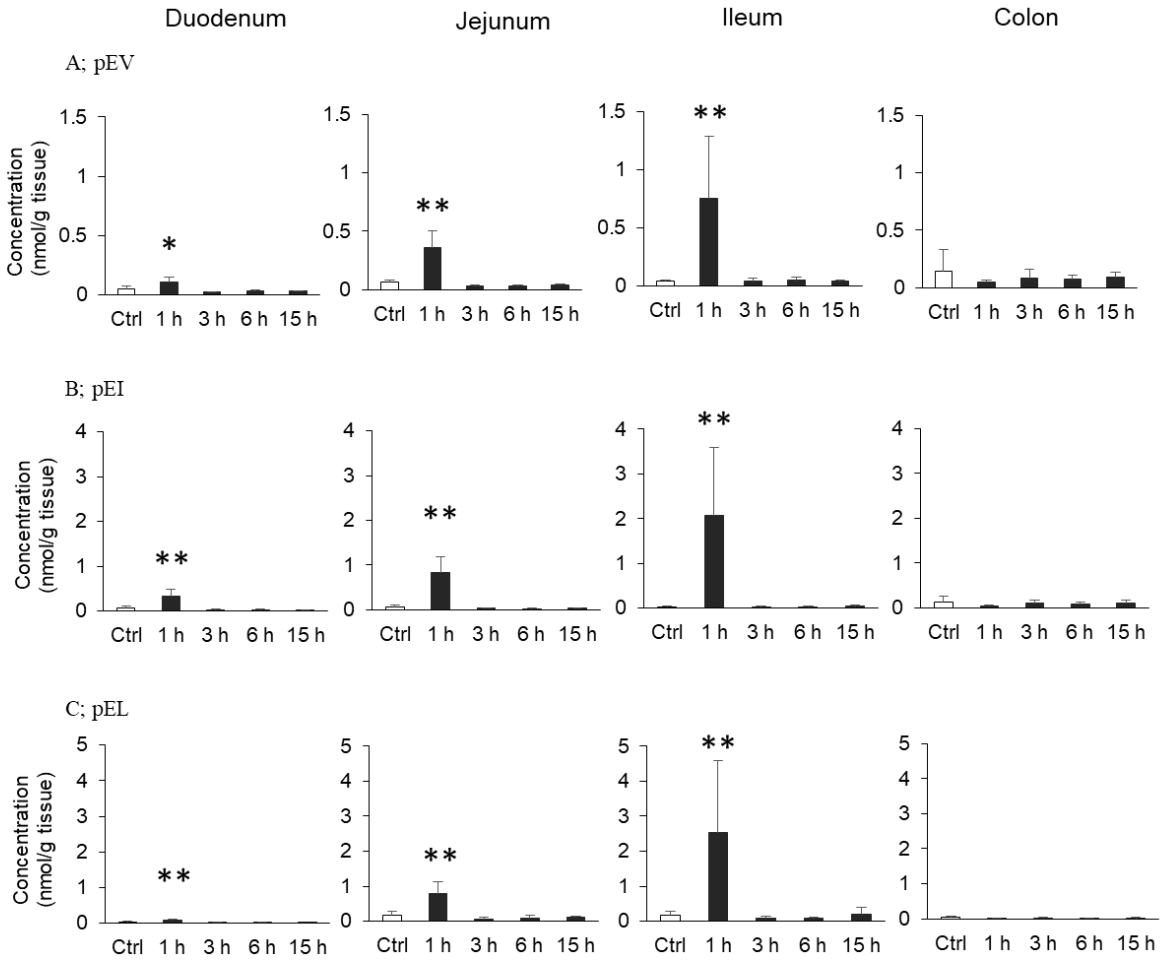

Figure 3-3. Comparison of concentration of pyroglutamyl peptides after oral administration of mixture of pyroglutamyl peptides in intestines

Refer the figure legend of Figure 3-1 for affiliation of animal groups. Contents of each pyroglutamyl peptide; pEV (A), pEI (B), and pEL (C) in duodenum, jejunum, ileum, and colon were determined by LC-MS/MS. Data are shown in mean ± SD (n=4). * and ** represent significant differences of $p<0.05$ and $p<0.01$, respectively, by Dunnett's test vs Ctrl.

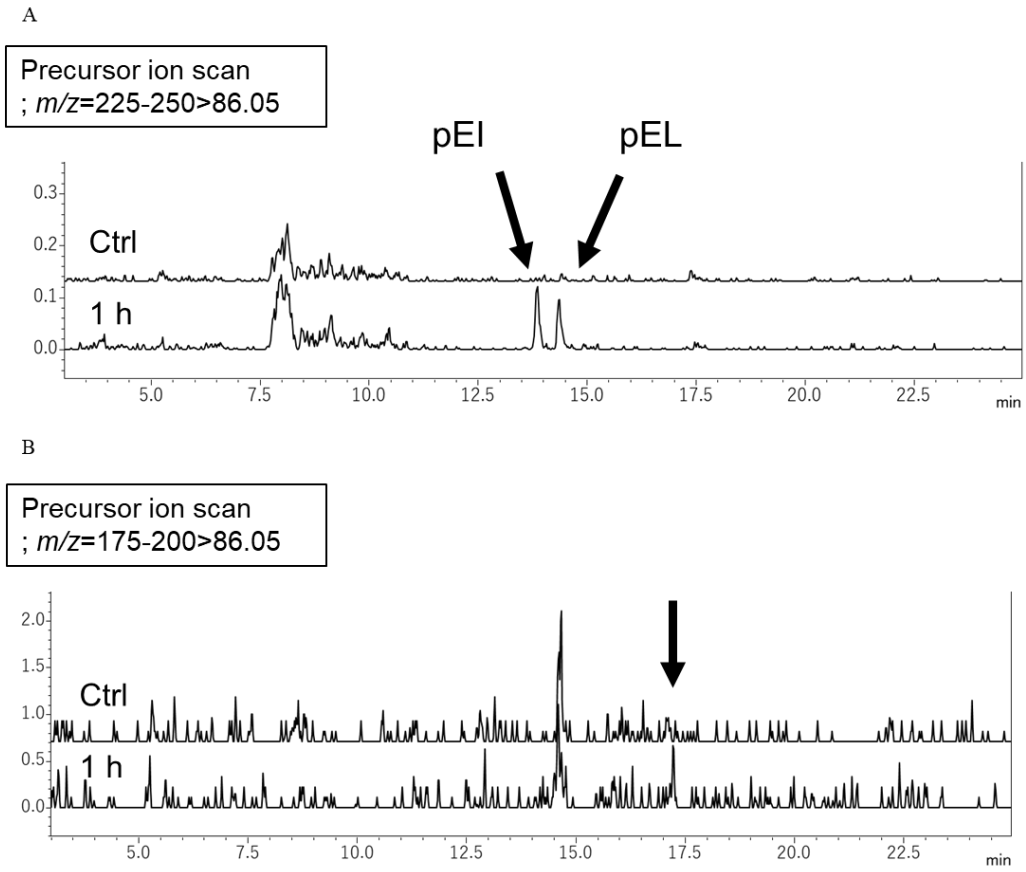

Figure 3-4. MS chromatograms obtained from LC-MS/MS in precursor ion scan mode in ethanol-soluble fraction of ileum of Control and 1 h after the administration.

Refer the figure legend of Figure 3-1 for affiliation of ctrl and 1 h. Ethanol-soluble fractions of ileum of Ctrl (upper) and 1 h (bottom) were subjected to LC-MS/MS in precursor ion scan mode, targeting immonium ion of Ile and Leu. Mass chromatograms, obtained from precursor ion scan mode of *m/z*=225-250>86.05 (A) and *m/z*=175-200>86.05 (B), respectively. Peaks identified as pEI and pEL are indicated arrows. The peak with *m/z*=188.1 indicates with arrow (B) was further subjected to LC-MS/MS in product ion scan mode.

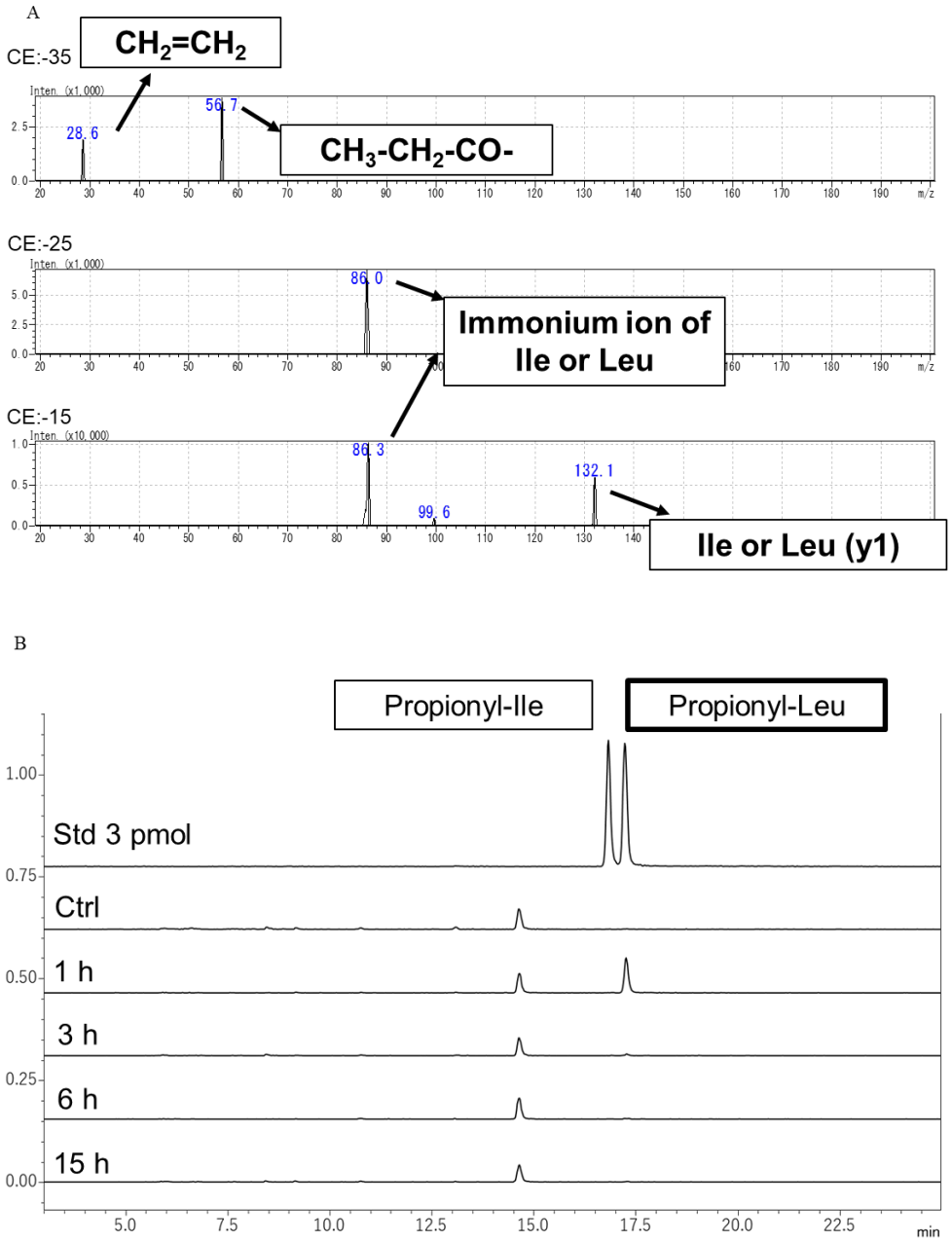

Figure 3-5. Identification and determination of propionyl-Leu

MS spectrums of compound with *m/z*=188.1 were obtained from different collision energies (A). The peak of *m/z*=188.1 was identified as propiomyl-Leu and detected in ethanol-soluble fraction of ileum of 1 h (B).

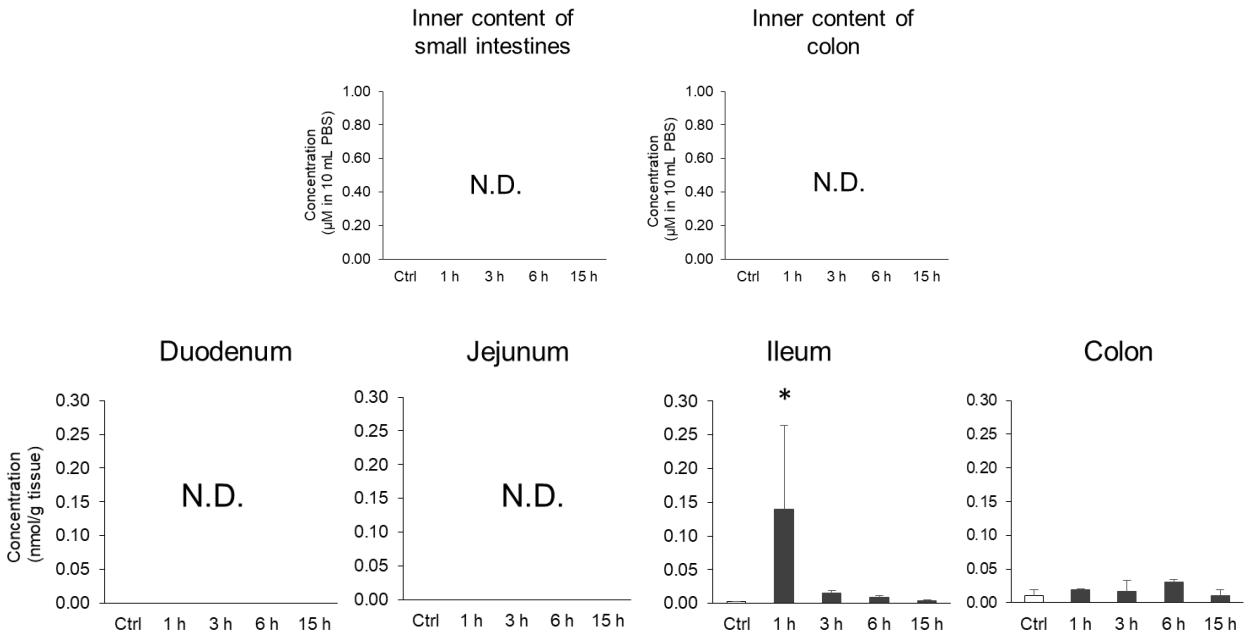

Figure 3-6. Concentration of propionyl-Leu after the oral administration of pyrogltamyl peptides in rats.

Refer the figure legend of Figure 3-1 for affiliation of animal groups. Contents of propionyl-Leu in inner contents of small intestine and colon, duodenum, jejunum, ileum and colon were determined by LC-MS/MS. Data are shown in mean ± SD (n=4). * represents significant differences of $p<0.05$ by Dunnett's test vs Ctrl.

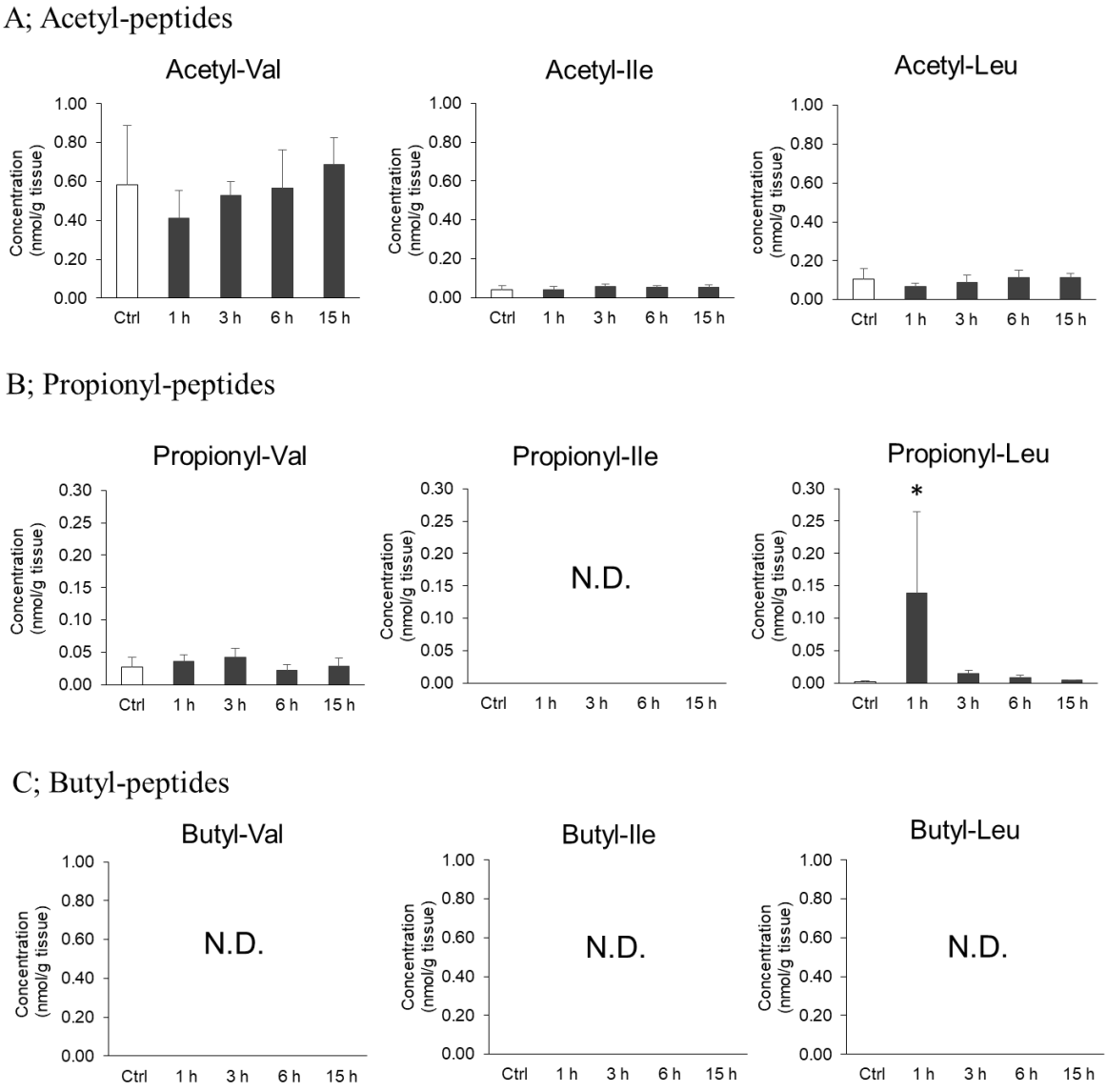

Figure 3-7. Concentration of propionyl-Leu and other related peptides in ileum after the oral administration of pyrogltamyl peptides in rats.

Refer the figure legend of Figure 3-1 for affiliation of animal groups. Contents of acetyl-peptides (A), propionyl-peptides (B), and butyl-peptides (C) in ileum were determined by LC-MS/MS. Data are shown in mean ± SD (n=4). * represents significant differences of $p<0.05$ by Dunnett's test vs Ctrl.

Supplemental Figure 3

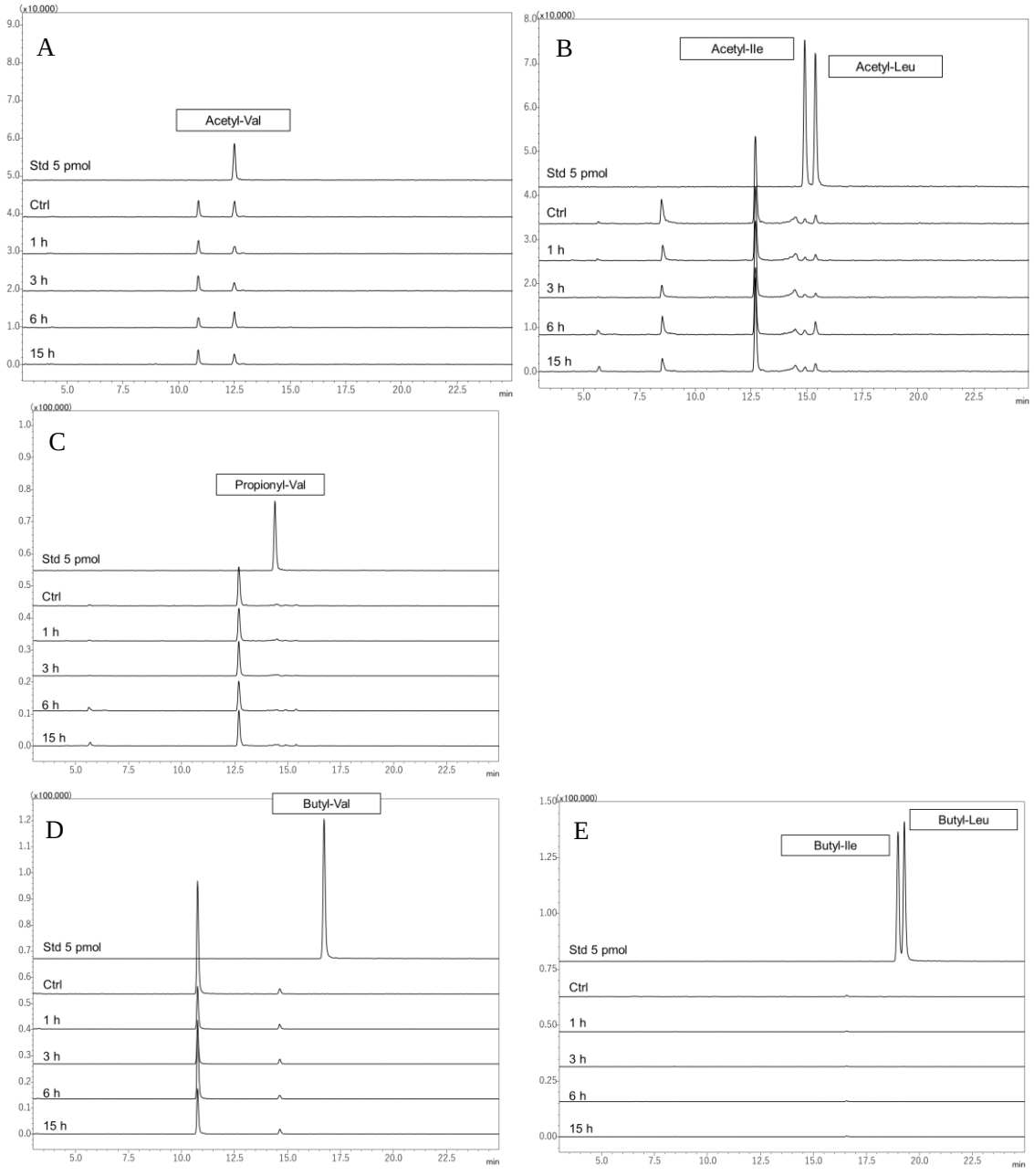

Supplemental Figure 3. Detection of propionyl-Leu-related peptides in ileum.

Refer the figure legend of Figure 3-1 for affiliation of animal groups. The presences of acetyl-Val (A), acetyl-Ile and Leu (B), propionyl-Val (C), butyl-Val (D), and butyl-Ile and Leu (E) in ileum were compared to their standards by LC-MS/MS in MRM mode. Elution was compared with each standard peptide (first chromatogram; referred to Std).

References for Chapter 3

1. Fernández-Tomé, S., Sanchón, J., Recio, I. & Hernández-Ledesma, B. Transepithelial transport of lunasin and derived peptides: inhibitory effects on the gastrointestinal cancer cells viability. *J. Food Compos. Anal.* **68**, 101–110 (2018).
2. Ding, L., Wang, L., Zhang, T., Yu, Z. & Liu, J. Hydrolysis and transepithelial transport of two corn gluten derived bioactive peptides in human Caco-2 cell monolayers. *Food Res. Int.* **106**, 475–480 (2018).
3. Wada, S. *et al.* Ingestion of Low dose pyroglutamyl leucine improves dextran sulfate sodium-induced colitis and intestinal microbiota in mice. *J. Agric. Food Chem.* **61**, 8807–8813 (2013).
4. Sato, K. *et al.* Identification of a hepatoprotective peptide in wheat gluten hydrolysate against D-galactosamine-induced acute hepatitis in rats. *J. Agric. Food Chem.* **61**, 6304–6310 (2013).
5. Foltz, M., van der Pijl, P. C. & Duchateau, G. S. M. J. E. Current in vitro testing of bioactive peptides is not valuable. *J. Nutr.* **140**, 117–118 (2010).
6. Lin, H. V. *et al.* Butyrate and propionate protect against diet-induced obesity and regulate gut hormones via free fatty acid receptor 3-independent mechanisms. *PLoS One* **7**, e35240 (2012).
7. Arora, T., Sharma, R. & Frost, G. Propionate. Anti-obesity and satiety enhancing factor? *Appetite* **56**, 511–515 (2011).
8. Chambers, E. S. *et al.* Effects of targeted delivery of propionate to the human colon on appetite regulation, body weight maintenance and adiposity in overweight adults. *Gut* **64**, 1744–1754 (2015).
9. Hong, Y.-H. *et al.* Acetate and propionate short chain fatty acids stimulate adipogenesis via GPCR43. *Endocrinology* **146**, 5092–5099 (2005).
10. Zaibi, M. S. *et al.* Roles of GPR41 and GPR43 in leptin secretory responses of murine adipocytes to short chain fatty acids. *FEBS Lett.* **584**, 2381–2386 (2010).
11. Al-Lahham, S. H. *et al.* Regulation of adipokine production in human adipose tissue by propionic acid. *Eur. J. Clin. Invest.* **40**, 401–407 (2010).

12. Higashimura, Y. *et al.* Propionate promotes fatty acid oxidation through the up-regulation of peroxisome proliferator-activated receptor α in intestinal epithelial cells. *J. Nutr. Sci. Vitaminol. (Tokyo).* **61**, 511–515 (2015).

Conclusion and Prospective Research

Pyroglutamyl peptides are widely distributed in food protein hydrolysates[1–3] and some pyroglutamyl peptides, such as pyroGlu-Leu, pyroGlu-Asn-Ile, exert anti-inflammatory effect and suppress hepatitis and colitis in animal models.[2,4–7] In addition, these peptides suppress DSS-induced dysbiosis, while its mechanism remained unknown. Pyroglutamyl peptides are also present in Japanese rice wine, one of Japanese traditional fermented foods.[8] Presence of pyroglutamyl peptides in other Japanese fermented food, such as miso, has been suggested.[9] However, structure and contents of pyroglutamyl peptides in miso remained unknown due to complicity of food matrix.

In Chapter 1, newly developed LC-MS/MS method based on precursor scan targeting immonium ion of pyroglutamic acid residue revealed the presences of 13 pyroglutamyl peptides in miso. In addition, potential anti-obesity effect of hydrophobic pyroglutamyl peptides were demonstrated in rats fed high fat diet.

In Chapter 2, the oral administration of pyroGlu-Leu attenuated high fat diet-induced dysbiosis by increasing host antimicrobial peptides. This is novel concept for modulation of gut microbiota by food component. For this purpose, low molecular weight basic proteins including antimicrobial peptides were directly detected by LC-MS based on multivalent ions, which provides powerful tool to examine antimicrobial peptides. It has been demonstrated that dysbiosis induces obesity.[10,11] Thus, it could be assumed that attenuation of dysbiosis by increasing host antimicrobial peptide by hydrophobic short chain pyroglutamyl peptides including pyroGlu-Leu suppresses high fat diet-induced body weight gain.

In Chapter 3, it was demonstrated that three hydrophobic pyroglutamyl peptides (pyroGlu-Val, pyroGlu-Ile, pyroGlu-Leu) were mainly absorbed into ileum. Moreover, administration of the mixture of them generated a novel peptide, propionyl-Leu, in ileum, which might be involved in suppression of body weight gain and increase of host antimicrobial peptide. As there are no reports demonstrating the presence of propionyl-Leu, biological activity of propionyl-Leu remains unknown. However, it could be

assumed that propionyl-Leu acts like short chain fatty acids (SCFAs). Propionate is one of short chain fatty acids (SCFAs), which are produced by fermentation by microbiota and are present in gut lumen, as well as acetate and butyrate.[12] It has been shown that butyrate and propionate suppress high fat diet-induced obesity partially by inhibiting food intake.[12] It has been also shown that butyrate is a ligand for GPR109A.[13] Therefore, there is a possibility that propionyl-Leu might be excreted from cells and be ligand for GPR109A. Alternatively, hydrophobic short chain pyroglutamyl peptides might act on cell surface receptor, which might generate propionyl-Leu in cell and act as second messenger. To solve these possibilities, further studies are necessary.

Some epidemiological and animal studies have demonstrate that intake of Japanese diet (washoku) and Japanese traditional fermented foods have positive effects on health propmotion.[14–18] However, the active compounds in them have not been fully understood. Recent intervention study demonstrates that the intake of the 1975 type of Japanese diet decreases body weight and improves lipid metabolic parameter than the 2015 type of Japanese modern diet in healthy subjects.[19] Dishes using Japanese traditional fermented foods, such as miso, soy sauce (shoyu), and Japanese rice wine (sake), decreased in the modern Japanese diet (2005) compared to 1970's diet.[20] Sake is not only consumed as an alcoholic beverage, but is also used as a seasoning in traditional Japanese dishes. Sake contains approximately 1.0-1.5 mg/100 mL of pyroGlu-Leu.[8] Both miso and shoyu contain higher contents of pyroGlu-Leu than sake.[9] Therefore, significant amounts of pyroglutamyl peptides can be obtained by the consumption of washoku resulting in health benefits. Therefore, the decrease of consumption of these Japanese traditional fermented foods might be associated to the risk of obesity and dyslipidemia.

In conclusion, the present study suggests that hydrophobic short chain pyroglutamyl peptides may be key players in health benefits by consumption of washoku and Japanese traditional fermented foods. Effects of the administration of pyroglutamyl peptides should be further confirmed by well-designed human clinical study.

References for Conclusion and Prospective Research

1. Sato, K. *et al.* Occurrence of indigestible pyroglutamyl peptides in an enzymatic hydrolysate of wheat gluten prepared on an industrial scale. *J. Agric. Food Chem.* **46**, 3403–3405 (1998).
2. Sato, K. *et al.* Identification of a hepatoprotective peptide in wheat gluten hydrolysate against D-galactosamine-induced acute hepatitis in rats. *J. Agric. Food Chem.* **61**, 6304–6310 (2013).
3. Ejima, A., Nakamura, M., Suzuki, Y. A. & Sato, K. Identification of food-derived peptides in human blood after ingestion of corn and wheat gluten hydrolysates. *J. Food Bioact.* **2**, 104–111 (2018).
4. Wada, S. *et al.* Ingestion of Low dose pyroglutamyl leucine improves dextran sulfate sodium-induced colitis and intestinal microbiota in mice. *J. Agric. Food Chem.* **61**, 8807–8813 (2013).
5. Hirai, S. *et al.* Anti-inflammatory effect of pyroglutamyl-leucine on lipopolysaccharide-stimulated RAW 264.7 macrophages. *Life Sci.* **117**, 1–6 (2014).
6. Oishi, M. *et al.* pyroGlu-Leu inhibits the induction of inducible nitric oxide synthase in interleukin-1β-stimulated primary cultured rat hepatocytes. *Nitric Oxide* **44**, 81–87 (2015).
7. Kiyono, T. *et al.* Identification of pyroglutamyl peptides with anti-colitic activity in Japanese rice wine, sake, by oral administration in a mouse model. *J. Funct. Foods* **27**, 612–621 (2016).
8. Kiyono, T. *et al.* Identification of pyroglutamyl peptides in Japanese rice wine (sake): Presence of hepatoprotective pyroGlu-Leu. *J. Agric. Food Chem.* **61**, 11660–11667 (2013).
9. Sato, K. & Kiyono, T. Modified peptides in foods; Structure and function of pyroglutamyl peptides. *FFI J.* **222**, 216–222 (2017).
10. Ley, R. E., Turnbaugh, P. J., Klein, S. & Gordon, J. I. Human gut microbes associated with obesity. *Nature* **444**, 1022–1023 (2006).

11. Turnbaugh, P. J. *et al.* An obesity-associated gut microbiome with increased capacity for energy harvest. *Nature* **444**, 1027–1031 (2006).
12. Lin, H. V. *et al.* Butyrate and propionate protect against diet-induced obesity and regulate gut hormones via free fatty acid receptor 3-independent mechanisms. *PLoS One* **7**, e35240 (2012).
13. Thangaraju, M. *et al.* GPR109A is a G-protein-coupled receptor for the bacterial fermentation product butyrate and functions as a tumor suppressor in colon. *Cancer Res.* **69**, 2826–2832 (2009).
14. Tomata, Y. *et al.* Dietary patterns and incident dementia in elderly Japanese: The Ohsaki cohort 2006 study. *Journals Gerontol. Ser. A Biol. Sci. Med. Sci.* **71**, 1322–1328 (2016).
15. Zhang, S., Tomata, Y., Sugawara, Y., Tsuduki, T. & Tsuji, I. The Japanese dietary pattern is associated with longer disability-free survival time in the general elderly population in the Ohsaki cohort 2006 study. *J. Nutr.* **149**, 1245–1251 (2019).
16. Nozue, M. *et al.* Fermented soy product intake is inversely associated with the development of high blood pressure: The Japan public health center–based prospective study. *J. Nutr.* **147**, 1749–1756 (2017).
17. Yang, X. *et al.* Associations between intake of dietary fermented soy food and concentrations of inflammatory markers: a cross-sectional study in Japanese workers. *J. Med. Investig.* **65**, 74–80 (2018).
18. Ikeda, K. *et al.* Dietary habits associated with reduced insulin resistance: The Nagahama study. *Diabetes Res. Clin. Pract.* **141**, 26–34 (2018).
19. Sugawara, S. *et al.* The 1975 type Japanese diet improves lipid metabolic parameters in younger adults: A randomized controlled trial. *J. Oleo Sci.* **67**, 599–607 (2018).
20. Yamamoto, K. *et al.* The Japanese diet from 1975 delays senescence and prolongs life span in SAMP8 mice. *Nutrition* **32**, 122–128 (2016).

Acknowledgements

I am grateful to Dr. Kenji Sato for supporting my research life warmly with kindness and thoughtfulness, for giving me great opportunities to experience latest research field, and for teaching me the interest of research. I am really happy to spend my student days under his instruction in his lab.

I also would like to thank Dr. Haruhiko Toyohara and Dr. Masato Kinoshita for their so much advice on my research. I have learned a lot in the seminar.

I also would like to thank Dr. Vadivel Ganapathy of Texas Tech University Health Sciences Center for giving me an opportunity to study on binding assay under his instruction. I also would like to thank Dr. Yangzom D. Butia, Dr. Sabarish Ramachandran, Dr. Sathish Sivaprakasam, Dr. Jiro Ogura, Dr. Toshihiro Sato, Dr. Kei Higuchi, and all students of Dr. Vadivel Ganapathy's lab and staff of TTUHSC for teaching me the experiment. I had a really great, fruitful, and meaningful time during my stay in America in virtue of their so much support.

I also would like to thank Dr. Yasushi Nakamura and Dr. Eun Young Park of Kyoto Prefectural University and Dr. Takeshi Hasegawa of Louis Pasteur Research Center for supporting the animal experiment.

I also would like to thank Dr. Naohiro Tomari and the staff of the Kyoto Integrated Science and Technology Bio-Analysis Center for allowing me to use their MALDI-TOFMS (AXIMA Performance).

I sincerely thank all the current and former members of laboratory of Marine Biological Function for helping my experiment, as well as for supporting my research and private life. Especially, I am grateful to Ms. Yumi Kojima and Mr. Satoshi Miyauchi for supporting animal experiment, peptide synthesis, and participating in discussion many times. I am so glad to be a member of "pyroglutamyl peptide group" with them. Also, I am grateful to all the member of Dr. Sato's group for supporting my experiment.

Finally, I appreciate my family for supporting me so warmly all the time.